

Diffusion-weighted MRI in head and neck squamous cell carcinomas

Juliette Pauline Driessen

Cover design by Ubo van der Burg
Photograph of the diffusion of a drop of ink in water

Layout and printed by Gildeprint, Enschede, the Netherlands.

ISBN: 978-94-6233-266-9

Copyright © by J.P. Driessen 2016. All rights reserved. No part of this publication may be reproduced in any form, by print, photocopy, electronic data transfer or any other means, without prior permission.

Diffusion-weighted MRI in head and neck squamous cell carcinomas

Diffusie gewogen MRI bij plaveiselcelcarcinomen van het hoofd-halsgebied
(met een samenvatting in het Nederlands)

Proefschrift

ter verkrijging van de graad van doctor
aan de Universiteit Utrecht
op gezag van de rector magnificus,
prof.dr. G.J. van der Zwaan,
ingevolge het besluit van het college voor promoties
in het openbaar te verdedigen
op donderdag 19 mei 2016 des middags te 2.30

door

Juliette Pauline Driessen

geboren op 9 oktober 1986
te 's-Gravenhage

Promotoren:

Prof. dr. W. Grolman
Prof. dr. C.H.J. Terhaard

Copromotoren:

Dr. L.M. Janssen
Dr. ir. M.E.P. Philippens

Contents

Chapter 1	Introduction and outline	7
Chapter 2	Follow-up of head and neck cancer after (chemo)radiotherapy A nationwide survey of 58 head and neck oncology specialists in the Netherlands	19
Chapter 3	Diffusion-weighted imaging in head and neck squamous cell carcinomas: A systematic review	35
Chapter 4	Diffusion-weighted MR imaging in laryngeal and hypopharyngeal carcinoma: Association between apparent diffusion coefficient and histologic findings	57
Chapter 5	Correlation of human papillomavirus status with apparent diffusion coefficient of diffusion-weighted MRI in head and neck squamous cell carcinomas	73
Chapter 6	Is pretreatment apparent diffusion coefficient a predictor of radiosensitivity of head and neck squamous cell carcinomas?	89
Chapter 7	Prospective comparative study of diffusion-weighted MRI versus FDG PET-CT for the detection of recurrent head and neck squamous cell carcinomas after (chemo)radiotherapy.	103
Chapter 8	Summary and general discussion	119
Chapter 9	Summary in Dutch - Nederlandse samenvatting	133
	Acknowledgments - Dankwoord	139
	Curriculum Vitae	147





1

Introduction and outline

Chapter 1

R1
R2
R3
R4
R5
R6
R7
R8
R9
R10
R11
R12
R13
R14
R15
R16
R17
R18
R19
R20
R21
R22
R23
R24
R25
R26
R27
R28
R29
R30
R31
R32
R33
R34
R35
R36
R37
R38
R39

Epidemiology of head and neck cancer

Head and neck cancer is a malignant tumor that originates in the upper aerodigestive tract situated between the thoracic outlet and the skull base. The majority of head and neck cancers are squamous cell carcinomas, they originate from the mucosal layer of the upper aerodigestive tract. In the Netherlands, head and neck cancer occupies the seventh place in cancer incidence in males and the ninth place in females. Approximately 3000 patients were diagnosed with head and neck cancer in 2014 and over the last years the incidence is increasing. (1) Head and neck squamous cell carcinomas (HNSCC) typically start to occur at the age of 35-40 years with a peak incidence at the age of 55-60 years. The anatomical subsite most frequently involved in head and neck cancer varies per country, region and sex and relates in part to the underlying carcinogenic factors. In the Netherlands, the most common affected subsites of HNSCC are the oral cavity, the larynx and the oro- and hypopharynx (figure 1). Other, in the Netherlands less frequent affected subsites, are the sinonasal cavity, nasopharynx and salivary glands. (1)

Alcohol and tobacco are the most important risk factors for HNSCC. Combined they have a synergistic carcinogenic effect. For laryngeal cancer exposure to asbestos and wood dust is also described as a risk factor. (2) In addition, an association between viral infections and HNSCC has been found. Epstein-Barr virus has been associated to the development of nasopharyngeal cancer, and more recently human papillomavirus is associated with oral cavity and oropharyngeal carcinomas. (3, 4) Continuation of smoking and excessive alcohol consumption adversely influences survival as it contributes to the development of second primary tumors and recurrences, but also reduces the effectiveness of some of the treatment modalities. (5, 6)

Staging

HNSCC is staged according to the TNM classification of the Union Against Cancer and the American Joint Committee on Cancer (seventh edition, 2010). This classification is based on the anatomic extent of the primary tumor (T-stage), lymph node metastases (N-stage) and presence of distant metastases (M-stage). The criteria for T-stage is diameter dependent in case of oral and oropharyngeal carcinomas, and for laryngeal carcinoma it's based on invasion of laryngeal subsites and vocal cord mobility. N-stage is based on side, size and number of involved lymph nodes. The most common route of lymphatic spread is towards the ipsilateral cervical lymph nodes. The N-stage is one of the most important prognostic factors in patients suffering from HNSCC. M-stage is based on the existence of distant metastases, which most common occur in the lungs, bone and liver. Distant metastases change prognosis dramatically

and generally no curative options are available. Based on the TNM classification patients can be divided in clinical stages I to IV. Approximately one-third of the patients present with early stage disease (stage I and II) and two-third of the patients present with advanced disease (stage III and IV).

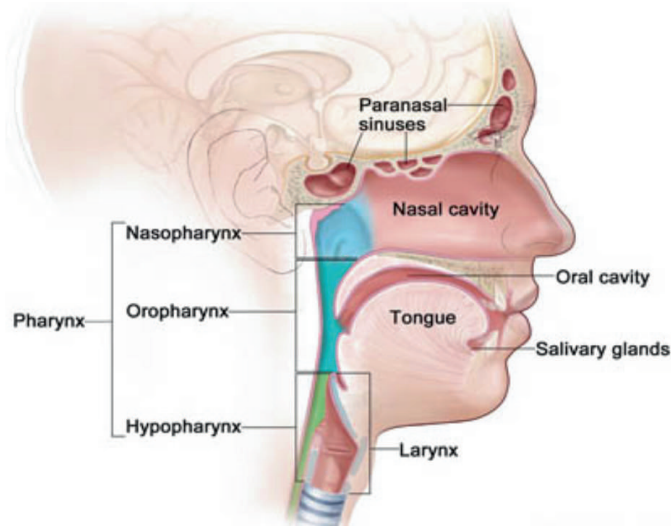


FIGURE 1. Sites of origin of head and neck cancer.

Treatment

Treatment of HNSCC is based on surgery, radiotherapy, systemic therapy or a combination. The choice of optimal treatment is based on subsite and stage, and is aimed to achieve high locoregional control with maximal organ function and minimal therapy-induced side effects. For early stage HNSCC first choice is often (laser assisted) surgery or radiotherapy. For locally advanced HNSCC the first choice treatment is often radiotherapy (RT) combined with chemotherapy or Cetuximab because of the advantage of organ preservation.

Recently, intensity modulated radiotherapy (IMRT) has been developed. This technique is based on a three-dimensional delineation of the target volume. Varying the beam intensity results in a dose distribution with a steep dose gradient outside the target volume. This enables high dose of radiation given on the target volume and simultaneous preservation of nearby organs at risk. (7) This high-precision technique has been a great progress in the radiotherapy of HNSCC, as it reduces the side effects of radiotherapy on organs at risk nearby the target volume without compromising overall survival. This has led to increasing use of radiotherapy in primary HNSCC. Consequently, instead of primary surgery, surgery has become increasingly important as a salvage procedure in case of recurrent or persistent disease after (chemo)radiation. (8)

1	R1
	R2
	R3
	R4
	R5
	R6
	R7
	R8
	R9
	R10
	R11
	R12
	R13
	R14
	R15
	R16
	R17
	R18
	R19
	R20
	R21
	R22
	R23
	R24
	R25
	R26
	R27
	R28
	R29
	R30
	R31
	R32
	R33
	R34
	R35
	R36
	R37
	R38
	R39

Post treatment surveillance

As the role of radiotherapy grows in the management of HNSCC, so does the challenge of post treatment surveillance. Local recurrences occur in up to 50% depending on subsite and T-stage (9-11) Local recurrence is clinically defined as the existence of another squamous cell carcinoma within three years after and within two centimetres of the index tumor. (12) Early detection of residual or recurrent disease after (chemo)radiation ((C)RT) is one of the main objectives during follow-up as it enhances the chance of successful salvage surgery. (13, 14) Delayed detection might lead to increased number of patients with irresectable tumors and therefore decreased survival rates. (15, 16) This often leads to a clinical dilemma as post radiation side effects such as oedema and inflammation may mimic recurrent local disease. (17, 18) Reference standard for proven residual or recurrent local disease is biopsy, however unnecessary biopsies in previously radiated areas are undesirable because of pain and wound healing problems. This causes a dilemma when patients present with symptoms after radiotherapy which might reflect residual disease but also might be caused by radiation itself. Ideally, an accurate selection strategy would reduce the number of patients requiring a biopsy without compromising early detection of residual disease.

With the use of conventional imaging such as computed tomography (CT) and magnetic resonance imaging (MRI) the differentiation of recurrence and post therapeutic alterations remains a challenge. Fluorine 18 fluorodeoxyglucose positron emission tomography combined with CT (FDG PET-CT) is a modality often used in the post treatment surveillance after radiotherapy for HNSCC. FDG PET-CT has a high sensitivity and negative predictive value which makes it suitable for the use of detection of recurrence. (19, 20) However FDG PET-CT has several shortcomings such as high costs, patient exposure to ionizing radiation and changes in tracer uptake in irradiated areas. (21-23) Also, FDG PET-CT is limited by a high false positive rate caused by the avidity of inflammatory mucosae to the FDG-tracer. Therefore, recent developments focus on modern imaging techniques to enhance the diagnostic accuracy in the early post radiation surveillance. (24)

Treatment stratification

Another challenge in the treatment of HNSCC is to identify patients who will benefit from radiotherapy. Although most tumors respond well to radiotherapy, there are tumors with less sensitivity to radiotherapy. Reliable pre-treatment identification of (non)responders would be a valuable way to enable future personalized therapy stratification. (25) Identification of nonresponders to radiotherapy would enable surgery to be given earlier in the treatment process and avoid treatment induced side effects of failed radiotherapy. Techniques for

pre-therapeutic prediction of radiosensitivity in an individual patient is limited, but modern imaging techniques might have potential.

Diffusion-weighted MR imaging

Diffusion-weighted MR imaging (DW-MRI) is a functional MRI technique that measures microscopic water mobility in tissues. In free surrounding, water molecules migrate at microscopic level driven by thermal energy. However, the distance of this diffusion is dependent on the medium in which the water molecule is situated. This is known as the diffusion coefficient. For water at body temperature of 37°C this diffusion coefficient is approximately 3×10^{-3} mm²/sec. However, the diffusivity of water molecules in the human body is hindered by numerous things such as cell membranes, macromolecules and organelles. As a result, water molecules inside the human body are not entirely free in diffusion but partly restricted dependent on the composition of the specific tissue it is situated in. DW-MRI has the ability to measure diffusion of water molecules by sensitizing a MRI sequence with 2 equal but opposing gradients. Magnetization of protons is dephased by the first gradient and rephased by the second gradient. Motion of non-stationary water molecules in tissues between the two opposing gradients will result in incomplete rephasing, which is translated in a loss of signal in the images. A DWI sequence's diffusion sensitivity (e.g. b-value) is determined by the strength, duration and time interval between the opposing gradients. The higher the b-value, the more sensitive the technique is to the effects of diffusion. By repeating the sequence with consecutive and increasing b-values, the progressive signal decay over the images with increasing b-value can be quantified using the apparent diffusion coefficient (ADC). Hereby, ADC provides an objective measure of the diffusivity of water protons. (26, 27) As diffusion restriction is considered to be caused by cellular components it correlates to cellular density. As tumors generally present with higher cellularity, they will present greater diffusion restriction and, consequently, a lower ADC compared to normal tissues. The correlation between cellularity and ADC makes DW-MRI interesting in numerous applications in the often so challenging radio diagnostics of HNSCC. (28, 29) Figure 2 shows a typical example of a DW-MRI of a patient with an oropharyngeal carcinoma.

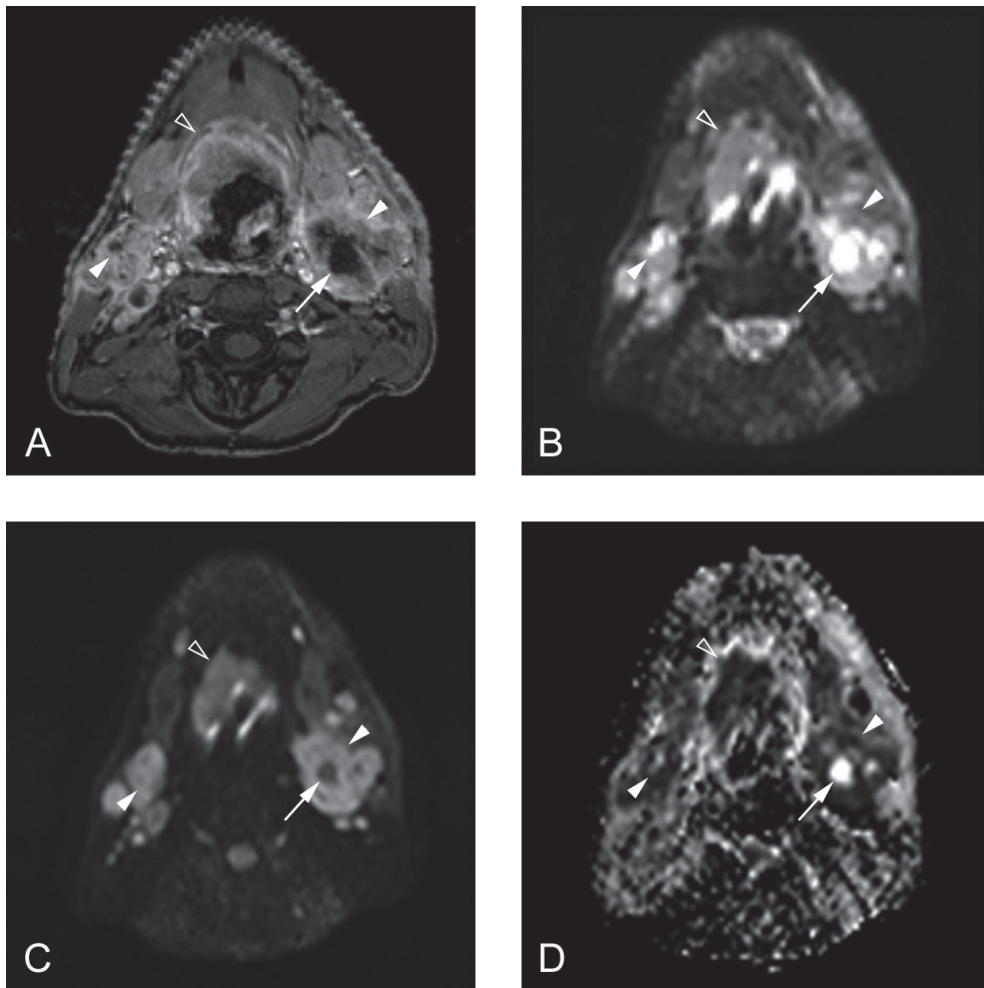


FIGURE 2. Diffusion-weighted MR images of a squamous cell carcinoma in the base of tongue of a 50-year-old male. **(A)** Axial T1-weighted gadolinium MR image shows primary tumor and malignant lymph nodes (arrowheads) and necrotic centre within the lymph nodes on the left (arrow). **(B)** The primary tumor (open arrowhead), lymph adenopathy on both sides (arrowheads), and the necrotic centre on the left (arrow) show hyperintense signal on spin-echo echo-planar DWI $b\ 0\ \text{s/mm}^2$. **(C)** The vital malignant areas remain hyperintense (arrowheads) on $b\ 800\ \text{s/mm}^2$, whereas the signal in the necrotic core is hypointense. **(D)** Apparent diffusion coefficient (ADC) map shows hypointense signal in the primary tumor and malignant lymph nodes, corresponding with a low ADC and a high signal in the necrotic core, corresponding with a high ADC.

1

R1
R2
R3
R4
R5
R6
R7
R8
R9
R10
R11
R12
R13
R14
R15
R16
R17
R18
R19
R20
R21
R22
R23
R24
R25
R26
R27
R28
R29
R30
R31
R32
R33
R34
R35
R36
R37
R38
R39

Outline of this thesis

In this thesis we study the use of DW-MRI in HNSCC. The main goal of this thesis is to evaluate the potential of DW-MRI to benefit the current clinical practise of HNSCC, from early after diagnosis, in the reflection of tumor microbiology, to later on in the post treatment phase to enable early detection of recurrent disease.

In **chapter 2** we inventoried the place for DW-MRI in the follow-up of HNSCC after (C)RT by performing a survey on the clinical practise of follow-up among all members of the Dutch Head and Neck Society. Among other things we focussed on the use of imaging for response evaluation, early detection of local recurrence and the imaging modalities of choice.

In **chapter 3** we addressed this topic by reviewing the current literature on the use of DW-MRI in HNSCC. We divided this review in three main usages of DW-MRI in HNSCC; detection of primary tumors, nodal staging and detection of local recurrences.

In the next chapters we studied the biophysical background of DW-MRI; **Chapter 4** correlates histopathological findings on whole mount laryngectomy specimens with the presurgical ADC. We investigated the correlation between cellular density, amount of nuclear, cytoplasmic and stromal area to ADC. In **chapter 5** we investigated the correlation between human papillomavirus status and ADC. These two chapters aim to give us insight and understanding of the reflection of ADC on microscopic level. In **chapter 6** we investigated the prediction of radiosensitivity using pretreatment ADC. The aim of this study is to evaluate if DW-MRI could be used as an accurate modality for treatment stratification before onset. Using multivariate logistic regression, we study the ability of ADC to predict local response after (C)RT for HNSCC.

In **chapter 7** we focus on the diagnostic accuracy of DW-MRI to detect local recurrence after (C)RT. We present the results of a prospective comparative study between the current standard, FDG PET-CT, and DW-MRI for the detection of local recurrence in patients clinically suspected for local recurrence after (C)RT for HNSCC. With this study we investigated the hypothesis that DW-MRI reduces false-positive results compared to FDG PET-CT while maintaining the high negative predictive value of FDG PET-CT.

Throughout this thesis we aim to investigate the use of DW-MRI for HNSCC in a broad sense. The result of this work can be helpful for future studies investigating the clinical use of DW-MRI in HNSCC. **Chapter 8** contains a summary and future prospects, followed by a Dutch summary in **chapter 9**.

1. Netherlands Cancer Registry. Incidence of cancer in the Netherlands 2014.; Available from: www.cijfersoverkanker.nl.
2. Burch, J.D., et al., Tobacco, alcohol, asbestos, and nickel in the etiology of cancer of the larynx: a case-control study. *J Natl Cancer Inst*, 1981. 67(6): p. 1219-24.
3. Coghill, A.E. and A. Hildesheim, Epstein-Barr virus antibodies and the risk of associated malignancies: review of the literature. *Am J Epidemiol*, 2014. 180(7): p. 687-95.
4. Ringstrom, E., et al., Human papillomavirus type 16 and squamous cell carcinoma of the head and neck. *Clin Cancer Res*, 2002. 8(10): p. 3187-92.
5. Schwartz, L.H., et al., Synchronous and metachronous head and neck carcinomas. *Cancer*, 1994. 74(7): p. 1933-8.
6. Farshadpour, F., et al., Survival analysis of head and neck squamous cell carcinoma: influence of smoking and drinking. *Head Neck*, 2011. 33(6): p. 817-23.
7. Gregoire, V., et al., Intensity-modulated radiation therapy for head and neck carcinoma. *Oncologist*, 2007. 12(5): p. 555-64.
8. Wong, L.Y., et al., Salvage of recurrent head and neck squamous cell carcinoma after primary curative surgery. *Head Neck*, 2003. 25(11): p. 953-9.
9. Ritoe, S.C., et al., Screening for local and regional cancer recurrence in patients curatively treated for laryngeal cancer: definition of a high-risk group and estimation of the lead time. *Head Neck*, 2007. 29(5): p. 431-8.
10. Spector, G.J., Distant metastases from laryngeal and hypopharyngeal cancer. *ORL J Otorhinolaryngol Relat Spec*, 2001. 63(4): p. 224-8.
11. Terhaard, C.H., et al., T3 laryngeal cancer: a retrospective study of the Dutch Head and Neck Oncology Cooperative Group: study design and general results. *Clin Otolaryngol Allied Sci*, 1992. 17(5): p. 393-402.
12. Braakhuis, B.J., et al., Second primary tumors and field cancerization in oral and oropharyngeal cancer: molecular techniques provide new insights and definitions. *Head Neck*, 2002. 24(2): p. 198-206.
13. Cooney, T.R. and M.G. Poulsen, Is routine follow-up useful after combined-modality therapy for advanced head and neck cancer? *Arch Otolaryngol Head Neck Surg*, 1999. 125(4): p. 379-82.
14. Merckx, M.A., et al., Effectiveness of routine follow-up of patients treated for T1-2N0 oral squamous cell carcinomas of the floor of mouth and tongue. *Head Neck*, 2006. 28(1): p. 1-7.
15. Ho, A.S., et al., Decision making in the management of recurrent head and neck cancer. *Head Neck*, 2014. 36(1): p. 144-51.
16. Goodwin, W.J., Jr., Salvage surgery for patients with recurrent squamous cell carcinoma of the upper aerodigestive tract: when do the ends justify the means? *Laryngoscope*, 2000. 110(3 Pt 2 Suppl 93): p. 1-18.
17. Weissman, J.L. and R. Akindele, Current imaging techniques for head and neck tumors. *Oncology (Williston Park)*, 1999. 13(5): p. 697-709; discussion 713.
18. Wang, S.J., Surveillance radiologic imaging after treatment of oropharyngeal cancer: a review. *World J Surg Oncol*, 2015. 13: p. 94.
19. Isles, M.G., C. McConkey, and H.M. Mehanna, A systematic review and meta-analysis of the role of positron emission tomography in the follow up of head and neck squamous cell carcinoma following radiotherapy or chemoradiotherapy. *Clin Otolaryngol*, 2008. 33(3): p. 210-22.
20. Terhaard, C.H., et al., F-18-fluoro-deoxy-glucose positron-emission tomography scanning in detection of local recurrence after radiotherapy for laryngeal/ pharyngeal cancer. *Head Neck*, 2001. 23(11): p. 933-41.
21. Kostakoglu, L., et al., Early detection of recurrent disease by FDG-PET/CT leads to management changes in patients with squamous cell cancer of the head and neck. *Oncologist*, 2013. 18(10): p. 1108-17.

- R1
- R2
- R3
- R4
- R5
- R6
- R7
- R8
- R9
- R10
- R11
- R12
- R13
- R14
- R15
- R16
- R17
- R18
- R19
- R20
- R21
- R22
- R23
- R24
- R25
- R26
- R27
- R28
- R29
- R30
- R31
- R32
- R33
- R34
- R35
- R36
- R37
- R38
- R39
22. Valk, P.E., et al., Cost-effectiveness of PET imaging in clinical oncology. *Nucl Med Biol*, 1996. 23(6): p. 737-43.
 23. Yao, M., et al., The role of FDG PET in management of neck metastasis from head-and-neck cancer after definitive radiation treatment. *Int J Radiat Oncol Biol Phys*, 2005. 63(4): p. 991-9.
 24. de Bree, R., et al., Advances in imaging in the work-up of head and neck cancer patients. *Oral Oncol*, 2009. 45(11): p. 930-5.
 25. Bourhis, J., Hypoxia response pathways and radiotherapy for head and neck cancer. *J Clin Oncol*, 2006. 24(5): p. 725-6.
 26. Koh, D.M. and A.R. Padhani, Diffusion-weighted MRI: a new functional clinical technique for tumour imaging. *Br J Radiol*, 2006. 79(944): p. 633-5.
 27. Padhani, A.R., Diffusion magnetic resonance imaging in cancer patient management. *Semin Radiat Oncol*, 2011. 21(2): p. 119-40.
 28. Hatakenaka, M., et al., Pretreatment apparent diffusion coefficient of the primary lesion correlates with local failure in head-and-neck cancer treated with chemoradiotherapy or radiotherapy. *Int J Radiat Oncol Biol Phys*, 2011. 81(2): p. 339-45.
 29. Vandecaveye, V., et al., Detection of head and neck squamous cell carcinoma with diffusion weighted MRI after (chemo)radiotherapy: correlation between radiologic and histopathologic findings. *Int J Radiat Oncol Biol Phys*, 2007. 67(4): p. 960-71.

1

- R1
- R2
- R3
- R4
- R5
- R6
- R7
- R8
- R9
- R10
- R11
- R12
- R13
- R14
- R15
- R16
- R17
- R18
- R19
- R20
- R21
- R22
- R23
- R24
- R25
- R26
- R27
- R28
- R29
- R30
- R31
- R32
- R33
- R34
- R35
- R36
- R37
- R38
- R39





2

**Follow-up of head and neck cancer after (chemo)radiotherapy
A nationwide survey of 58 head and neck oncology specialists
in the Netherlands**

J.P. Driessen
R. Puijk
L.M. Janssen
W. Grolman
I. Stegeman
C.H.J. Terhaard

Submitted

Abstract

Background: After (chemo)radiotherapy for head and neck squamous cell carcinomas (HNSCC), early detection of recurrences is of great importance to enable salvage surgery. However, international guidelines lack consensus concerning the follow-up strategy. This survey aims to evaluate the current clinical practice in the Netherlands.

Methods: An online questionnaire was sent to all physicians treating HNSCC in the Netherlands. Response rate was 52% and covered all institutions.

Results: The interval and duration of follow-up have been standardized in most institutions. However, the use of standard response evaluation and chosen imaging technique during follow-up varied widely. When clinical suspicion of local recurrence exists, most physicians perform biopsy without the use of imaging beforehand.

Conclusions: This variation illustrates the need of guidelines for the follow-up of HNSCC. These should not only focus on the interval of consultations, but also address the use of imaging modalities as well as the modality of preference.

R1
R2
R3
R4
R5
R6
R7
R8
R9
R10
R11
R12
R13
R14
R15
R16
R17
R18
R19
R20
R21
R22
R23
R24
R25
R26
R27
R28
R29
R30
R31
R32
R33
R34
R35
R36
R37
R38
R39

Introduction

Today, head and neck squamous cell carcinoma (HNSCC) is the sixth most common cancer worldwide. (1) Nowadays, HNSCC is increasingly being treated by (chemo)radiotherapy (CRT). CRT has the advantage of organ preservation with less cosmetic morbidity. Loco-regional recurrence rate varies from less than 5% up to 55% within 5 years after CRT, depending on subsite and tumor stage. (2,3) From these recurrences, the majority will manifest within 3 years after treatment. (4,5) Early detection of loco-regional recurrences is one of the main objectives during follow-up as it enhances the chance of successful salvage surgery, where delayed detection might lead to irresectability and decreased survival rates. (6-8) Discrimination between tumor recurrence and post-radiation effects has been proven to be difficult, as post-radiation effects may mimic tumor recurrence after CRT. (9) Furthermore, unnecessary biopsies in previously radiated areas are undesirable as they can lead to pain and wound healing problems and often need general anesthesia. (10) Ideally, an accurate selection strategy would reduce the number of patients requiring a biopsy without compromising early detection of residual disease. Regrettably, national and international practical guidelines vary widely according to the optimal approach of post-treatment routine follow-up. (5,6,11-13) There is no consensus concerning the frequency of consultation, duration of follow-up and the indication and use of additional imaging modalities. (9) With this study we aim to evaluate the current clinical practice in the Netherlands concerning the follow-up strategy after CRT in HNSCC patients.

Methods

Questionnaire

An online questionnaire was developed by a team consisting of one epidemiologist/methodologist, one resident otorhinolaryngology, one head and neck surgeon and one radiation oncologist. A literature search was conducted to investigate the main differences and questions in the follow-up of HNSCC after CRT.

Recipients

The questionnaire (appendix 1) was sent by email to all clinical physicians treating HNSCC in the Netherlands connected to the Dutch Head and Neck Oncology Society (Nederlandse Werkgroep Hoofd-Hals Tumoren). Respondents had 4 weeks to complete the questionnaire, a reminder was sent after 2 weeks to non-respondents. Of the recipients, 73% were otorhinolaryngology/maxillofacial head and neck surgeons and the remaining 27% were head and neck radiation oncologists. Data was collected and answers were compared to available literature.

R1
R2
R3
R4
R5
R6
R7
R8
R9
R10
R11
R12
R13
R14
R15
R16
R17
R18
R19
R20
R21
R22
R23
R24
R25
R26
R27
R28
R29
R30
R31
R32
R33
R34
R35
R36
R37
R38
R39

Results

Response rate

One hundred eleven questionnaires were sent to 13 institutions. A total of 58 (52%) questionnaires were returned, representing 13 institutions. Of the respondents, 38 (62%) were otorhinolaryngology/maxillofacial head and neck surgeons and the remaining were head and neck radiation oncologists.

Follow-up interval and duration

The Dutch oncology guideline for HNSCC is sparse in concrete recommendations for follow-up of HNSCC, but does have recommendation concerning the interval of consultation during follow-up. It advises 5-year follow-up, with intervals of 2-3 months for the first two years, 4-6 months for the third year and 6 months of the fourth and fifth year. (12,13) For oropharyngeal carcinomas, 54 (93%) respondents followed this advice, for hypopharyngeal/laryngeal carcinomas this was 49 (85%). If not, the main difference was prolongation of follow-up after 5 years. Table 1 shows the results.

TABLE 1. Result of survey, question 1 and 2

	Oropharynx N (%)	Hypopharynx/ Larynx N (%)
Q1 Do you use the interval of follow-up as recommended by the Dutch oncological guideline?		
Yes	51 (88)	45 (78)
Yes, but I also differ from it	3 (5)	4 (7)
No	4 (7)	6 (10)
Missing *	-	3 (5)
Q2 Do you routinely perform response evaluation (e.g. baseline) imaging to evaluate (chemo) radiotherapy response?		
Yes	31 (53)	27 (47)
Not always, but sometimes	22 (38)	23 (40)
Never	5 (9)	5 (9)
Missing *	-	3 (5)

* Three respondents did not answer the questions of oropharyngeal carcinomas as they reported to only treat hypopharyngeal carcinomas and laryngeal carcinomas

Response evaluation, e.g. baseline imaging

Standard response evaluation was done by approximately half of all respondents (53% oropharyngeal cancer vs 47% hypopharyngeal/laryngeal cancer). Five (9%) respondents never performed response evaluation (table 1). If response evaluation was done, the majority

(71%) performed it 3 months after end of radiation, and 19% at 2 months after treatment. MRI and CT were the most used imaging modalities.

Diagnostic modalities

When asked what the most important requirement is for a diagnostic imaging technique in follow-up of HNSCC, high positive predictive value (PPV) was reported as the most important (29%), followed by high negative predictive value (NPV) (22%), cost-benefit (12%) and high sensitivity (10%). Least important are logistics (7%) and invasiveness (3%). See table 2 for additional answers.

TABLE 2. Result of survey, question 3, and 7-10

	N (%)
Q3 What is your most important requirement with respect to diagnostics/imaging?	
Cost-benefit	7 (12)
Logistics / management / availability	4 (7)
Invasiveness	2 (3)
High positive predictive value	17 (29)
High negative predictive value	13 (22)
High sensitivity	6 (10)
High specificity	3 (5)
Other, i.e.: *	5 (9)
missing	1 (2)
Q7 Should it be preferable for patients to get their follow-up at the nearest hospital?	
Yes	9 (15)
No	46 (79)
Missing	3 (5)
Q8 Should patients be more informed/educated about symptoms of early recurrences?	
Yes	44 (76)
No	11 (19)
Missing	3 (5)
Q9 If a patient is non-curative in case of a recurrence, will you still use diagnostics to conform the recurrence??	
Yes	13 (22)
Sometimes	40 (69)
No	2 (3)
Missing	3 (5)
Q10 Are you satisfied with the current available guidelines in the Netherlands concerning evaluation of local and regional response?	
Yes	30 (52)
No	23 (40)
Missing	5 (8)

*: Please explain you answer

Imaging during follow-up

Findings at physical examination, continuous/progressive symptoms and the start of a new symptom were listed as the most decisive facts to perform extra diagnostics during follow-up. Also weight loss and advanced TNM stage were listed as important facts. Continuing smoking was only sparsely mentioned.

In case of clinical suspicion of a local recurrence, the preferred diagnostic technique varied among the respondents. Most respondents used examination under general anesthesia (EUA) with biopsy, without prior imaging (32-37%). If they used imaging, the majority used PET-CT (19-20%). In case of a suspect regional recurrence, most respondents used ultrasound with fine needle aspiration (US-FNA) (72%). See table 3.

TABLE 3. Routine diagnostic modality when clinically suspected of local-regional recurrence (Q5)

Imaging modality	Oropharynx	Hypopharynx/ larynx	Regional
	N (%)	N (%)	N (%)
EUA with biopsy, without prior imaging	17 (29.3%)	18 (31.0%)	inapplicable
CT	1 (1.7%)	5 (8.6%)	1 (1.7%)
MRI	8 (13.8%)	1 (1.7%)	1 (1.7%)
FDG PET	-	1 (1.7%)	-
FDG PET-CT	10 (17.2%)	10 (17.2%)	7 (12.1%)
DW-MRI	2(3.4%)	2 (3.4%)	-
US with FNA	inapplicable	Inapplicable	39 (67.2%)
Other *	15 (25.9%)	12 (20.7%)	6 (10.3%)
Total	53 (91.3%)	49 (84.5%)	54 (93.1%)

Five oropharyngeal, 9 hypopharyngeal/laryngeal and 4 regional answers were not eligible to evaluate. EUA: examination under general anesthesia, CT: computed tomography, MRI: magnetic resonance imaging, FDG PET: 18F-fluorodeoxyglucose

Positron emission tomography-computed tomography, DW-MRI: diffusion-weighted MRI, US with FNA: ultrasound with fine needle aspiration

*: Alternative combinations, such as direct laryngoscopy combined with FDG PET-CT.

Imaging during follow-up

Findings at physical examination, continuous/progressive symptoms and the start of a new symptom were listed as the most decisive facts to perform extra diagnostics during follow-up. Also weight loss and advanced TNM stage were listed as important facts. Continuing smoking was only sparsely mentioned.

In case of clinical suspicion of a local recurrence, the preferred diagnostic technique varied among the respondents. Most respondents used examination under general anesthesia (EUA) with biopsy, without prior imaging (32-37%). If they used imaging, the majority used

PET-CT (19-20%). In case of a suspect regional recurrence, most respondents used ultrasound with fine needle aspiration (US-FNA) (72%). See table 3.

Institution of follow-up and patients' education

Forty-six (79%) physicians did not prefer referral of patient to their regional hospital for follow-up after treatment. Nine respondents (16%) did prefer referral, mainly because of patient interest. Out of all respondents 4 (7%) felt that referral was licit two years after treatment.

Forty-four (76%) physicians wanted to provide more information or education about alarm symptoms that could occur in early recurrences. Of them, 19 (43%) felt that more education would provide earlier detection and diagnosis.

Additional diagnostics in non-curative patients

If successful salvage treatment would be impossible due to patients' comorbidity or tumor irresectability, 13 respondents (22%) would still perform diagnostics/imaging to confirm a suspected recurrence, 40 respondents (69%) sometimes and 2 respondents (3%) would not. Patients' wish and palliative therapeutic options are most mentioned matters (total of 77%).

Guidelines

Overall, 23 respondents (40%) were not satisfied with current guidelines. They perceived them to be outdated, have limited evidence and lack of well-defined follow-up and diagnostic indications.

Discussion

Our study shows that clinical practice concerning the follow-up of HNSCC after CRT varies widely even in a relative small country as the Netherlands. As early detection of loco-regional recurrences of HNSCC after CRT enhances the chance of successful salvage surgery it should be one of the main objectives during follow-up. Therefore, it is important to have knowledge of the most effective strategy to detect residual or recurrent disease in these patients. Regrettably, international guidelines have well defined pretreatment and treatment recommendations, but their suggestions concerning follow-up is mostly limited to an advice for the interval and duration of consultation during follow-up. They lack concrete recommendations concerning the use of imaging for the detection of residual disease, or the imaging modality of choice. (4-6, 11-13) With this survey we aimed to investigate the current clinical practice in the follow-up of HNSCC after CRT.

R1
R2
R3
R4
R5
R6
R7
R8
R9
R10
R11
R12
R13
R14
R15
R16
R17
R18
R19
R20
R21
R22
R23
R24
R25
R26
R27
R28
R29
R30
R31
R32
R33
R34
R35
R36
R37
R38
R39

R1 ***Follow-up interval and duration***

R2 The frequency and duration of follow-up has been questioned over the past few decades.
R3 (4,5,9,14,15) Most guidelines recommend 5-year follow-up, with high frequency intervals
R4 during the first 3 years after CRT, when loco-regional recurrence is known to be high. In
R5 this survey, majority of the physicians systematically used the interval a duration of follow-
R6 up advised by the Dutch guideline. (12,13) The main way to differ from the advice was
R7 prolongation of follow-up after 5 years. In accordance, it has been reported that 34% of the
R8 British physicians followed patients for 10 years up to lifelong. (16)
R9

R10 ***Response evaluation, e.g. baseline imaging***

R11 About half of the respondents systematically performed baseline post-treatment imaging, all
R12 between 2-3 months' post-treatment using CT or MRI. However, after CRT, CT and MRI can be
R13 difficult to interpret, since post-treatment changes may mimic residual disease. The optimal
R14 time interval between treatment and imaging remains a debate, but in clinical practice it is
R15 often used 3 months after end of radiotherapy. (17)
R16

R17 ***Imaging during follow-up***

R18 In this study, continuous or progressive complaints, new suspicious symptoms and findings at
R19 physical examination are the main decisive facts for the decision to use additional diagnostics.
R20 Continuing consumption of tobacco after CRT is associated with significant increased risk of
R21 developing a loco-regional recurrence. (18,19) Remarkably, it wasn't often mentioned in this
R22 study.
R23

R24 ***Diagnostic modalities***

R25 Most respondents (29%) found high PPV is the most important requirement of a diagnostic
R26 imaging technique in the follow-up of HNSCC. Twenty-two percent found a high NPV the
R27 most important. As early detection is of great importance for successful secondary salvage
R28 treatment, our opinion is that the most important requirement of an imaging modality should
R29 be to reliably rule out tumor recurrence, and therefore NPV is of greater importance than the
R30 PPV. (20)

R31 The majority of the respondents used EUA with biopsy without prior imaging in case of a
R32 clinical suspicion of a recurrence. Second, FDG PET-CT scan, with or without EUA was used.
R33 FDG PET-CT has less false positive scans compared to stand-alone FDG PET and is reported
R34 to have a NPV approximately 95% and a PPV 65% for detection of local recurrences. (20,21)
R35 The exceptionally high NPV and accuracy are especially found when FDG PET-CT is performed
R36 after more than 12 weeks' post-treatment. (21,22) However, FDG PET-CT is limited by its false
R37 positive results due to FDG's avidity to inflammation. (21)
R38
R39

Sparsely mentioned by our respondents, diffusion-weighted MRI (DW-MRI) is an effective modality with promising results in detection of loco-regional recurrences. (23-25) It is reported to have a NPV and PPV of >90-95% (25,26) Nevertheless, DW-MRI is slightly being used according to this study, which might be because of technical challenges and learning curves as this technique is known for artifacts and distortions. (25)

US-FNA is mostly used to detect regional recurrences. That's in accordance with literature where it is reported to have an accuracy of 97.5%. (27)

Institution of follow-up and patients' education

The majority of the physicians preferred follow-up at their own institution. In literature it has been suggested to combine hospital with general practitioner visits to increase follow-up frequency and thereby improve surveillance sensitivity. (16,28,29)

Respondents showed high preference for providing more education as it could contribute to earlier self-detection, diagnosis and better salvage treatment. Flynn et al. showed that 61-68% of recurrences were self-detected. (28) On the other hand, stand-alone self-detection is noticed to be unacceptable. (28,29)

Additional diagnostics in non-curative patients

Only 2 respondents will refrain from additional diagnostics or imaging when a patient is not suitable for salvage. This is in accordance with the fact that the respondents did not find cost-effectiveness one of the main requirements of a diagnostic imaging technique.

Guidelines

Forty percent of our respondents were not satisfied with the current available guidelines. Most given reasons were that they are based on outdated data, have limited evidence and are lacking well-defined follow-up and diagnostic indications.

Strengths and limitations

This survey is an attempt to reflect the current clinical practice in the Netherlands. In the Netherlands the oncologic care of HNSCC is centralized, and there is a well-organized coordination through the Dutch Head and Neck Oncology Cooperative Group. This enabled us to contact all physicians who treat HNSCC. Furthermore, we decided, in contrary to other survey concerning HNSCC, to include both surgeons and radiation oncologist in this survey, as they are both involved in the early follow-up after CRT. We had a 52% response rate, which is a reasonable response rate for this kind of survey and comparable to other survey of this kind. (16,19) A limitation is that there might be a bias in the respondents, and that it might not reflect the total of current practice in the Netherlands.

R1
R2
R3
R4
R5
R6
R7
R8
R9
R10
R11
R12
R13
R14
R15
R16
R17
R18
R19
R20
R21
R22
R23
R24
R25
R26
R27
R28
R29
R30
R31
R32
R33
R34
R35
R36
R37
R38
R39

Conclusion and recommendations

This survey gives an insight on the current clinical practice in the Netherlands concerning the follow-up strategy in HNSCC patients after (chemo)radiotherapy. The interval and duration of follow-up have been standardized in most institutions according to the advice of the Dutch oncology guideline for HNSCC. However, the use of standard response evaluation and chosen imaging technique during follow-up varied widely. This substantial variation illustrates the need for guidelines for the follow-up strategy in HNSCC. These guidelines should not only focus on the duration and interval of consultations, but also include recommendations concerning the indication and use of additional imaging modalities as well as the imaging modality of preference. Functional imaging techniques such as FDG PET-CT or modern imaging such as DW-MRI are interesting techniques in this context. However, prospective comparative imaging studies in HNSCC after CRT are sparse. Future research should focus on these clinical important matters.

R1
R2
R3
R4
R5
R6
R7
R8
R9
R10
R11
R12
R13
R14
R15
R16
R17
R18
R19
R20
R21
R22
R23
R24
R25
R26
R27
R28
R29
R30
R31
R32
R33
R34
R35
R36
R37
R38
R39

1. Ferlay, J., et al., Cancer incidence and mortality worldwide: sources, methods and major patterns in GLOBOCAN 2012. *Int J Cancer*, 2015. 136(5): p. E359-86.
2. Spector, G.J., et al., Management of stage IV glottic carcinoma: therapeutic outcomes. *Laryngoscope*, 2004. 114(8): p. 1438-46.
3. Forastiere, A.A., et al., Concurrent chemotherapy and radiotherapy for organ preservation in advanced laryngeal cancer. *N Engl J Med*, 2003. 349(22): p. 2091-8.
4. Ritoe, S.C., et al., Effect of routine follow-up after treatment for laryngeal cancer on life expectancy and mortality: results of a Markov model analysis. *Cancer*, 2007. 109(2): p. 239-47.
5. Lester, S.E. and R.G. Wight, 'When will I see you again?' Using local recurrence data to develop a regimen for routine surveillance in post-treatment head and neck cancer patients. *Clin Otolaryngol*, 2009. 34(6): p. 546-51.
6. Cooney, T.R. and M.G. Poulsen, Is routine follow-up useful after combined-modality therapy for advanced head and neck cancer? *Arch Otolaryngol Head Neck Surg*, 1999. 125(4): p. 379-82.
7. Merkkx, M.A., et al., Effectiveness of routine follow-up of patients treated for T1-2N0 oral squamous cell carcinomas of the floor of mouth and tongue. *Head Neck*, 2006. 28(1): p. 1-7.
8. Wong, L.Y., et al., Salvage of recurrent head and neck squamous cell carcinoma after primary curative surgery. *Head Neck*, 2003. 25(11): p. 953-9.
9. Digonnet, A., et al., Post-therapeutic surveillance strategies in head and neck squamous cell carcinoma. *Eur Arch Otorhinolaryngol*, 2013. 270(5): p. 1569-80.
10. Valentino, J., et al., Interval pathologic assessments in patients treated with concurrent hyperfractionated radiation and intraarterial cisplatin (HYPERRADPLAT). *Head Neck*, 2002. 24(6): p. 539-44.
11. Schwartz, D.L., et al., Postradiotherapy surveillance practice for head and neck squamous cell carcinoma--too much for too little? *Head Neck*, 2003. 25(12): p. 990-9.
12. Dutch Head and Neck Oncology Cooperative Group, Guideline oral cavity- and oropharyngeal squamous cell Carcinoma (2004), http://www.nwhht.nl/files/user/orofarynxcarcinoom_2004.pdf.
13. Dutch Head and Neck Oncology Cooperative Group, Guideline Laryngeal carcinoma (2010), www.oncoline.nl.
14. Boysen, M., et al., The value of follow-up in patients treated for squamous cell carcinoma of the head and neck. *Eur J Cancer*, 1992. 28(2-3): p. 426-30.
15. Ritoe, S.C., et al., Value of routine follow-up for patients cured of laryngeal carcinoma. *Cancer*, 2004. 101(6): p. 1382-9.
16. Joshi, A., et al., Current trends in the follow-up of head and neck cancer patients in the UK. *Clin Oncol (R Coll Radiol)*, 2010. 22(2): p. 114-8.
17. Schouten, C.S., et al., Response evaluation after chemoradiotherapy for advanced staged oropharyngeal squamous cell carcinoma: a nationwide survey in the Netherlands. *Eur Arch Otorhinolaryngol*, 2014.
18. Browman, G.P., et al., Influence of cigarette smoking on the efficacy of radiation therapy in head and neck cancer. *N Engl J Med*, 1993. 328(3): p. 159-63.
19. Hoff, C.M., C. Grau, and J. Overgaard, Effect of smoking on oxygen delivery and outcome in patients treated with radiotherapy for head and neck squamous cell carcinoma--a prospective study. *Radiother Oncol*, 2012. 103(1): p. 38-44.
20. Terhaard, C.H., et al., F-18-fluoro-deoxy-glucose positron-emission tomography scanning in detection of local recurrence after radiotherapy for laryngeal/ pharyngeal cancer. *Head Neck*, 2001. 23(11): p. 933-41.
21. Gupta, T., et al., Diagnostic performance of post-treatment FDG PET or FDG PET/CT imaging in head and neck cancer: a systematic review and meta-analysis. *Eur J Nucl Med Mol Imaging*, 2011. 38(11): p. 2083-95.
22. Krabbe, C.A., et al., 18F-FDG PET as a routine posttreatment surveillance tool in oral and oropharyngeal squamous cell carcinoma: a prospective study. *J Nucl Med*, 2009. 50(12): p. 1940-7.

R1
R2
R3
R4
R5
R6
R7
R8
R9
R10
R11
R12
R13
R14
R15
R16
R17
R18
R19
R20
R21
R22
R23
R24
R25
R26
R27
R28
R29
R30
R31
R32
R33
R34
R35
R36
R37
R38
R39

- R1
R2
R3
R4
R5
R6
R7
R8
R9
R10
R11
R12
R13
R14
R15
R16
R17
R18
R19
R20
R21
R22
R23
R24
R25
R26
R27
R28
R29
R30
R31
R32
R33
R34
R35
R36
R37
R38
R39
23. Vandecaveye, V., et al., Diffusion-weighted magnetic resonance imaging early after chemoradiotherapy to monitor treatment response in head-and-neck squamous cell carcinoma. *Int J Radiat Oncol Biol Phys*, 2012. 82(3): p. 1098-107.
 24. Vandecaveye, V., et al., Detection of head and neck squamous cell carcinoma with diffusion weighted MRI after (chemo)radiotherapy: correlation between radiologic and histopathologic findings. *Int J Radiat Oncol Biol Phys*, 2007. 67(4): p. 960-71.
 25. Driessen, J.P., et al., Diffusion-weighted imaging in head and neck squamous cell carcinomas: a systematic review. *Head Neck*, 2015. 37(3): p. 440-8.
 26. Tshering Vogel, D.W., et al., Diffusion-weighted MR imaging including bi-exponential fitting for the detection of recurrent or residual tumour after (chemo)radiotherapy for laryngeal and hypopharyngeal cancers. *Eur Radiol*, 2013. 23(2): p. 562-9.
 27. Manikantan, K., et al., Making sense of post-treatment surveillance in head and neck cancer: when and what of follow-up. *Cancer Treat Rev*, 2009. 35(8): p. 744-53.
 28. Flynn, C.J., et al., The value of periodic follow-up in the detection of recurrences after radical treatment in locally advanced head and neck cancer. *Clin Oncol (R Coll Radiol)*, 2010. 22(10): p. 868-73.
 29. Paniello, R.C., et al., Practice patterns and clinical guidelines for posttreatment follow-up of head and neck cancers: a comparison of 2 professional societies. *Arch Otolaryngol Head Neck Surg*, 1999. 125(3): p. 309-13.

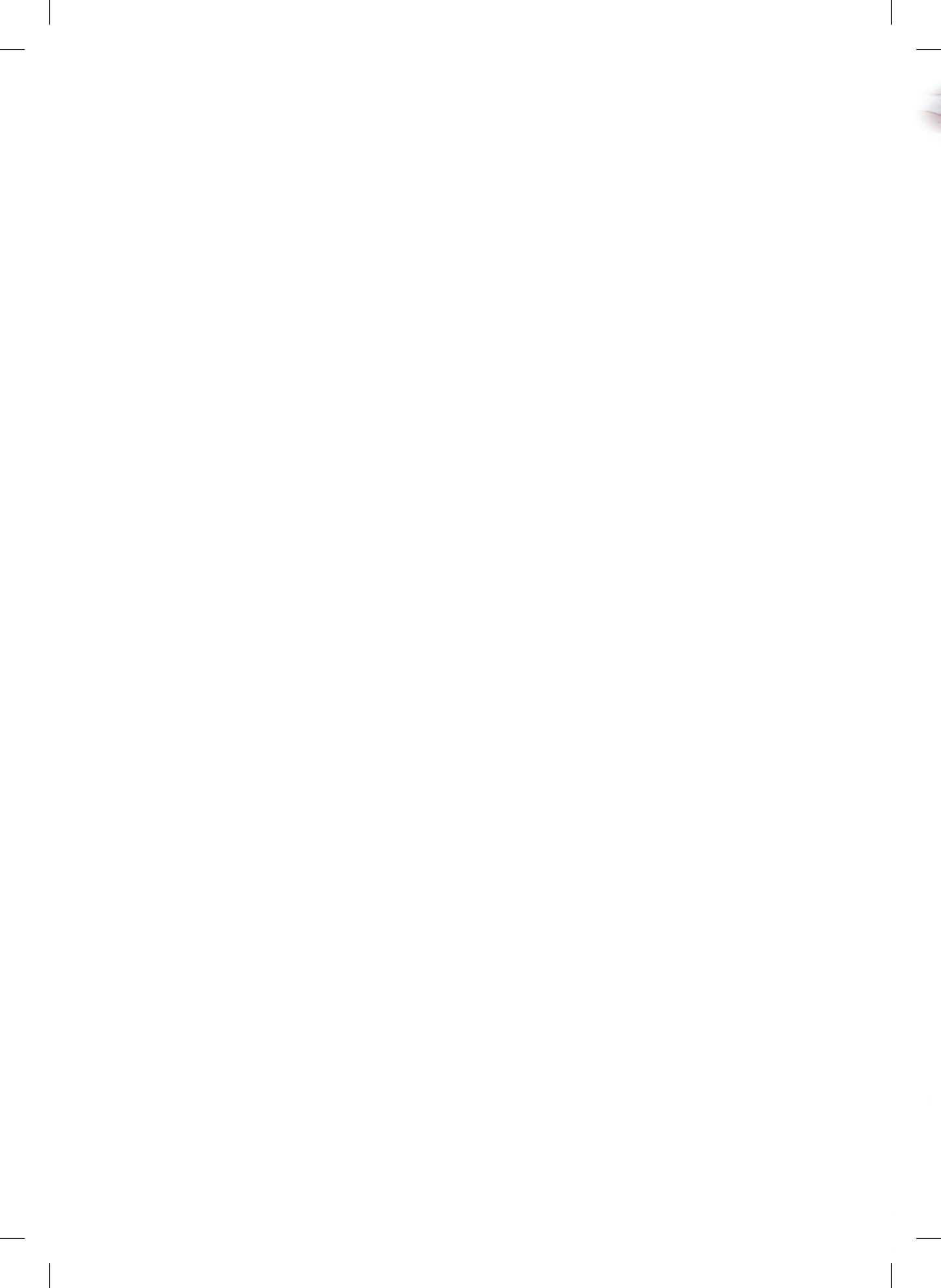
APPENDIX 1. Routine diagnostic modality when clinically suspected of local regional recurrence

<p>Q.1 After treatment, do you systematically use the interval of follow-up as recommended by the Dutch oncological guideline?</p>	<p>Oropharynx: 1) Yes 2) Yes, but I also differ from it, because* 3) No, because</p>	<p>Hypopharynx/larynx: 1) Yes 2) Yes, but I also differ from it, because* 3) No, because</p>
<p>Q.2 To evaluate (chemo)radiotherapy response, you routinely use the patient history, physical examination and flexible fiberoptic endoscopy. Do you routinely perform response evaluation (e.g. baseline) imaging?</p>	<p>Oropharynx: 1) Yes, at * months after treatment 2) No, but I will decide to use it when* 3) No, I never use additional baseline imaging</p>	<p>Hypopharynx/larynx: 1) Yes, at * months after treatment 2) No, but I will decide to use it when* 3) No, I never use additional baseline imaging</p>
<p>Q.3 What is your most important requirement with respect to diagnostics/imaging?</p>	<p>1) Cost-benefit 2) Logistics / management / availability 3) Invasiveness 4) High positive predictive value (actual having the disease with a positive test result) 5) High negative predictive value (not having the disease with a negative test result) 6) High sensitivity 7) High specificity 8) Other, i.e.:</p>	

R1 R2 R3 R4 R5 R6 R7 R8 R9 R10 R11 R12 R13 R14 R15 R16 R17 R18 R19 R20 R21 R22 R23 R24 R25 R26 R27 R28 R29 R30 R31 R32 R33 R34 R35 R36 R37 R38 R39	<p>Q.4 What are the most decisive facts to decide to perform extra diagnostics/imaging to detect a local recurrence? Please fill in 5 options for both oropharynx and hypopharynx/larynx: with '1' counting for the most important fact, and '5' for the least important.</p> <table border="1"> <tr> <td> <p>Oropharynx:</p> <ul style="list-style-type: none"> • Continuous or progressive complaints • New suspicious symptoms • Continuing smoking during/after treatment • Continuing drinking alcohol during/after treatment • Patients' vitality • Weight loss • Findings at physical examination (e.g. evident tumor, edema, ulcer, lymph nodes) • Primary tumor site • Primary (high) TNM staging • Patients' wishes </td> <td> <p>Hypopharynx/larynx:</p> <ul style="list-style-type: none"> • Continuous or progressive complaints • New suspicious symptoms • Continuing smoking during/after treatment • Continuing drinking alcohol during/after treatment • Patients' vitality • Weight loss • Findings at physical examination (e.g. evident tumor, edema, ulcer, lymph nodes) • Primary tumor site • Primary (high) TNM staging • Patients' wishes </td> </tr> </table>	<p>Oropharynx:</p> <ul style="list-style-type: none"> • Continuous or progressive complaints • New suspicious symptoms • Continuing smoking during/after treatment • Continuing drinking alcohol during/after treatment • Patients' vitality • Weight loss • Findings at physical examination (e.g. evident tumor, edema, ulcer, lymph nodes) • Primary tumor site • Primary (high) TNM staging • Patients' wishes 	<p>Hypopharynx/larynx:</p> <ul style="list-style-type: none"> • Continuous or progressive complaints • New suspicious symptoms • Continuing smoking during/after treatment • Continuing drinking alcohol during/after treatment • Patients' vitality • Weight loss • Findings at physical examination (e.g. evident tumor, edema, ulcer, lymph nodes) • Primary tumor site • Primary (high) TNM staging • Patients' wishes
<p>Oropharynx:</p> <ul style="list-style-type: none"> • Continuous or progressive complaints • New suspicious symptoms • Continuing smoking during/after treatment • Continuing drinking alcohol during/after treatment • Patients' vitality • Weight loss • Findings at physical examination (e.g. evident tumor, edema, ulcer, lymph nodes) • Primary tumor site • Primary (high) TNM staging • Patients' wishes 	<p>Hypopharynx/larynx:</p> <ul style="list-style-type: none"> • Continuous or progressive complaints • New suspicious symptoms • Continuing smoking during/after treatment • Continuing drinking alcohol during/after treatment • Patients' vitality • Weight loss • Findings at physical examination (e.g. evident tumor, edema, ulcer, lymph nodes) • Primary tumor site • Primary (high) TNM staging • Patients' wishes 		
	<p>Q.5 If you use diagnostics/imaging to detect a local/regional recurrence, which technique is your first choice?</p> <table border="1"> <tr> <td> <p>Oropharynx:</p> <ol style="list-style-type: none"> 1) EUA with biopsy 2) CT 3) MRI 4) FDG PET 5) FDG PET-CT 6) Diffusion-weighted MRI 7) Other, i.e.: </td> <td> <p>Hypopharynx/larynx:</p> <ol style="list-style-type: none"> 1) EUA with biopsy 2) CT 3) MRI 4) FDG PET 5) FDG PET-CT 6) Diffusion-weighted MRI 7) Other, i.e.: </td> </tr> </table>	<p>Oropharynx:</p> <ol style="list-style-type: none"> 1) EUA with biopsy 2) CT 3) MRI 4) FDG PET 5) FDG PET-CT 6) Diffusion-weighted MRI 7) Other, i.e.: 	<p>Hypopharynx/larynx:</p> <ol style="list-style-type: none"> 1) EUA with biopsy 2) CT 3) MRI 4) FDG PET 5) FDG PET-CT 6) Diffusion-weighted MRI 7) Other, i.e.:
<p>Oropharynx:</p> <ol style="list-style-type: none"> 1) EUA with biopsy 2) CT 3) MRI 4) FDG PET 5) FDG PET-CT 6) Diffusion-weighted MRI 7) Other, i.e.: 	<p>Hypopharynx/larynx:</p> <ol style="list-style-type: none"> 1) EUA with biopsy 2) CT 3) MRI 4) FDG PET 5) FDG PET-CT 6) Diffusion-weighted MRI 7) Other, i.e.: 		
	<p>Q.6 What are the most decisive facts to decide to perform extra diagnostics/imaging to detect a regional recurrence? Please fill in 5 options with '1' counting for the most important fact, and '5' for the least important.</p> <ul style="list-style-type: none"> • Continuous or progressive complaints • New suspicious symptoms • Continuing smoking during/after treatment • Continuing drinking alcohol during/after treatment • Patients' vitality • Weight loss • Findings at physical examination (e.g. evident tumor, edema, ulcer, lymph nodes) • Primary tumor site • Primary (high) TNM staging • Patients' wishes 		

Q.7	Should it be preferable for patients to get their follow-up at the nearest (regional) hospital, because of logistical reasons?
	1) Yes, because* 2) No, because*
Q.8	Should patients be more informed/educated about relevant (alarming) symptoms of early recurrences?
	1) Yes, because* 2) No, because*
Q.9	If you suspect a recurrent carcinoma, but the patient will not be suitable for salvage surgery or other curative treatment, will you still use diagnostics/imaging to confirm this recurrence?
	1) Yes, because* 2) Sometimes, depends on* 3) No, because*
Q.10	Are you satisfied with the current available guidelines in the Netherlands concerning evaluation of local and regional response?
	1) Yes, because* 2) No, because*
Q.11	Do you have any suggestions regarding the current clinical practice in the Netherlands concerning evaluation of local and regional response?

* : Please explain your answer, EUA: examination under general anesthesia, CT: computed tomography, MRI: magnetic resonance imaging, FDG PET: 18F-fluorodeoxyglucose Positron emission tomography, DW-MRI: diffusion-weighted MRI, US with FNA: Ultra sound with fine needle aspiration.





3

Diffusion-weighted imaging in head and neck squamous cell carcinomas: a systematic review

J.P. Driessen
P.M.W. van Kempen
G.J. van der Heijden
M.E.P. Philippens
F.A. Pameijer
I. Stegeman
C.H.J. Terhaard
L.M. Janssen
W. Grolman

Head Neck. 2015 Mar;37(3):440-8

R1
R2
R3
R4
R5
R6
R7
R8
R9
R10
R11
R12
R13
R14
R15
R16
R17
R18
R19
R20
R21
R22
R23
R24
R25
R26
R27
R28
R29
R30
R31
R32
R33
R34
R35
R36
R37
R38
R39

Abstract

Background: The purpose of this study was for us to review diagnostic accuracy of diffusion-weighted imaging (DW-MRI) in primary head and neck squamous cell carcinomas (HNSCCs), detection of metastatic lymph nodes, and recurrences.

Methods: A systematic review for studies concerning DW-MRI was performed.

Results: Ten studies fulfilled inclusion criteria. All studies showed significant higher “apparent diffusion coefficient” (ADC) in benign compared to malignant lesions. ADC thresholds for optimal discrimination varied. In detection of primary HNSCC, the accuracy of DW-MRI ranged from 66% to 86%. In metastatic lymph nodes, the accuracy of DW-MRI was 85% to 91% and the negative predictive value (NPV) was higher than 91%. For recurrences, the accuracy of DW-MRI was 78% to 100% and the NPV ranged from 77% to 100%.

Conclusion: DW-MRI showed consistent high accuracy and high NPV. However, available literature is sparse and varying ADC thresholds were reported. Compared to current imaging techniques, DW-MRI showed the most potential in lymph node staging and detection of recurrences.

Introduction

In the care of patients with head and neck squamous cell carcinoma (HNSCC), imaging is of great importance in tumor staging and follow-up after treatment. For primary staging, conventional CT and MRI are widely used. (1) However, these imaging techniques rely on morphological and size-related criteria and, hereby, the diagnosis of small tumors or micrometastatic nodes remains challenging. (1,2) After treatment, this challenge remains with difficulties in discrimination of tumor recurrence and post-therapeutic effects after surgery or (chemo)radiation. (3) Especially in the post-therapeutic setting, numerous studies have demonstrated the potential of 18F-fluorodeoxyglucose (FDG) positron emission tomography (PET), however, this technique is limited because of the substantial number of false positive results because of FDG avidity to inflammation. (4) Moreover, FDG PET scans are expensive, include exposure to ionizing radiation, and suffer from low resolution. FDG PET-CT partly resolves resolution limitations and increases diagnostic accuracy, however, false-positive results based on inflammation remain a challenge.

A relative new imaging technique is diffusion-weighted imaging (DW-MRI). DW-MRI is an established technique in the early detection of acute stroke, and is increasingly subject of research in several oncologic imaging applications. (5–7) For background on DW-MRI see appendix 1 and figure 1. DW-MRI can be performed with most standard MRI systems, takes only a few minutes, and needs no contrast agent administration. Unfortunately, DW-MRI is sensitive to many artifacts, especially in the heterogeneous head and neck region. (8,9) Optimization of techniques and growing experience resulted in an increasing number of articles reporting DW-MRI in the head and neck region recently.

The purpose of this review was to determine the diagnostic accuracy of DW-MRI in head and neck oncology divided into 3 main purposes: (1) tumor detection in patients clinically suspected of HNSCC; (2) differentiation of metastatic and benign cervical nodes in patients with HNSCC; and (3) detection of tumor recurrence after treatment of HNSCC.

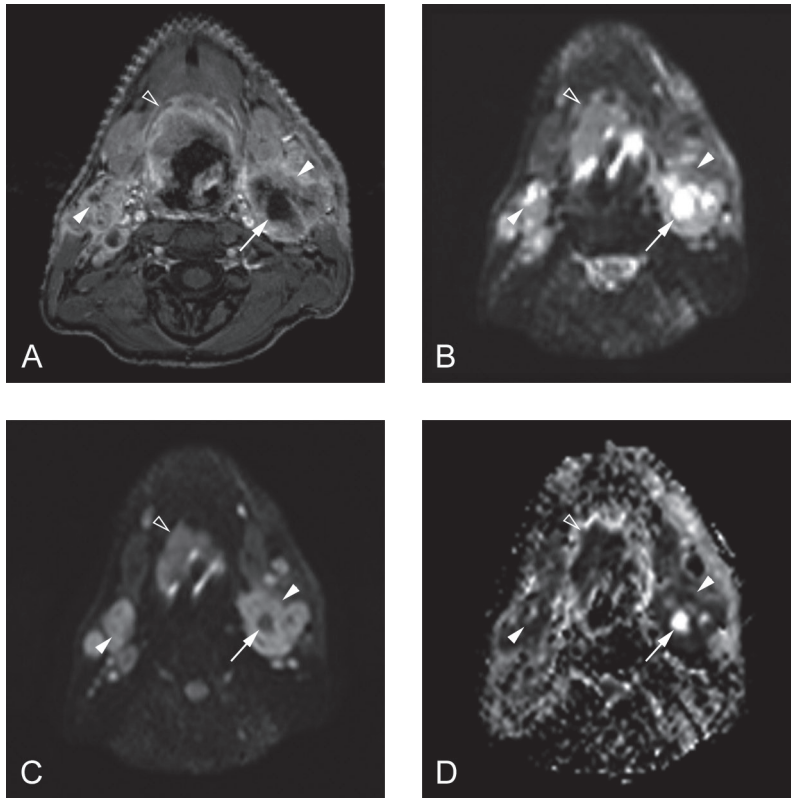


FIGURE 1. Diffusion-weighted MR images of a squamous cell carcinoma in the base of tongue of a 50-year-old male. **(A)** Axial T1-weighted gadolinium MR image shows primary tumor and malignant lymph nodes (arrowheads) and necrotic centre within the lymph nodes on the left (arrow). **(B)** The primary tumor (open arrowhead), lymph adenopathy on both sides (arrowheads), and the necrotic centre on the left (arrow) show hyperintense signal on spin-echo echo-planar DWI b 0 s/mm². **(C)** The vital malignant areas remain hyperintense (arrowheads) on b 800 s/mm², whereas the signal in the necrotic core is hypointense. **(D)** Apparent diffusion coefficient (ADC) map shows hypointense signal in the primary tumor and malignant lymph nodes, corresponding with a low ADC and a high signal in the necrotic core, corresponding with a high ADC.

Materials and Methods

Search strategy

A systematic search was conducted using PubMed, Embase, and Cochrane databases for original articles published until September 2012. Search terms were “head and neck cancer,” “DW-MRI,” and their synonyms in the titles or abstracts, combined with the associated Mesh terms. Appendix 2 displays the full search strategy. Citations and references of selected articles and reviews were checked to identify missed potentially relevant articles. Using predefined inclusion and exclusion criteria, 2 reviewers (J.P.D. and P.M.W.K.) independently

selected all relevant articles by title and abstract. Subsequently, full texts of relevant articles were screened for a more detailed selection.

Inclusion criteria

We included studies concerning original reports on the diagnostic accuracy of DW-MRI in (1) patients clinically suspected of having HNSCC, (2) differentiation of metastatic and benign cervical lymph nodes in patients with HNSCC, and (3) detection of tumor recurrence of HNSCC after therapy. Studies should have confirmed the presence or absence of squamous cell carcinoma (SCC) with cytology, histopathology, or follow-up.

Exclusion criteria

Studies published only as abstracts, case reports, editorials, technical notes, and (partial) duplicate publications of the same dataset were excluded. Articles not written in English, German, French, or Dutch were excluded. We excluded diagnostic case control studies in which the diagnosis is already known; as such, patients are not representative of patients suspected of having HNSCC.

In addition, we excluded studies only reporting on patients with nasal cavity and paranasal sinus SCC, because they are infrequent in Europe and differ in pathophysiology. (10) Studies conducted on lesions with a mixture of subsites, including some patients with nasal cavity or paranasal sinuses, were not excluded.

Quality assessment

The remaining eligible articles were assessed for quality by 2 reviewers (J.P.D. and P.M.W.K.) independently, using criteria of the Quality Assessment of Diagnostic Accuracy Studies (QUADAS-2) tool. (11) As proposed by the QUADAS guidelines, the following 4 items were scored on having a low, high, or unknown risk of bias: (1) patient selection: consecutive patients, avoidance of case-control, and avoidance of inappropriate exclusions; (2) index test: blinding to reference standard, pre-specified, or derived threshold; (3) reference standard: validity of reference standard, and blinding to index test; and (4) flow and timing: interval between and standardization of test and reference standard, and completeness of data. Patient selection, index test, and reference standard were also assessed in terms of applicability. Initial disagreement between reviewers was resolved by discussion.

Data extraction and analysis

Each study was categorized into diagnostics of primary HNSCC, nodal staging, or recurrences. Using a standardized data extraction form, we extracted sample size, tumor subsite, MRI acquisition, b-values, delineation method and reference standard, mean apparent diffusion coefficient (ADC) of malign and benign lesions or nodes, and the optimal thresholds between malignant and benign from each study. In addition, negative predictive value (NPV), positive

predictive value (PPV), accuracy, the sensitivity, and specificity were extracted or recalculated. For statistical analysis, SPSS Statistics version 16.0 (SPSS, Chicago, IL) was used.

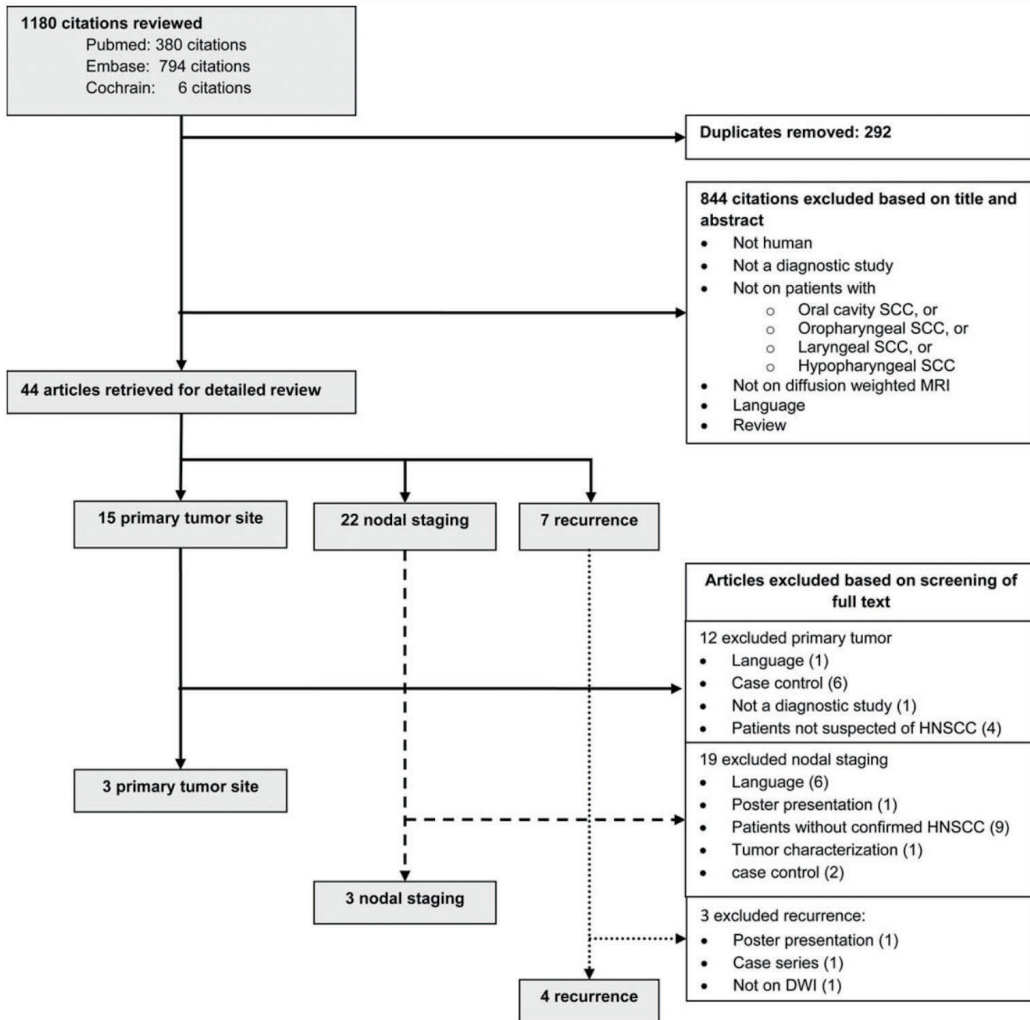


FIGURE 2. Flowchart of included and excluded studies. SCC: squamous cell carcinomas, HNSCC: head and neck: squamous cell carcinomas, DWI: diffusion-weighted imaging.

Results

Search results

The search retrieved 827 unique articles. Of these, 43 articles were selected for detailed review of full text. Finally, 10 articles were included (figure 2). (12–21) Of these 10 included articles, 3 studied diagnostic accuracy of DW-MRI in primary HNSCC, (12–14) 3 studied nodal staging, (15–17) and 4 studied the detection of recurrence. (18–21) All included studies were written in English.

Quality assessment

Table 1 shows the result of the quality assessment according to the QUADAS-2 tool of diagnostic studies. (12–21) One study (16) scored all 7 items as having a low risk of bias and applicability concerns, whereas 4 studies scored 5 or fewer items as having a low risk of bias and applicability concerns. (12,14,18,19) All studies, except Dirix et al (16) scored high risk of bias on the “Index test.” Although the radiologist was often blinded to the pathology when making the delineation, the ADC threshold for a positive test was determined afterward and derived from own data. Although all studies had an appropriate reference standard, 4 studies did not perform the same reference sets in all patients. (14,18,19,21) Overall, the quality of the 10 articles varied from intermediate to good, according to the QUADAS-2 tool.

Study characteristics

Overall, the selected 10 studies included 370 patients (range, 16–81 patients); 222 patients suspected of having HNSCC, 71 patients with HNSCC suspected of lymph node metastasis, and 77 patients suspected of having recurrence of HNSCC after treatment. The mean prevalence of malignancy in primary suspected lesions was 46%, in suspected nodes 20%, and 49% in lesions suspected of recurrence after treatment. Most studies used 1.5 Tesla field strength, echo planar imaging (EPI) sequence, and b-values 0 and 1000 for calculation of the ADC. An exception was Sakamoto et al, (12) using a split acquisition of fast spin-echo signals (SPICE) sequence and a maximal b-value of 771. There was wide variation in calculation of the lesions’ mean ADC; some studies calculated mean ADC of the whole tumor volume, (15,20) whereas other studies used the mean ADC of 1 axial slice (16,17,19) or even a region of interest (ROI) within the tumor. (12–14,18,21) The studies varied in inclusion or exclusion of necrotic or cystic parts of the lesion. Study characteristics are summarized in table 2.

TABLE 1. Quality assessment of studies included

Study first author	Risk of bias				Applicability concerns			
	Patient selection	Index test	Reference standard	Flow and timing	Patient selection	Index test	Reference standard	
Primary tumor								
Sakamoto et al (12)	■	◇	■	■	■	■	◇	
Srinivasan et al (13)	■	◇	■	■	■	■	■	
Wang et al (14)	■	◇	■	◇	■	■	■	
Nodal staging								
Bondt et al (15)	■	◇	■	■	■	■	■	
Dirix et al (16)	■	■	■	■	■	■	■	
Vandecaveye et al (17)	■	◇	■	■	■	■	■	
Recurrence								
Gouhar et al (18)	■	◇	◇	■	■	?	■	
Razek et al (19)	■	◇	◇	◇	■	■	◇	
Vandecaveye et al (20)	■	◇	■	■	■	■	■	
Tshering Vogel et al (21)	■	◇	■	■	■	■	■	

■ : low risk, ◇ : high risk, ? : unclear

TABLE 2. Study characteristics

Study first author	Year	N	N ^{LN}	N ^{LN} <10mm (%)	b-value	Pulse sequence	Field strength (Tesla)	Delineation method	Exclusion NC or C	Delineation	Reference standard
Primary tumor											
Sakamoto et al (12)	2009	62			0, 771	SPLICE	1,5	ROI	no	1 radiologist	HP
Srinivasan et al (13)	2008	33			0, 800 and 0, 1000*	EPI	3	ROI	yes	1 radiologist	HP, FU
Wang et al (14)	2001	81			0, 1000	EPI	1,5	ROI	yes	1 radiologist	HP, FU
Nodal staging											
Bondt et al (15)	2009	16	219	209 (95.4)	0, 1000	EPI	1,5	TV	yes	2 radiologists	HP
Dirix et al (16)	2010	22	198	171 (86.4)	0, 1000	EPI	1,5	TL	no	2 radiologists	HP
Vandecaveye et al (17)	2009	33	301	259 (86.0)	0, 1000	EPI	1,5	TL	yes	2 radiologists	HP
Recurrence											
Gouhar et al (18)	2011	21			0, 1000	EPI	1,5	ROI	no	2 radiologists	HP
Razek et al (19)	2007	30			0, 1000	EPI	1,5	TL	yes	1 radiologist	CYT, HP
Vandecaveye et al (20)	2007	22			0, 50, 100, 500, 750, 1000	EPI	1,5	TV	no	2 radiologists	HP
Tshering Vogel et al (21)	2012	46			0, 50, 100, 500, 750, 1000	EPI	1,5	ROI	yes	2 radiologists	HP, FU

N: number of included patients, N^{LN}: number of lymph nodes (%), NC: necrosis, C: cysts, TL: total lesion one axial slide, TV: tumor volume in all axial slides, HP: histopathology, FU: follow up, CYT: cytology

* 2 different protocols were used; b0 and b800 or b0 and b1000

Primary tumor site

Three articles studied diagnostic accuracy of DW-MRI in detection of primary HNSCC. (12–14) All patients presented with a lesion that was clinically suspected of a primary HNSCC. Sakamoto et al (12) supplied additional data at our request. Mean ADC of benign and malignant lesions are shown in the first column of figure 3. All studies showed significantly higher ADC in benign lesions compared to malignant lesions. Although, the mean ADC of both groups showed wide variation. Sakamoto et al (12) found the highest ADC for malignant lesions, whereas Srinivasan et al (13) found the lowest mean ADC of benign lesions. The incidence of malignancy varied widely, from 28% to 61%. In the study of Sakamoto et al, (12) the malignant lesions consisted of 58% HNSCC, compared to 81% HNSCC in the study of Srinivasan et al (13) and 45% HNSCC in the study of Wang et al. (14) The calculated optimal ADC threshold for discrimination of benign and malignant lesions. was comparable in Srinivasan et al (13) and Wang et al. (14) Adversely, Sakamoto et al (12) found a higher optimal ADC threshold. With the optimal ADC threshold, Wang et al (14) obtained the highest diagnostic accuracy of DW-MRI in detection of malignant lesions of 86%, compared to 76% and 66% in Srinivasan et al (13) and Sakamoto et al, (12) respectively. The NPV ranged from 88% to 78% and the PPV from 44% to 93%. The diagnostic accuracy of all studies is summarized in table 3.

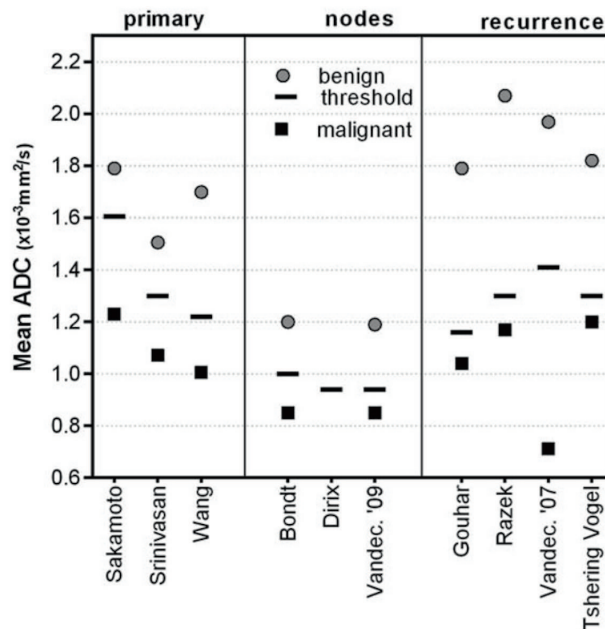


FIGURE 3. Mean apparent diffusion coefficient (ADC) of malignant and benign head and neck lesions and optimal discriminating ADC threshold. ADC threshold are calculated to maximize accuracy, except for de Bondt et al¹⁵ who preferred to maximize sensitivity and Dirix et al¹⁶ who predefined an ADC threshold derived from Vandecaveye et al¹⁷.

TABLE 3. Diagnostic accuracy of diffusion-weighted MRI

Study first author	Meth	Prev	Threshold	PPV	NPV	AC	SE	SP
Primary tumor								
Sakamoto et al (12)	Qn	28	1.61	44	88	66	79	60
Srinivasan et al (13)	Qn	48	1.30	72	80	76	81	71
Wang et al (14)	Qn	61	1.22	93	78	86	84	91
Nodal staging								
Bondt et al (15)	Qn	12	1.00	44	99	85	92	84
Dirix et al (16)	Qn	23	0.94	91	97	95	89	97
Vandecaveye et al (17)	Qn	25	0.94	82	91	91	84	94
Recurrence								
Gouhar et al (18)	Qn	62	1.16	92	78	86	85	88
Razek et al (19)	Qn	63	1.30	94	77	87	84	91
Vandecaveye et al (20)	Qn	68	1.41	100	100	100	100	100
Tshering Vogel et al (21)	Qn	39	130	75	80	78	67	86
	Ql	39	NA	100	97	98	94	100

Values represent numbers, unless stated otherwise

Meth: methodology (Qn: Quantitative assessment, Ql: Qualitative assessment)

Prev: prevalence, Threshold: ADC value to discriminate between malignant and benign lesions ($\times 10^{-3}$ mm²/sec) PPV: positive predictive value, NPV: negative predictive value, AC: accuracy, SE: sensitivity, SP: specificity

Nodal staging

Three articles studied the diagnostic accuracy of DW-MRI in detection of malignant nodes in patients with known HNSCC without previous treatment. (15–17) All patients had proven HNSCC with risk of lymph node metastasis and were planned for a (selective) neck dissection. After neck dissection, all identified lymph nodes were matched to the preoperative DW-MRI. The second column of figure 3 shows mean ADC and ADC thresholds. Dirix et al (16) did not report the mean ADC of benign and malignant nodes, but only reported obtained diagnostic accuracy by the use of a predefined ADC threshold of 0.94 derived from Vandecaveye et al. (17) They reported the highest accuracy in discrimination of benign and malignant nodes of 97%. Vandecaveye et al (17) and de Bondt et al (15) reported identical mean ADCs, which were significantly different in malignant and benign nodes. However, Vandecaveye et al (17) subsequently chose an ADC threshold resulting in maximal diagnostic accuracy, whereas de Bondt et al (15) preferred an ADC threshold, which resulted in a high sensitivity and consequently compromised with a lower accuracy. All studies showed high accuracy above 85% and an NPV of 91%, which is summarized in table 3. Vandecaveye et al (17) performed a sub-analysis for nodes smaller than 1 cm and reported a sensitivity of 76%. All studies had low incidence of malignant nodes, because all matched nodes were taken into account individually, regardless of size or presentation on other imaging modalities.

Recurrence

Four articles studied the diagnostic accuracy of DW-MRI in detection of recurrent HNSCC after treatment. (18–21) Vandecaveye et al supplied additional data at our request. Gouhar and El-Hariri (18) included patients clinically suspected of a local recurrence of laryngeal carcinoma within 2 to 6 months after radiotherapy. Abdel Razek et al (19) included patients clinically suspected of local recurrence, based on symptoms or findings, within 4 to 14 months after treatment of HNSCC. Treatment consisted of radiotherapy, surgery, or both. Vandecaveye et al (17) included patients after (chemo)radiotherapy with or without surgery with a suspicion of local recurrence, regional recurrence, or both. For this review, only the 22 patients suspected of a local recurrence were included. Finally, Tshering Vogel et al (21) included patients clinically suspected of local recurrence of laryngeal or hypopharyngeal carcinoma within 3 to 108 months after (chemo)radiotherapy. Tshering Vogel et al (21) is the only study that not only used quantitative analyses (e.g., ADC), but also used qualitative visual assessment of DW-MRI b 1000 s/mm², ADC map, and corresponding morphological MR images. All studies found significantly higher mean ADC in benign lesions compared to recurrences. All studies except Gouhar and El-Hariri¹⁸ found identical optimal ADC thresholds. By quantitative assessment, diagnostic accuracy varied from 78% to 100%, but all found high NPV of 78% to 100%, with a PPV of 75% to 100%. Compared to the other quantitative studies, Vandecaveye et al (17) reported remarkable high diagnostic accuracy of 100%. The qualitative study of Tshering Vogel et al²¹ also achieved high diagnostic accuracy, with sensitivity, specificity, accuracy, NPV and PPV all above 94%. Figure 3 displays the mean ADC values and table 3 summarizes the diagnostic accuracy. In addition, figure 4 displays the posterior probabilities compared to the prior probability (e.g., prevalence). All studies were within the upper triangle, indicating that they have both added positive value as well as added negative value. The added value of a positive test, defined as the difference between the prevalence of recurrence and the positive predictive value, ranged between 30% and 61%. The added value of a negative test, defined as the difference between (1-prevalence) and the negative predictive value, ranged between 19% and 40%.

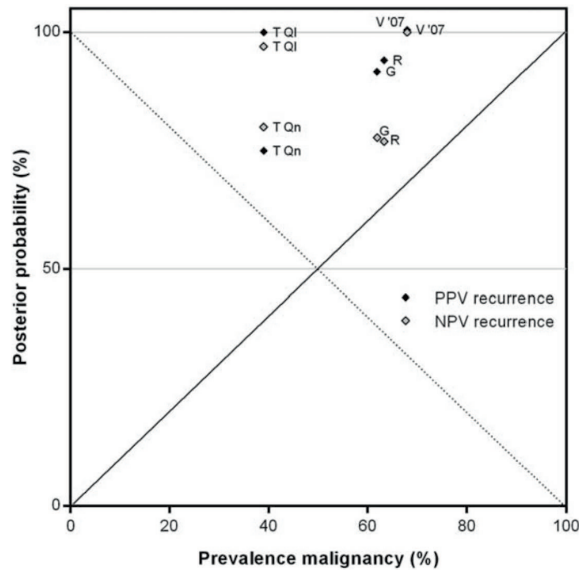


FIGURE 4. Positive and negative predictive value of diffusion-weighted imaging (DWI) in detection of recurrence compared to prevalence (prior probability). All studies are plotted in the upper triangle, which indicates both an added positive and an added negative value of DWI. G: Gouhar and El-Hariri¹⁸, R: Abdel Razek et al¹⁹, V '07: Vandecaveye et al. 2007²⁰, T Qn: Tshering Vogel et al²¹ quantitative assessment, T Ql: Tshering Vogel et al²¹ qualitative assessment.

Discussion

Although DW-MRI in the head and neck is challenging, numerous recent articles study its use for a variety of purposes. We systematically reviewed the literature for diagnostic studies covering DW-MRI in head and neck oncology, divided into 3 review questions; the diagnostic accuracy of DW-MRI in (1) patients clinically suspected of having HNSCC; (2) differentiation metastatic and benign cervical lymph nodes in patients with HNSCC; and (3) detection of tumor recurrence of HNSCC after therapy.

We selected studies according to the recommendations of the QUADAS team and used the QUADAS-2 tool to judge the quality of the selected studies. (11) The first striking point of our search was the sparseness of literature with a suitable methodology to address our research question. Most studies have a case-control design, comparing ADC of known carcinomas with normal tissues. These studies all find significant differences between malignant and benign tissues, and calculate high diagnostic accuracy of this technique. However, this design is not appropriate to study diagnostic accuracy, because patient selection is not comparable to daily practice. An appropriate design to study diagnostic accuracy is to include patients suspected or at risk of a specific diagnosis. (11) The exclusion of studies with a case-control design

R1
R2
R3
R4
R5
R6
R7
R8
R9
R10
R11
R12
R13
R14
R15
R16
R17
R18
R19
R20
R21
R22
R23
R24
R25
R26
R27
R28
R29
R30
R31
R32
R33
R34
R35
R36
R37
R38
R39

R1 limited our included articles; however, inclusion of case-control studies introduces a bias in
R2 patient selection and risks the chance of overestimation of the diagnostic accuracy. (11)

R3 In oncology, accuracy of an imaging technique must be preferably high, but maybe even
R4 more important is to reliably exclude the presence of a tumor, because false negative results
R5 have serious consequences. (22) They can lead to delayed detection or under-treatment,
R6 with possibly compromised survival. Therefore, a reliable test for this purpose must have a
R7 high NPV and high sensitivity. On the other hand, false-positive results can lead to the use of
R8 extra diagnostics and unnecessary invasive biopsies. In the ideal situation, both NPV and PPV
R9 of the diagnostic test are low.

R10 **Primary tumor site**

R11 Three studies investigated DW-MRI in detection of primary HNSCC. (12–14) Although all
R12 studies found significantly higher ADC in benign lesions compared to malignant lesions,
R13 the reported mean ADC of both malignant and benign lesions and hereby the optimal ADC
R14 threshold showed wide variation. In correspondence with the varying mean ADC, optimal
R15 ADC thresholds for discrimination varied as well. This variation can be explained by multiple
R16 factors; the use of different b-values, pulse sequence, and field strength, and also by the
R17 variation in histology of included lesions. Malignant lesions did not only consist of HNSCC
R18 but also included malignant lymphomas. Malignant lymphomas show lower ADC values than
R19 SCC. (23) Wang et al (14) included most malignant lymphomas leading to the lowest mean
R20 ADC of malignant lesions. Within the benign lesions, Srinivasan et al (13) only included solid
R21 lesions, whereas the other studies had cystic lesions as well, resulting in a higher mean ADC.
R22

R23 The reported NPV of DW-MRI in the diagnostics of malignancy is not superior to the
R24 currently used diagnostics of MRI and CT and FDG PET-CT, which have NPV and accuracy up to
R25 94%. (1,22,24) In conclusion, conventional MRI, CT, and FDG PET-CT remain good diagnostic
R26 tools for the detection of primary malignancy in the head and neck and DW-MRI shows no
R27 additional diagnostic value.
R28

R29 **Nodal staging**

R30 Because the status of the cervical lymph nodes is the most important prognostic factor,
R31 optimal staging of the neck is of great importance. Two studies reporting mean ADC of benign
R32 and malignant nodes showed very similar results. (15,17) Mean ADC values of benign nodes
R33 were comparable and higher compared to metastatic nodes. Although these studies found
R34 almost identical mean ADC in their study, they used different ADC thresholds corresponding
R35 with different diagnostic accuracies. Vandecaveye et al (17) calculated the ADC threshold for
R36 the optimal accuracy of 91% with a receiver operating characteristic (ROC) curve, whereas de
R37 Bondt et al (15) chose an ADC threshold with less accuracy (84%), but with a higher sensitivity
R38 and NPV. Dirix et al (16) was the only study that did not derive the threshold from its own
R39

data, but used a predefined threshold derived from the study of Vandecaveye et al. (17) The reported results of DW-MRI are superior to those reported of FDG PET-CT, in which a recent review of Al-Ibraheem et al (25) reported an average sensitivity of 97% to 90%, and a specificity of 80% to 93%. (26–28)

In addition, Vandecaveye et al (20) performed a sub-analysis on lymph nodes smaller than 1 cm and found a sensitivity of 76% in this category. This is comparable to the detection of occult metastatic lymph nodes by FDG PET-CT, which has a sensitivity of around 75%. In conclusion, these scarce results suggest that DW-MRI might be superior in discrimination of metastatic and benign lymph nodes compared to nuclear imaging.

Recurrence

Imaging after treatment of HNSCC is challenging. However, accurate selection of suspected patients is of great importance to avoid unnecessary biopsies in previously irradiated or surgically treated areas, and early detection of recurrence improves outcome and survival. (29) Conventional imaging has poor capacity in discrimination of post-treatment effects from tumor recurrence, and even nuclear imaging (FDG PET-CT) has potential for false positive results because of FDG avidity to inflammation. (4,30,31) As in primary tumors, there was a large variation in mean ADC values of post-treatment effects and recurrence between different studies. Difference in reported ADC of post-treatment effects might be explained by the difference in treatment, as Gouhar and El-Hariri (18) solely included patients after radiotherapy and Abdel Razek et al (19) also included surgically treated patients. These approaches caused different ADC thresholds, but the threshold of Gouhar and El-Hariri (18) to discriminate benign lymph nodes was even lower than the mean ADC of malignant lesions in Abdel Razek et al. (19) This makes it hazardous to translate the reported thresholds. Although ADC values differed among the studies, DW-MRI showed good diagnostic accuracy in detection of recurrent HNSCC, with NPV ranging from 77% to 100%.

DW-MRI has, compared to other imaging modalities of which FDG PET-CT shows best results, comparably reported high sensitivity and NPV starting from 85% to 100%. (25,32,33) However, FDG PET-CT is limited by false positive results because of inflammation. As mentioned, the NPV and sensitivity is the most important in oncology, but especially in case of recurrence after radiotherapy (unnecessary) biopsies can damage already fragile tissue and superimpose infection, necrosis, or failure to heal. The reported PPV of DW-MRI is 91% to 100%, much higher than the 64% to 77% PPV of FDG PET-CT. (32,33) Another advantage of DW-MRI is that it is based on restriction of water molecules, therefore, it is not influenced by post-radiotherapy effects and inflammation. This might enable early detection of recurrences after treatment. This in contrast to FDG PET-CT, which is less reliable in the early post-(radio) therapy setting. (34) In conclusion, DW-MRI seems superior to FDG PET-CT for detection of recurrent HNSCC after treatment, especially caused by the higher PPV.

Limitations

The strength of a systematic review depends on the quality of the included studies. For this systematic review, we performed a comprehensive search with transparent methods, quality assessment, and extracted and recalculated study outcomes. The following limitations should be taken into account; the quality of the studies was intermediate, we found only 1 study that used a predefined ADC threshold not derived from own data. (16) This might cause best-case scenarios and has risk of overestimation of accuracy in daily practice. In addition, diagnostic studies have a trend toward positive publication bias. Second, we found a large variation in the method of ADC calculation. The variety of b-values, pulse sequences, field strength, and delineation methods all influence ADC values. This makes statistical pooling unable to do and makes it hard to translate the reported ADC thresholds. Finally, for the studies concerning detection of metastatic nodes, there is a risk of overestimation of the results. All studies use multiple cervical lymph nodes in 1 patient as independent events. This increases the power of studies and has the risk of introducing positive bias. However, the presence of multiple nodes in a neck dissection makes it impossible to assess this data on a per-patient basis. It is important, however, to realize that the actual number of included patients is rather low, and these finding should ideally be confirmed in larger studies.

In conclusion, according to current available evidence, DW-MRI shows no added value in detection of primary HNSCC, but might show potential in nodal staging and discrimination of recurrence from post-treatment changes. For nodal staging and detection of recurrence, we found diagnostic accuracies varying from 78% to 100% and NPV from 77% to 100%. However, these results are based on few studies, and small patient groups and needs to be confirmed in larger head-to-head studies comparing DW-MRI to other imaging modalities. In addition, large variations in optimal ADC thresholds are reported among the various studies, which make it difficult to establish which ADC threshold to use. In daily practice, one could start using DW-MRI as a complementary sequence to standard diagnostic MRI, in which lesions with high signal at high b-values and low ADC are more likely to be malignant. Therefore, we recommend incorporating DW-MRI in the standard MRI protocol of head and neck lesions. This way, DW-MRI sequence can be optimized to reduce artefacts and gather experience in the interpretation of DW-MRI and ADC maps. For future research, we recommend focus on nodal staging and detection of recurrences with uniform DW-MRI protocols and a proper design for diagnostic studies preferably according to the guidelines of QUADAS-2.

Acknowledgments

The authors thank Mrs. B. Kramer for her help with the design of the systematic search, and Dr. J. Sakamoto and Dr. V. Vandecaveye for providing us with supplementary data of their studies.

- [R1](#)
- [R2](#)
- [R3](#)
- [R4](#)
- [R5](#)
- [R6](#)
- [R7](#)
- [R8](#)
- [R9](#)
- [R10](#)
- [R11](#)
- [R12](#)
- [R13](#)
- [R14](#)
- [R15](#)
- [R16](#)
- [R17](#)
- [R18](#)
- [R19](#)
- [R20](#)
- [R21](#)
- [R22](#)
- [R23](#)
- [R24](#)
- [R25](#)
- [R26](#)
- [R27](#)
- [R28](#)
- [R29](#)
- [R30](#)
- [R31](#)
- [R32](#)
- [R33](#)
- [R34](#)
- [R35](#)
- [R36](#)
- [R37](#)
- [R38](#)
- [R39](#)

1. de Bree R, Castelijns JA, Hoekstra OS, Leemans CR. Advances in imaging in the work-up of head and neck cancer patients. *Oral Oncol* 2009;45(11):930-5.
2. de Bondt RB, Nelemans PJ, Hofman PA, et al. Detection of lymph node metastases in head and neck cancer: a meta-analysis comparing US, USgFNAC, CT and MR imaging. *Eur J Radiol* 2007;64(2):266-72.
3. Brouwer J, Bodar EJ, De Bree R, et al. Detecting recurrent laryngeal carcinoma after radiotherapy: room for improvement. *Eur Arch Otorhinolaryngol* 2004;261(8):417-22.
4. de Bree R, van der Putten L, Brouwer J, Castelijns JA, Hoekstra OS, Leemans CR. Detection of locoregional recurrent head and neck cancer after (chemo)radiotherapy using modern imaging. *Oral Oncol* 2009;45(4-5):386-93.
5. Dunithan AJ, Cox LA, Long BW. Detection of acute stroke with diffusion-weighted MRI. *Radiol Technol* 1998;69(6):559-65.
6. Padhani AR. Diffusion magnetic resonance imaging in cancer patient management. *Semin Radiat Oncol* 2011;21(2):119-40.
7. Koh DM, Padhani AR. Diffusion-weighted MRI: a new functional clinical technique for tumour imaging. *Br J Radiol* 2006;79(944):633-5.
8. Lambrecht M, Dirix P, Vandecaveye V, De Keyzer F, Hermans R, Nuyts S. Role and value of diffusion-weighted MRI in the radiotherapeutic management of head and neck cancer. *Expert Rev Anticancer Ther* 2010;10(9):1451-9.
9. Thoeny HC, De Keyzer F, King AD. Diffusion-weighted MR imaging in the head and neck. *Radiology* 2012;263(1):19-32.
10. Hildesheim A, Wang CP. Genetic predisposition factors and nasopharyngeal carcinoma risk: a review of epidemiological association studies, 2000-2011: Rosetta Stone for NPC: genetics, viral infection, and other environmental factors. *Semin Cancer Biol* 2012;22(2):107-16.
11. Whiting PF, Rutjes AW, Westwood ME, et al. QUADAS-2: a revised tool for the quality assessment of diagnostic accuracy studies. *Ann Intern Med* 2011;155(8):529-36.
12. Sakamoto J, Yoshino N, Okochi K, et al. Tissue characterization of head and neck lesions using diffusion-weighted MR imaging with SPLICE. *Eur J Radiol* 2009;69(2):260-8.
13. Srinivasan A, Dvorak R, Perni K, Rohrer S, Mukherji SK. Differentiation of benign and malignant pathology in the head and neck using 3T apparent diffusion coefficient values: early experience. *AJNR Am J Neuroradiol* 2008;29(1):40-4.
14. Wang J, Takashima S, Takayama F, et al. Head and neck lesions: characterization with diffusion-weighted echo-planar MR imaging. *Radiology* 2001;220(3):621-30.
15. de Bondt RB, Hoerberigs MC, Nelemans PJ, et al. Diagnostic accuracy and additional value of diffusion-weighted imaging for discrimination of malignant cervical lymph nodes in head and neck squamous cell carcinoma. *Neuroradiology* 2009;51(3):183-92.
16. Dirix P, Vandecaveye V, De Keyzer F, et al. Diffusion-weighted MRI for nodal staging of head and neck squamous cell carcinoma: impact on radiotherapy planning. *Int J Radiat Oncol Biol Phys* 2010;76(3):761-6.
17. Vandecaveye V, De Keyzer F, Vander Poorten V, et al. Head and neck squamous cell carcinoma: value of diffusion-weighted MR imaging for nodal staging. *Radiology* 2009;251(1):134-46.
18. Abdel Razek AA, Kandeel AY, Soliman N, et al. Role of diffusion-weighted echo-planar MR imaging in differentiation of residual or recurrent head and neck tumors and posttreatment changes. *AJNR Am J Neuroradiol* 2007;28(6):1146-52.
19. Gouhar G, El-Hariri M. Feasibility of diffusion weighted MR imaging in differentiating recurrent laryngeal carcinoma from radionecrosis. *The Egyptian Journal of Radiology and Nuclear Medicine* 2011(42):169-175.
20. Vandecaveye V, De Keyzer F, Nuyts S, et al. Detection of head and neck squamous cell carcinoma with diffusion weighted MRI after (chemo)radiotherapy: correlation between radiologic and histopathologic findings. *Int J Radiat Oncol Biol Phys* 2007;67(4):960-71.

21. Tshering Vogel DW, Zbaeren P, Geretschlaeger A, Vermathen P, De Keyzer F, Thoeny HC. Diffusion-weighted MR imaging including bi-exponential fitting for the detection of recurrent or residual tumour after (chemo)radiotherapy for laryngeal and hypopharyngeal cancers. *Eur Radiol* 2012.
22. Rumboldt Z, Gordon L, Bonsall R, Ackermann S. Imaging in head and neck cancer. *Curr Treat Options Oncol* 2006;7(1):23-34.
23. Fong D, Bhatia KS, Yeung D, King AD. Diagnostic accuracy of diffusion-weighted MR imaging for nasopharyngeal carcinoma, head and neck lymphoma and squamous cell carcinoma at the primary site. *Oral Oncol* 2010;46(8):603-6.
24. Branstetter BFT, Blodgett TM, Zimmer LA, et al. Head and neck malignancy: is PET/CT more accurate than PET or CT alone? *Radiology* 2005;235(2):580-6.
25. Al-Ibraheem A, Buck A, Krause BJ et al. Clinical applications of FDG PET and PET/CT in head and neck cancer. *J Oncol*. 2009;2009:208725.
26. Nahmias C, Carlson ER, Duncan LD, et al. Positron emission tomography/computerized tomography (PET/CT) scanning for preoperative staging of patients with oral/head and neck cancer. *Journal of Oral and Maxillofacial Surgery*. 2007;65(12):2524–2535
27. Schöder H, Yeung HW. Positron emission imaging of head and neck cancer, including thyroid carcinoma. *Seminars in Nuclear Medicine*. 2004;34(3):180–197.
28. Jeong HS, Baek CH, Son YI, et al. Use of integrated 18F-FDG PET/CT to improve the accuracy of initial cervical nodal evaluation in patients with head and neck squamous cell carcinoma. *Head Neck* 2007;29(3):203-10.
29. Agra IM, Carvalho AL, Ulbrich FS, et al. Prognostic factors in salvage surgery for recurrent oral and oropharyngeal cancer. *Head Neck* 2006;28(2):107-13.
30. Terhaard CH, Bongers V, van Rijk PP, Hordijk GJ. F-18-fluoro-deoxy-glucose positron-emission tomography scanning in detection of local recurrence after radiotherapy for laryngeal/ pharyngeal cancer. *Head Neck* 2001;23(11):933-41.
31. Brouwer J, de Bree R, Comans EF, et al. Improved detection of recurrent laryngeal tumor after radiotherapy using (18)FDG-PET as initial method. *Radiother Oncol* 2008;87(2):217-20.
32. Ryan WR, Fee WE, Jr., Le Q-T, Pinto HA. Positron-emission tomography for surveillance of head and neck cancer. *Laryngoscope*. 2005;115(4):645–650.
33. Abgral R, Querellou S, Potard G, et al. Does ¹⁸F-FDG PET/CT improve the detection of posttreatment recurrence of head and neck squamous cell carcinoma in patients negative for disease on clinical follow-up? *Journal of Nuclear Medicine*. 2009;50(1):24–29
34. McCollum AD, Burrell SC, Haddad RI, et al. Positron emission tomography with 18F-fluorodeoxyglucose to predict pathologic response after induction chemotherapy and definitive chemoradiotherapy in head and neck cancer. *Head Neck* 2004;26(10):890-6.

APPENDIX 1: Background diffusion-weighted imaging.

Diffusion-weighted imaging (DW-MRI) reflects the microanatomy of tissues based the diffusion of water protons. Diffusion of water protons can be examined by sensitizing an MRI sequence with 2 equal but opposing gradients. Magnetization of protons are dephased by the first gradient and rephased by the second gradient. Motion of non-stationary water molecules in tissues between the 2 opposing gradients will result in incomplete rephrasing, which is translated in a loss of signal in the images. A DW-MRI sequence's diffusion sensitivity (e.g., b-value) is determined by the strength, duration and time interval between the opposing gradients. The higher the b-value, the more sensitive the technique is to the effects of diffusion. By repeating the sequence with consecutive and increasing b-values, the progressive signal decay over the images with increasing b-value can be quantified using the apparent diffusion coefficient (ADC). Hereby, ADC provides an objective measure of the diffusivity of water protons. As tumors generally present with higher cellularity, they will present greater diffusion restriction and, consequently, a lower ADC compared to normal tissues. (6,7,9) Figure 1 shows a typical example of DW-MRI of a patient with an oropharyngeal carcinoma.

APPENDIX 2: Search query September 2012.

(oncology [Title/Abstract]) OR (oncological [Title/ Abstract]) OR (tumor [Title/Abstract]) OR (tumors [Title/ Abstract]) OR (tumours [Title/Abstract]) OR tumour [Title/Abstract]) OR (carcinoma [Title/Abstract]) OR (carcinomas [Title/Abstract]) OR (cancer [Title/Abstract]) OR (cancers [Title/Abstract]) OR (malignancy [Title/ Abstract]) OR (malignancies [Title/ Abstract]) OR (neoplasm [Title/Abstract]) OR (SCC [Title/Abstract]) OR (SCCS [Title/ Abstract]) OR (malignant [Title/Abstract]) OR (cancerous [Title/Abstract]) OR (malignance [Title/ Abstract]) OR (neoplasms [Title/Abstract]) AND (head and neck [Title/Abstract]) OR (larynx [Title/Abstract]) OR (laryngeal [Title/Abstract]) OR (hypopharynx [Title/ Abstract]) OR (hypopharyngeal [Title/Abstract]) OR (oral cavity [Title/Abstract]) OR (oropharynx [Title/ Abstract]) OR (oropharyngeal [Title/Abstract]) OR (glottic [Title/ Abstract]) OR (subglottic [Title/Abstract]) OR (supraglottic [Title/Abstract]) OR (glottis [Title/Abstract]) OR (supraglottis [Title/Abstract]) OR (subglottis [Title/ Abstract]) OR (otolaryngology [Title/Abstract]) OR (otorhinolaryngology [Title/Abstract]) OR (nasopharynx [Title/Abstract]) OR (nasopharyngeal [Title/Abstract]) OR (nasopharynx [Title/Abstract]) OR (rhinopharynx [Title/ Abstract]) OR (nasopharynges [Title/Abstract]) OR (rhinopharynges [Title/Abstract]) OR (otolaryngologic [Title/ Abstract]) OR (otolaryngological [Title/Abstract]) OR (Neoplasms [Mesh]) AND (Larynx [Mesh]) OR (Pharynx [Mesh]) OR (Otolaryngology [Mesh]) OR (Head and Neck Neoplasms [Mesh]) OR (HNSCC [Title/Abstract]) OR (cervical lymph nodes [Title/Abstract]) OR (cervical lymph node [Title/Abstract]) AND (diffusion [Title/ Abstract]) OR (DWI [Title/Abstract]) OR (DW imaging [Title/Abstract]) OR (DW-MRI [Title/Abstract]) OR (Diffusion Magnetic Resonance Imaging [Mesh])

- R1
- R2
- R3
- R4
- R5
- R6
- R7
- R8
- R9
- R10
- R11
- R12
- R13
- R14
- R15
- R16
- R17
- R18
- R19
- R20
- R21
- R22
- R23
- R24
- R25
- R26
- R27
- R28
- R29
- R30
- R31
- R32
- R33
- R34
- R35
- R36
- R37
- R38
- R39





4

Diffusion-weighted MR imaging in laryngeal and hypopharyngeal carcinoma: Association between apparent diffusion coefficient and histologic findings

J.P. Driessen
J. Caldas-Magalhaes
L.M. Janssen
F.A. Pameijer
N. Kooij
C.H.J. Terhaard
W. Grolman
M.E.P. Philippens

Radiology. 2014 Aug;272(2):456-63

Abstract

Purpose: To investigate the relationship between the histologic characteristics of head and neck squamous cell carcinoma and apparent diffusion coefficient (ADC) at diffusion-weighted magnetic resonance (MR) imaging.

Materials and Methods: The institutional ethics committee approved this study and waived informed consent. In head and neck squamous cell carcinoma, local failure after chemotherapy and/or radiation therapy correlates with pretreatment ADC. However, the histopathologic basis of this correlation remains unclear. In this study, 16 patients with head and neck squamous cell carcinoma were enrolled (median age, 60 years; range, 49-78 years). Before undergoing total laryngectomy, patients underwent 1.5-T diffusion-weighted MR imaging. After resection, whole-mount hematoxylin-eosin stained sections were registered to the MR images. Cellular density; nuclear, cytoplasmic, and stromal area; and nuclear-cytoplasmic ratio within the tumor were calculated by using image-based segmentation on four consecutive slices. Mean ADC of the corresponding tumor region was calculated. Spearman correlations between ADC and histologic characteristics were calculated.

Results: ADC was significantly and inversely correlated with cell density ($n = 16$, $r = -0.57$, $P = .02$), nuclear area ($n = 12$, $r = -0.64$, $P = .03$), and nuclear-cytoplasmic ratio ($n = 12$, $r = -0.77$, $P \leq .01$). ADC was significantly and positively correlated with percentage area of stroma ($n = 12$, $r = 0.69$, $P = .01$). Additionally, the percentage area of stroma was strongly interdependent with the percentage area of nuclei ($n = 12$, $r = -0.97$, $P \leq .01$).

Conclusion: ADC was significantly correlated with cellularity, stromal component, and nuclear-cytoplasmic ratio. The positive correlation of ADC and stromal component suggests that the poor prognostic value of high pretreatment ADC might partly be attributed to the tumor-stroma component, a known predictor of local failure.

Advances in knowledge:

- Apparent diffusion coefficient (ADC) was positively related to the percentage area of stroma ($r = 0.69$, $P = .01$).
- ADC was negatively related to the absolute number of cells per square millimeter ($r = -0.57$, $P = .02$), the percentage area of nuclei ($r = -0.64$, $P = .03$), and the nuclear-cytoplasmic ratio ($r = -0.77$, $P \leq .01$).

Implications for patient care:

- Pretreatment ADC and corresponding microanatomic parameters are related, which may improve the interpretation of diffusion-weighted MR images.
- The reported poor prognostic value of high pretreatment ADC in head and neck squamous cell carcinoma might be explained by the corresponding high stromal content of the tumor.

Introduction

In head and neck squamous cell carcinomas, magnetic resonance (MR) imaging is increasingly used because it provides excellent soft-tissue contrast in this complex and heterogeneous region. Besides conventional anatomic images, there is a rising trend toward additional functional MR imaging, such as diffusion-weighted imaging (DW-MRI), for further characterization of tissues. (1) DW-MRI is an established imaging technique in the early detection of acute stroke, and it is gaining increasing importance in several oncologic applications. (2) DW-MRI is used to quantify the diffusional motion of water with the apparent diffusion coefficient (ADC). As such, the ADC provides information about the microenvironment of tissues. (3,4) DW-MRI has proven to be highly accurate in the differentiation of benign from malignant lesions, and it can be used for tissue characterization of primary tumors and metastasis. (5–7) DW-MRI seems particularly promising in the prediction of tumor radiosensitivity and the early assessment of treatment response, since high pretreatment ADC has been shown to be correlated with local failure of chemotherapy and/or radiation therapy and might therefore become an important application for treatment personalization. (8–13)

A number of variables are presumed to influence the mobility of water protons. Commonly, the restriction of water molecules in tumors is attributed to increased cellular density (CD) and decreased interstitial space. (14–16) However, perfusion, tortuosity of the extracellular space, and integrity of cellular membranes affect diffusivity. In prostate tissue and central nervous system lymphomas, an inverse correlation between ADC and CD has been found. (15–18) However, limited studies have been conducted to investigate the relationship between ADC and other microanatomic features, and the histopathologic basis of the association between high ADC and local failure remains unclear. (19,20)

The aim of this study was to investigate the relationship between histologic characteristics of head and neck squamous cell carcinoma and ADC.

Materials and Methods

Patients

The institutional ethics committee approved this study and waived informed consent. Eighteen consecutive patients were enrolled between June 2009 and April 2011 as part of an ongoing study, and all data were reviewed retrospectively. Inclusion criteria were biopsy proven laryngeal or hypopharyngeal squamous cell carcinoma without prior treatment, stage T3 or T4 disease, and planned curative total laryngectomy with or without partial pharyngectomy. Before surgery, patients underwent a 1.5-T MR imaging examination that included DW-MRI. Two patients were excluded from analysis, owing to failure of the histologic section

R1 preparation (n = 1) or incomplete DW-MRI protocol (n = 1). Sixteen patients remained for
R2 analysis. Eight patients (50%) were included in our previous publication on the development
R3 of the registration method for the imaging validation study by Caldas-Magalhaes et al. (21)
R4

R5 **MR Imaging Protocol**

R6 Before undergoing surgery, all patients underwent MR imaging performed with a 1.5-T MR
R7 imaging system (Intera; Philips Medical Systems) with a small, two-element flexible surface
R8 receiver coil. MR sequences included T1-weighted imaging before and after administration
R9 of gadolinium-based contrast agent (repetition time msec/echo time msec, 593/15) and T2-
R10 weighted (4200/130) imaging. DW-MRI images were obtained by using a multisection single-
R11 shot spin-echo echo-planar imaging sequence, with short inversion time inversion-recovery
R12 fat suppression (5872/70, inversion time of 180 msec, four signals acquired, field of view of
R13 25 x 20 cm², section thickness of 4 mm, acquisition matrix of 121 x 101 mm², intersection gap
R14 of 0 mm, and b-values of 0, 150, and 800 sec/mm²). ADC values were calculated with b-values
R15 of 150 and 800 sec/mm². The median time interval between MR imaging and surgery was 9
R16 days (range, 1–34 days).
R17

R18 **Whole-Mount Histologic Section Preparation**

R19 Histologic section preparation and imaging registration were described previously. (21)
R20 Briefly, the following steps were performed. After surgery, the fresh surgical specimen was
R21 fixed in 10% formaldehyde for at least 48 hours. After fixation, computed tomography of
R22 the specimen was performed. Subsequently, to prevent deformations during the slicing
R23 procedure, the specimen was solidified in 5% agarose before it was sliced in 3-mm thick
R24 slices and photographed. Special attention was paid to the orientation of the specimen in
R25 the agarose block, so that the slice direction was comparable to the pre-surgical images.
R26 Finally, after removal of the agarose and decalcification, 4-mm whole-mount microscopic
R27 slices were cut from the macroscopic slices and stained with hematoxylin-eosin (H-E) with
R28 standard histologic procedure. Cross-sectional area of the tumor was outlined on the H-E
R29 sections by an experienced pathologist (N.K., with 6 years of experience).
R30

R31 **Registration of MR Images and Pathologic Specimens**

R32 The MR images were registered semi automatically to the H-E sections as described
R33 previously. (21. Briefly, each H-E section was first registered to the corresponding
R34 photographed macroscopic slice. Second, a three-dimensional specimen was reconstructed
R35 from the stacked photographs of the macroscopic slices, and, finally, the reconstructed three-
R36 dimensional specimen was registered to the T1-weighted MR images after gadolinium-based
R37 contrast material administration by using the outlining of the thyroid and cricoid cartilage
R38 as a reference. The DW-MRI MR sections were registered by using the same transformation
R39

as that used for the T1-weighted MR images. This method provides a highly accurate three-dimensional registration, with a mean error of 3 mm in the axial plane owing to registration errors and specimen deformation. (21)

Selection of Regions of Interest

Four consecutive microscopic slides per patient, containing the largest tumor diameter, were chosen for further analysis and digitized at histologic resolution (objective magnification, $\times 20$) (ScanScope XT bright-field scanner; Aperio Technologies, Vista, Calif). The corresponding level of DW-MRI sections was identified by using the three-dimensional registration. DW-MRI sections have geometric distortions compared with native MR images, but only in the phase-encoded direction (anterior-posterior direction). Therefore, we could not transfer the delineation of the pathologist directly from the H-E sections to the DW-MRI sections. The tumor was thus manually delineated on images with a b-value of 0 sec/mm² by using the additional information from all other MR images by two physicians in consensus, independent of the delineation of the pathologist (J.P.D., a resident otorhinolaryngologist with 2 years of experience in DW-MRI; and F.A.P., a radiologist with more than 15 years of experience in head and neck radiology). Figure 1 shows an H-E section, including the pathologists' delineation, registered to the MR images and the manual delineation of the DW-MRI on the corresponding level.

Microanatomic Parameters from H-E Sections

Microanatomic analysis was performed on the cross-sectional tumor area, delineated by the pathologist on the four selected consecutive H-E sections per patient. The absolute number of cell nuclei (the CD) within the tumor was identified by using the IHC Nuclear Algorithm v8 in ImageScope v10.0 (Aperio Technologies) in the region delineated by the pathologist. The nuclear algorithm is based on color, size, shape, and surroundings nuclei (negative setting 1). (19) Finally, the nuclear-cytoplasmic (NC) ratio was calculated.

Statistical Analysis

For each tumor, median ADC, CD, and proportion of cellular components were calculated. Spearman correlation coefficients were calculated. The Student *t* test was used to test the difference between ADC values in different histologic tumor grades. Two-tailed *P* values of up to .05 were considered to indicate a significant difference. For the correlation of simultaneously tested hypotheses (percentage area of nuclei, stroma, and cytoplasm and the NC ratio), the Holm-Bonferroni adjustment for multiple comparisons was used (GraphPad Prism 6; GraphPad, La Jolla, Calif).

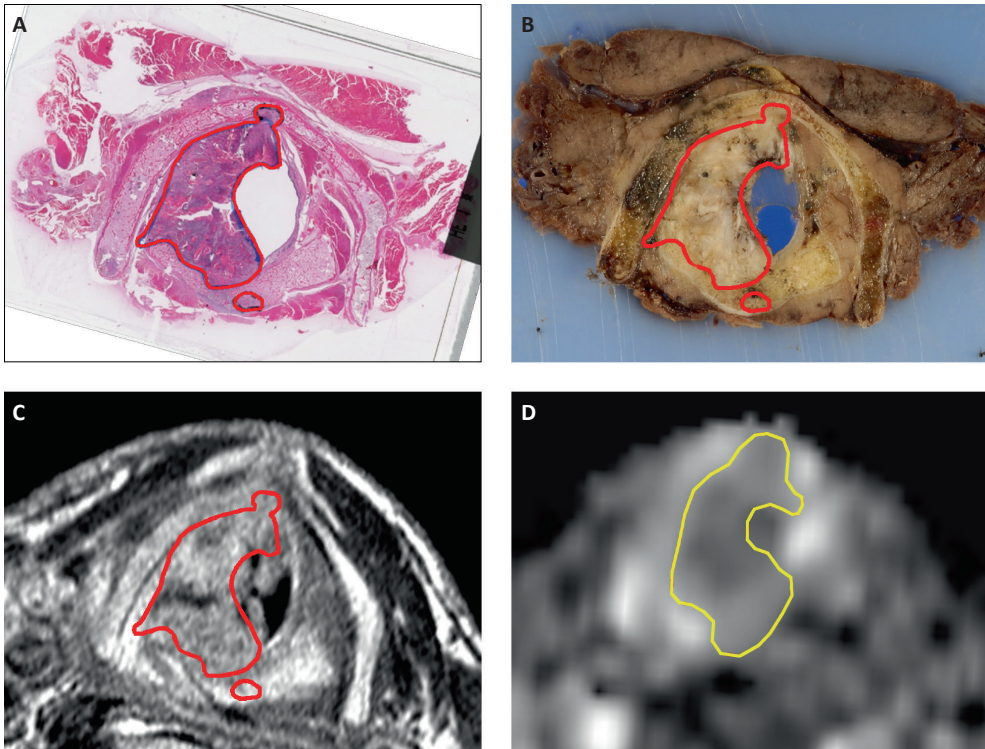


FIGURE 1. Images show DWI sections registered with pathologic and histologic specimens from a 78-year-old man with a T3 glottic carcinoma. The tumor is depicted in **(a)** the whole-mount digitized H-E section, **(b)** the corresponding macroscopic slice of the specimen, **(c)** the axial registered T1-weighted MR image acquired after injection of gadolinium-based contrast material, and **(d)** the ADC map. The delineation made by the pathologist on the H-E section (red outlines on **a**) was transferred to the MR image with an error of less than 3 mm to ensure the corresponding level of the DWI. A manual delineation was made on the DWI ($b = 0 \text{ mm/sec}^2$) section on the corresponding level, and ADC values were calculated (yellow outline on **d**).

Results

Sixteen patients were eligible for analysis of the CD. For the analyses of the cellular components with a color based segmentation method, 12 patients were eligible, as four patients were excluded because poor staining intensity hindered reliable separation of cytoplasm and nuclei. Patients' clinical characteristics are summarized in table 1.

TABLE 1. Patient characteristics

Characteristic	Value	
Age (y)*	60	(49-78)
Site †		
Supraglottic	6	(38)
Glottis	2	(13)
Transglottic	3	(18)
piriform sinus	5	(31)
Pathological tumor stage †		
T3	3	(18)
T4a	12	(75)
T4b	1	(6)
Differentiation †		
moderately	9	(56)
poorly	7	(44)
Interval MRI and surgery (days)*	9	(1-34)

Note. Unless specified otherwise, data are numbers of patients, with percentages in parentheses.

* Data are median values, with ranges in parentheses.

Figure 2 shows a typical example of the automatic segmentation on the H-E sections. The mean ADC of tumors showed wide variation, with a range of $(0.92-1.30) \times 10^{-3} \text{ mm}^2/\text{sec}$. ADC heterogeneity also varied widely among tumors, with a standard deviation range of $(0.15-0.34) \times 10^{-3} \text{ mm}^2/\text{sec}$. Table 2 displays the mean values of the microanatomic parameters and the Spearman correlations with ADC and with each other. ADC was significantly and inversely correlated to the CD, the nuclear area, and the NC ratio. ADC was significantly and positively correlated with the stromal area (figure 3). No significant correlation was found between ADC and cytoplasmic area.

TABLE 2. Microanatomical parameters and correlation with ADC

Parameter	CD (n=16)	Percentage Nuclei Area (n=12)	Percentage Cytoplasm Area (n=12)	Percentage Stroma Area (n=12)	N/C ratio (n=12)
Mean (range)	6406 (4806-8050)	43.1 (24.1-70.2)	19.6 (11.2-27.1)	39.6 (14.0-75.8)	2.4 (1.1-4.7)
Correlation with ADC					
<i>r</i> (<i>p</i> value)	- 0.57 (0.02)	- 0.66 (0.02)	0.45 (0.15)	0.68 (0.02)	- 0.78 (<0.01)
Correlation with percentage nuclei					
<i>r</i> (<i>p</i> value)	-	1.000	-0.01 (0.97)	-0.97 (<0.01)	0.64 (0.03)

Note. CD: absolute number of cells per mm^2 , *r*: Spearman's rho, N/C ratio: nuclear-cytoplasmic ratio

* Unless specified otherwise, data are mean values, with ranges in parentheses.

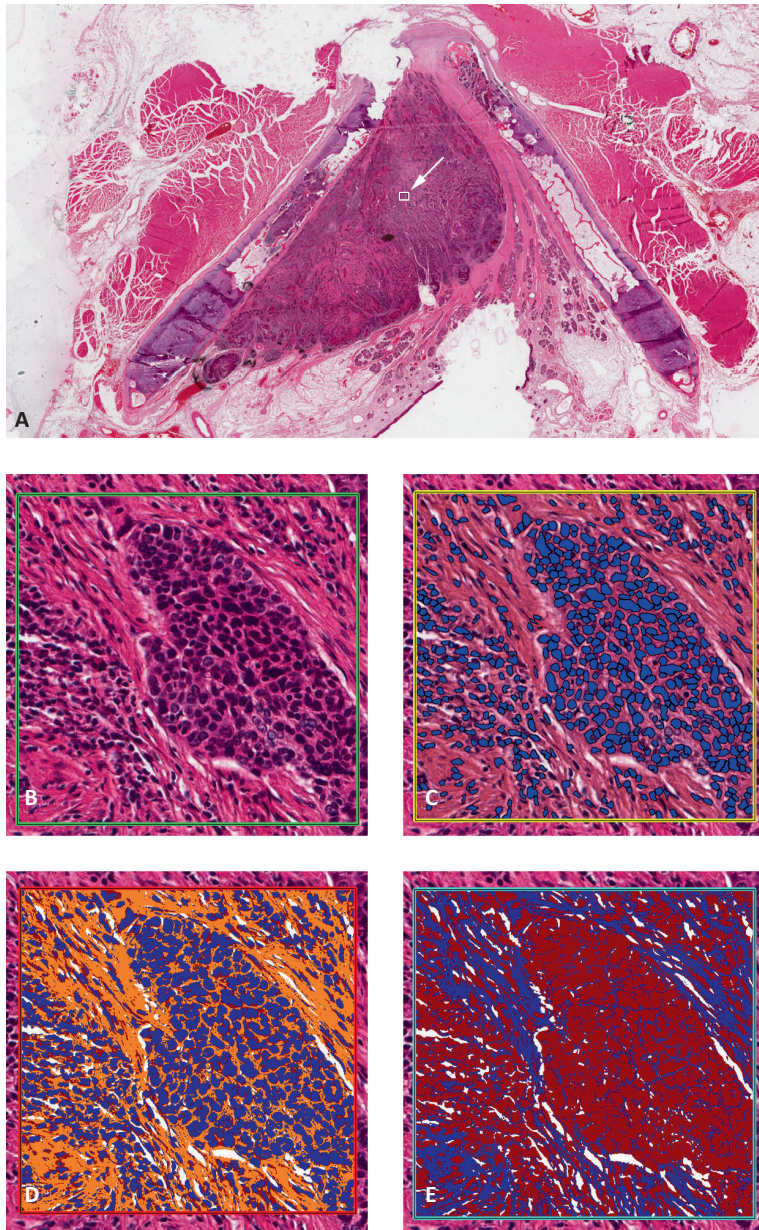


FIGURE 2. (a) Digitized whole-mount H-E section from a 70-year-old man with a T4 supraglottic laryngeal carcinoma. **b-e:** Original magnification, X20 of a random region within the tumor (arrow on a). **(b)** Microanatomic parameters were segmented automatically within the tumor. **(c)** The absolute number of cells (blue, IHC Nuclear Algorithm; Aperio Technologies), **(d)** percentage area of nuclei (blue, Positive Pixel Count Algorithm setting 1), and **(e)** percentage area of stroma (blue, Positive Pixel Count Algorithm setting 2) were segmented by using different algorithm settings. From these, the percentage area of cytoplasm (red area on **e** minus blue area on **d**) and NC ratio were calculated.

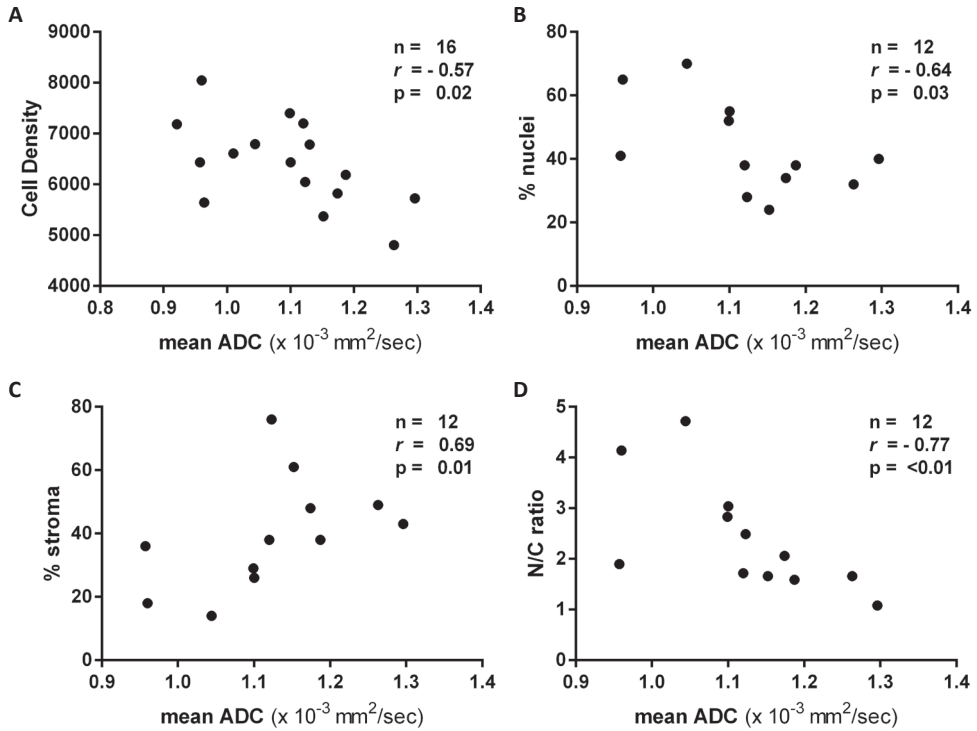


FIGURE 3. Plots show the correlation of mean ADC with (a) CD, (b) nuclear area, (c) stromal area, and (d) NC (N/C) ratio. Correlations were calculated with a nonparametric test. *r* : Spearman rho statistic.

Additionally, nuclear and stromal areas were very strongly and inversely correlated. This correlation shows their interdependence, although they result from different algorithm settings.

Figure 4 (A-C) shows examples of three tumors with different tissue microanatomy, the corresponding CD, ratios of cellular components, and ADC values. All tumors showed less than 5% necrosis (range, 1%-5%), and moderately differentiated tumors showed no difference in ADC compared with poorly differentiated tumors ((1.13 vs 1.05) x 10⁻³ mm²/sec; *P* = .20).

R1
R2
R3
R4
R5
R6
R7
R8
R9
R10
R11
R12
R13
R14
R15
R16
R17
R18
R19
R20
R21
R22
R23
R24
R25
R26
R27
R28
R29
R30
R31
R32
R33
R34
R35
R36
R37
R38
R39

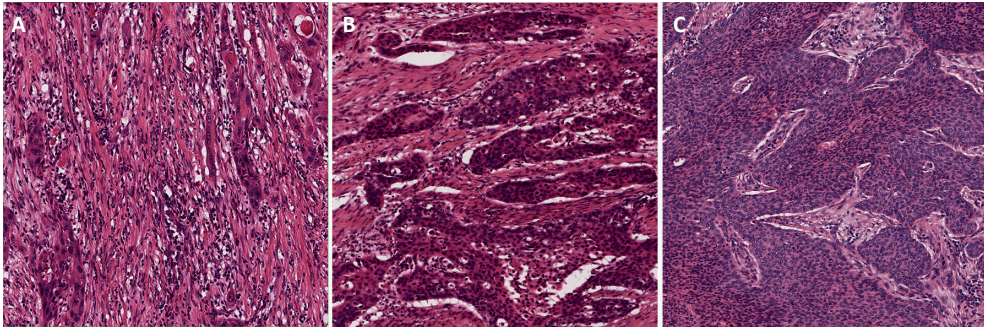


FIGURE 4. Digitized whole-mount H-E section (original magnification, X10) with different cell densities. **(a)** T4a laryngeal carcinoma. The tumor shows a low CD of 4806 cells per mm^2 , 32% nuclear area, 49% stromal area, NC ratio of 1.66, and high ADC of $1.26 \times 10^{-3} \text{ mm}^2/\text{sec}$. **(b)** T3 hypopharyngeal carcinoma. The tumor shows an intermediate CD of 6188 cells per mm^2 , 38% nuclear area, 38% stromal area, NC ratio of 1.59, and intermediate ADC of $1.19 \times 10^{-3} \text{ mm}^2/\text{sec}$. **(c)** T4a laryngeal carcinoma. The tumor shows a high CD of 8050 cells per mm^2 , 65% nuclear area, 18% stromal area, NC ratio of 4.14, and intermediate ADC of $0.96 \times 10^{-3} \text{ mm}^2/\text{sec}$.

Discussion

Exploration of the relationship between tissue microanatomy and ADC is of great importance to improve interpretation of DW-MRI findings and clarify the predictive value of ADC in treatment response.

In this study, we found a significant and inverse correlation between ADC and CD of moderate strength. Nuclear area and the NC ratio showed moderate to strong inverse correlation with ADC, and stromal area showed a moderate to strong positive correlation. Additionally, nuclear and stromal area showed strong interdependence.

The inverse correlation between ADC and CD reinforces the model that higher cellularity, with cells packed more densely, causes restriction of water diffusion. This inverse correlation has been reported previously in prostate cancer and lymphomas. (15–18) However, previous reports were limited to the percentage area of nuclei solely. Although the percentage area of nuclei is partly determined by the absolute number of cells, it is also influenced by the size of the nuclei, whereas CD is independent of nuclear size. The correlation between ADC and CD has been investigated previously by Barajas et al in central nervous system lymphomas by means of manual cell count from a core biopsy sample. (15) In that study, however, no registration was performed between pathologic specimens and imaging. Therefore, accurate location of the biopsy within the tumor was not taken into account. In squamous cell carcinomas of the head and neck, which are known for their heterogeneity, this method would be inappropriate. Instead, in our study, we used four consecutive whole-mount histologic sections, registered to MR images with a highly accurate and validated registration technique. (21) This method had a mean error of only 3 mm.

In contrast to prior literature, our study extended beyond tissue cellularity by including the investigation of numerous other tissue components. We found a moderate to strong significantly positive correlation of ADC and stromal area. Stromal area generally has more extracellular volume compared with a tumor with dense cellularity. A very strong interdependence between percentage area of nuclei and stroma was seen, which indicates that cellularity and stromal area were indistinguishable and interchangeable. The strong correlation between percentage area of nuclei and stroma might call into question the methodological independence; however, the two variables were calculated by using the Positive Pixel Count algorithm with different settings. Also, we found NC ratio to have a strong negative correlation with ADC, compared with the percentage area of nuclei. This NC ratio might be interpreted as the amount of cytoplasm per cell. The inverse correlation suggests that tumors with high NC ratio are likely to have densely packed cells with only a limited amount of cytoplasm, reflected by a low ADC.

Several studies have been conducted to investigate the prognostic value of ADC for determination of pre-therapeutic tumor radiosensitivity, and a high ADC was reported to be predictive for local nonresponders. (8,9) It is often hypothesized that this is due to necrotic parts within the tumor. Our study is the first to prove that low CD reflects a large stromal area that contributes to relatively high ADC values. Stromal component has shown to be an independent prognostic factor for a relapse-free period in several tumors, such as breast cancer, colon cancer, and esophageal squamous cell carcinoma. (23–27) Furthermore, it has been described that stromal cells play an important role in the support of tumor growth by promoting invasion and protection from apoptosis and potentially creating barriers to deliver systemic chemotherapy. (28–30) This might suggest that the poor prognostic value of a high pretreatment ADC might be partly attributed to the tumor-stromal component. In our study, we found no significant association between histologic tumor grade and mean ADC, although a trend was observed toward lower ADC values in poorly differentiated tumors compared with moderately differentiated tumors. The small sample size and the small variety in differentiation grade hamper the acquisition of significant results. However, a similar trend was reported recently. (31) In addition, all tumors showed less than 5% necrosis. Therefore, necrosis was not excluded or treated as a separate parameter.

Our study had several limitations. One limitation of this work was that the DW-MRI was affected by anterior-posterior geometrical distortions. To overcome this, the tumor was manually delineated on the DW-MRI sections on the corresponding cranio-caudal level. Clearly, a nonrigid registration method would have been preferable, enabling a voxel-based analysis that included analysis of tissue surrounding the tumor. The color-based segmentation and the usage of identical settings for all patients served to remove a large element of subjectivity and potential bias. The drawback of this method is that staining variability is not taken into account. For the absolute number of cells, we used an automatic segmentation technique

R1 with a 9.6% bias and a standard deviation of 11.4%, which we considered acceptable. This
R2 introduces some uncertainty in our data. Another limitation was that the number of patients
R3 was small, especially for the color-based segmentation, where four patients had to be
R4 excluded because of poor staining intensity. Still, even with this limited number of patients,
R5 we found significant correlations between ADC and tissue components.

R6 In conclusion, individual tissue components in laryngeal and hypopharyngeal squamous
R7 cell carcinomas significantly affected ADC. ADC inversely correlated with CD, nuclear area,
R8 and NC ratio and positively correlated with stromal area. Additionally, nuclear and stromal
R9 areas showed strong interdependence. These results give us insights into how ADC reflects
R10 the underlying microenvironment of laryngeal and hypopharyngeal cancers. The positive
R11 correlation of ADC and stromal component suggests that the poor prognostic value of high
R12 pretreatment ADC might partly be attributed to the tumor-stroma component, a known
R13 predictor of local failure.

R14 **Acknowledgment**

R15
R16 The authors thank Dr S. Willems, from the Department of Pathology, for his special help
R17 during the revision of this manuscript.
R18
R19
R20
R21
R22
R23
R24
R25
R26
R27
R28
R29
R30
R31
R32
R33
R34
R35
R36
R37
R38
R39

1. Padhani AR. Diffusion magnetic resonance imaging in cancer patient management. *Semin Radiat Oncol* 2011; 21:119-140.
2. Koh DM, Padhani AR. Diffusion-weighted MRI: a new functional clinical technique for tumour imaging. *Br J Radiol* 2006; 79:633-635.
3. Koh DM, Collins DJ. Diffusion-weighted MRI in the body: applications and challenges in oncology. *AJR Am J Roentgenol* 2007; 188:1622-1635.
4. Thoeny HC. Diffusion-weighted MRI in head and neck radiology: applications in oncology. *Cancer Imaging* 2011; 10:209-214.
5. Srinivasan A, Dvorak R, Perni K, Rohrer S, Mukherji SK. Differentiation of benign and malignant pathology in the head and neck using 3T apparent diffusion coefficient values: early experience. *AJNR Am J Neuroradiol* 2008; 29:40-44.
6. Vandecaveye V, De Keyzer F, Vander Poorten V, et al. Head and neck squamous cell carcinoma: value of diffusion-weighted MR imaging for nodal staging. *Radiology* 2009; 251:134-146.
7. Wang J, Takashima S, Takayama F, et al. Head and neck lesions: characterization with diffusion-weighted echo-planar MR imaging. *Radiology* 2001; 220:621-630.
8. Hatakenaka M, Nakamura K, Yabuuchi H, et al. Pretreatment apparent diffusion coefficient of the primary lesion correlates with local failure in head-and-neck cancer treated with chemoradiotherapy or radiotherapy. *Int J Radiat Oncol Biol Phys* 2011; 81:339-345.
9. Thoeny HC, Ross BD. Predicting and monitoring cancer treatment response with diffusion-weighted MRI. *J Magn Reson Imaging* 2010; 32:2-16.
10. Vandecaveye V, Dirix P, De Keyzer F, et al. Predictive value of diffusion-weighted magnetic resonance imaging during chemoradiotherapy for head and neck squamous cell carcinoma. *Eur Radiol* 2010; 20:1703-1714.
11. Hatakenaka M, Shioyama Y, Nakamura K, et al. Apparent diffusion coefficient calculated with relatively high b-values correlates with local failure of head and neck squamous cell carcinoma treated with radiotherapy. *AJNR Am J Neuroradiol* 2011; 32:1904-1910.
12. Lambrecht M, Vandecaveye V, De Keyzer F, et al. Value of diffusion-weighted magnetic resonance imaging for prediction and early assessment of response to neoadjuvant radiochemotherapy in rectal cancer: preliminary results. *Int J Radiat Oncol Biol Phys* 2012; 82:863-870.
13. Vandecaveye V, Dirix P, De Keyzer F, et al. Diffusion-weighted magnetic resonance imaging early after chemoradiotherapy to monitor treatment response in head-and-neck squamous cell carcinoma. *Int J Radiat Oncol Biol Phys* 2012; 82:1098-1107.
14. Lambrecht M, Dirix P, Vandecaveye V, De Keyzer F, Hermans R, Nuyts S. Role and value of diffusion-weighted MRI in the radiotherapeutic management of head and neck cancer. *Expert Rev Anticancer Ther* 2010; 10:1451-1459.
15. Barajas RF, Jr., Rubenstein JL, Chang JS, Hwang J, Cha S. Diffusion-weighted MR imaging derived apparent diffusion coefficient is predictive of clinical outcome in primary central nervous system lymphoma. *AJNR Am J Neuroradiol* 2010; 31:60-66.
16. Gibbs P, Liney GP, Pickles MD, Zelhof B, Rodrigues G, Turnbull LW. Correlation of ADC and T2 measurements with cell density in prostate cancer at 3.0 Tesla. *Invest Radiol* 2009; 44:572-576.
17. Zelhof B, Pickles M, Liney G, et al. Correlation of diffusion-weighted magnetic resonance data with cellularity in prostate cancer. *BJU Int* 2009; 103:883-888.
18. Wang XZ, Wang B, Gao ZQ, et al. Diffusion-weighted imaging of prostate cancer: correlation between apparent diffusion coefficient values and tumor proliferation. *J Magn Reson Imaging* 2009; 29:1360-1366.
19. Langer DL, van der Kwast TH, Evans AJ, et al. Prostate tissue composition and MR measurements: investigating the relationships between ADC, T2, K(trans), v(e), and corresponding histologic features. *Radiology* 2010; 255:485-494.

- R1
- R2
- R3
- R4
- R5
- R6
- R7
- R8
- R9
- R10
- R11
- R12
- R13
- R14
- R15
- R16
- R17
- R18
- R19
- R20
- R21
- R22
- R23
- R24
- R25
- R26
- R27
- R28
- R29
- R30
- R31
- R32
- R33
- R34
- R35
- R36
- R37
- R38
- R39
20. Ichikawa Y, Sumi M, Sasaki M, Sumi T, Nakamura T. Efficacy of diffusion-weighted imaging for the differentiation between lymphomas and carcinomas of the nasopharynx and oropharynx: correlations of apparent diffusion coefficients and histologic features. *AJNR Am J Neuroradiol* 2012; 33:761-766.
 21. Caldas-Magalhaes J, Kasperts N, Kooij N, et al. Validation of imaging with pathology in laryngeal cancer: accuracy of the registration methodology. *Int J Radiat Oncol Biol Phys* 2012; 82:e289-298.
 22. Borren A, Moman MR, Groenendaal G et al. Why prostate tumour delineation based on apparent diffusion coefficient is challenging: An exploration of the tissue microanatomy. *Acta Oncologica* 2013; early online; 1-8
 23. Wang K, Ma W, Wang J, et al. Tumor-stroma ratio is an independent predictor for survival in esophageal squamous cell carcinoma. *J Thorac Oncol* 2012; 7:1457-1461.
 24. de Kruijf EM, van Nes JG, van de Velde CJ, et al. Tumor-stroma ratio in the primary tumor is a prognostic factor in early breast cancer patients, especially in triple-negative carcinoma patients. *Breast Cancer Res Treat* 2011; 125:687-696.
 25. Huijbers A, Tollenaar RA, GW VP, et al. The proportion of tumor-stroma as a strong prognosticator for stage II and III colon cancer patients: validation in the VICTOR trial. *Ann Oncol* 2012. 24(1):179-185.
 26. Wiseman BS, Werb Z. Stromal effects on mammary gland development and breast cancer. *Science* 2002; 296:1046-1049.
 27. Mesker WE, Liefers GJ, Junggeburst JM, et al. Presence of a high amount of stroma and downregulation of SMAD4 predict for worse survival for stage I-II colon cancer patients. *Cell Oncol* 2009; 31:169-178.
 28. Koontongkaew S. The tumor microenvironment contribution to development, growth, invasion and metastasis of head and neck squamous cell carcinomas. *J Cancer*. 2013;4(1):66-83.
 29. Neesse A, Michl P, Frese KK, et al. Stromal biology and therapy in pancreatic cancer. *Gut*. 2011; 60:861-868.
 30. Muller MM, Fusenig NE. Friend or foes bipolar effects of the tumour stroma in cancer. *Nat Rev Cancer* 2004; 4:839-849.
 31. Varoquaux A, Rager O, Lovblad KO et al. Functional imaging of head and neck squamous cell carcinoma with diffusion-weighted MRI and FDG PET/CT: quantitative analysis of ADC and SUV. *Eur J Nucl Med Mol Imaging*. 2013 Jun; 40(6):842-52.

R1
R2
R3
R4
R5
R6
R7
R8
R9
R10
R11
R12
R13
R14
R15
R16
R17
R18
R19
R20
R21
R22
R23
R24
R25
R26
R27
R28
R29
R30
R31
R32
R33
R34
R35
R36
R37
R38
R39

4





5

Correlation of human papillomavirus status with apparent diffusion coefficient of diffusion-weighted MRI in head and neck squamous cell carcinomas

J.P. Driessen
A.J. van Bommel
P.M.W. van Kempen
L.M. Janssen
C.H.J. Terhaard
F.A. Pameijer
S.M. Willems
I. Stegeman
M.E.P. Philippens

Head Neck. 2015 Mar 17. doi: 10.1002/hed.24051.

Abstract

Background: Identification of prognostic patient characteristics in head and neck squamous cell carcinoma (HNSCC) is of great importance. Human papillomavirus (HPV)-positive HNSCCs have favorable response to (chemo)radiotherapy. Apparent diffusion coefficient, derived from diffusion-weighted MRI, has also shown to predict treatment response. The purpose of this study was to evaluate the correlation between HPV status and apparent diffusion coefficient.

Methods: Seventy-three patients with histologically proven HNSCC were retrospectively analyzed. Mean pretreatment apparent diffusion coefficient was calculated by delineation of total tumor volume on diffusion-weighted MRI. HPV status was analyzed and correlated to apparent diffusion coefficient.

Results: Six HNSCCs were HPV-positive. HPV-positive HNSCC showed significantly lower apparent diffusion coefficient compared to HPV-negative. This correlation was independent of other patient characteristics.

Conclusion: In HNSCC, positive HPV status correlates with low mean apparent diffusion coefficient. The favorable prognostic value of low pretreatment apparent diffusion coefficient might be partially attributed to patients with a positive HPV status.

R1
R2
R3
R4
R5
R6
R7
R8
R9
R10
R11
R12
R13
R14
R15
R16
R17
R18
R19
R20
R21
R22
R23
R24
R25
R26
R27
R28
R29
R30
R31
R32
R33
R34
R35
R36
R37
R38
R39

Introduction

Head and neck squamous cell carcinoma (HNSCC) ranks as the fifth cancer worldwide to date. (1) Because of the location of the primary tumor and the involved lymph nodes, surgical options are often hindered by functional losses and social isolation. Hence, patients are increasingly treated with organ-sparing treatments, such as (chemo)radiotherapy. (2) However, despite recent improvements in treatment and diagnostics, the 5-year overall survival remains relatively poor at approximately 50%. (3) In addition, although organ-sparing, all patients suffer from treatment-induced side effects. Therefore, the search for an optimized treatment strategy remains an important point of interest. Although most tumors show regression early after (chemo)radiotherapy, some tumors are nonresponsive to radiation. (4) Pretreatment identification of nonresponders to (chemo)radiation should enable better patient stratification; hopefully leading to improved survival rates and less treatment-induced side effects.

The apparent diffusion coefficient, a quantitative variable derived from diffusion-weighted MRI, seems to be an interesting parameter for pretreatment identification of nonresponders. Diffusion-weighted MRI is a relatively new MRI technique, which quantifies the restriction of random motion of water molecules in tissues by apparent diffusion coefficient. This diffusion coefficient reflects the microenvironment of tissues, in which higher cell density leads to more diffusion restriction of water molecules. (5–7) Apparent diffusion coefficient has shown to be useful in early treatment assessment, in patients treated by (chemo)radiotherapy, and it is also promising in pretreatment prediction of radiotherapy response. (8,9) A low pretreatment apparent diffusion coefficient has shown to correlate with good outcome after treatment with (chemo)radiotherapy. (8,9) A better understanding of the relationship between apparent diffusion coefficient and other prognostic factors is of great importance to understand the predictive value of apparent diffusion coefficient. This might help to comprehend the mechanisms at work at a microcellular level; facilitating the use of apparent diffusion coefficient for pre-therapy stratification, planning, and treatment personalization.

Human papillomavirus (HPV)-positive status in patients with HNSCC is a second patient characteristic that has been linked to a favorable outcome after treatment with (chemo) radiotherapy. (10) This specific subset of tumors exhibits better survival rate in comparison to their HPV-negative counterparts. HPV-positive HNSCC tends to show increased overall survival, as well as progression-free and disease-specific survival. (11–13) The difference in radiotherapy response is caused by the difference in carcinogenesis between HPV-positive and HPV-negative tumors. The most important difference is the inactivation of the tumor suppressor gene TP53 in HPV-positive tumors compared to a mutated TP53 in HPV-negative tumors. Therefore, in HPV-positive tumors TP53 can potentially be reactivated during radiotherapy, resulting in restoration of normal cell cycle control and apoptosis. (14,15) This mechanism results in a better prognosis for HPV-positive tumors.

R1 Patients with low pretreatment apparent diffusion coefficient are more responsive to
R2 treatment with chemoradiotherapy. HPV-associated HNSCC also shows a positive response
R3 to chemoradiotherapy.

R4 The purpose of this study was to investigate the relation between HPV status and apparent
R5 diffusion coefficient.

R6 **Patients and methods**

R7 ***Patient selection***

R8 Patients eligible for this study were those with histologically proven HNSCC treated with
R9 (chemo)radiotherapy between June 2009 and August 2011, who had a diagnostic MRI,
R10 including having a diffusion-weighted MRI sequence available. Inclusion criteria were T2, T3,
R11 and T4 cancers located in the oropharynx, hypopharynx, larynx, or oral cavity. Patients with
R12 T1 cancer were excluded because of inherent low resolution of diffusion-weighted MRI. T and
R13 N classifications were according to the American Joint Committee on Cancer. Clinical charts
R14 were retrospectively reviewed for clinical characteristics. Data were stored and coded before
R15 analysis.

R16 ***Diffusion-weighted MRI***

R17 All patients had undergone pretreatment MRI with diffusion-weighted MRI sequence for
R18 radiotherapy planning purposes. The MRIs were acquired on a 1.5 Tesla MRI scanner (Intera
R19 NT, Philips Medical Systems, Best, the Netherlands). Two surface coils were used as receivers.
R20 Diffusion-weighted MRI was acquired using a single-shot spin echo planar imaging (EPI) with
R21 3 b-values (0, 150, and 800 s/mm²) in 3 orthogonal directions with a 4-mm slice thickness.
R22 As part of the clinical protocol, gadolinium contrast-enhanced imaging was performed using
R23 a 3D T1 fast field echo after contrast administration. Apparent diffusion coefficient was
R24 calculated using all 3 b-values. The tumor was manually delineated on images with a b-value
R25 of 0 s/mm² by using the additional information of all other MRI scans by a radiologist and
R26 an Ear, Nose, and Throat resident in consensus (F.A.P. and J.P.D.). Evident cystic or necrotic
R27 regions were separately delineated and excluded from total tumor volume. All scans were
R28 acquired at a 1.5 Tesla Philips Intera scanner (Best). The T1weighted scan, a 3D T1 steady
R29 state free precession scan, after gadolinium administration was acquired with the following
R30 parameters: TR/TE 25/2.7 ms, flip angle 30, acquisition matrix: 256 x 256 x 80, acquired
R31 resolution: 1.0 x 1.0 x 2.2 mm³, reconstructed resolution: 1.0 x 1.0 x 1.1 mm³, number of
R32 averages: 1. The diffusion-weighted MRI was acquired using a single-shot spin EPI with
R33 the following acquisition parameters: TR/TE 5872/70 ms, flip angle 90, acquisition matrix:
R34 112 x 101, acceleration factor 2 (SENSE), EPI factor 51, acquired resolution: 2.1 x 2.1 mm²,
R35
R36
R37
R38
R39

reconstructed resolution: $1.7 \times 1.7 \text{ mm}^2$, number of averages 4. Fat suppression was applied using short tau inversion recovery with an inversion time of 180 ms.

Figure 1A-1F shows an example of tumor delineation on a 3D diffusion-weighted image and its automatic registration onto the apparent diffusion coefficient map. Mean apparent diffusion coefficient was calculated by the mean apparent diffusion coefficient of all voxels within the delineation.

Human papillomavirus status

HPV status of all primary tumors was determined on diagnostic biopsies. The standard treatment agreement with patients in our hospital includes anonymous use of redundant tissue for research purposes, therefore, no ethical approval is required (Code for proper secondary use of human tissue, Dutch Federation of Medical Scientific Societies). (16) HPV16 status was determined according to the algorithm of Smeets et al. (17) This protocol follows a 2-step procedure of p16 staining and polymerase chain reaction. The primary antibody used was a mouse antibody against p16INK4a (Neomarkers, Fremont, CA) after which a second antibody, a poly-HRP anti-mouse immunoglobulin G (Immunologic, Duiven, the Netherlands) was introduced to allow staining. The positive control was HPV16-positive tonsil tissue, and the negative control was skin tissue. Cases were considered p16-positive when at least 70% of neoplastic cells showed strong (21/31) nuclear and/or cytoplasmic staining. The p16 was scored by a dedicated head and neck pathologist (S.M.W.) blinded to the apparent diffusion coefficient results. In case of p16 overexpression, GP 51/61 PCR was performed to confirm HPV positivity. DNA isolation for this procedure was carried out using the Cobas DNA sample preparation kit (Roche Molecular Diagnostics, Branchburg, NJ), in accord with the protocol of the manufacturer.

Statistical analysis

HPV status was associated with clinical features, including age, sex, primary tumor site, tumor volume, stage, and T and N classifications. Statistical calculations were performed using appropriate tests; Student's t test for age, tumor volume and treatment, Fisher's exact for tumor and nodal stage, and chi-square for tumor subsite. The Shapiro-Wilk test was used to test normality of apparent diffusion coefficient distribution. To analyze differences in apparent diffusion coefficient per HPV group, the Student's t test was used. Correlation between apparent diffusion coefficient and HPV was calculated using Spearman's rho. Multivariate logistic regression was performed to correct for possible confounding factors in the correlation between HPV and apparent diffusion coefficient. For this, apparent diffusion coefficient was categorized in 5 percentiles (SPSS, version 20 and GraphPad, version 6, San Diego, CA). The p values $< .05$ were considered statistically significant.

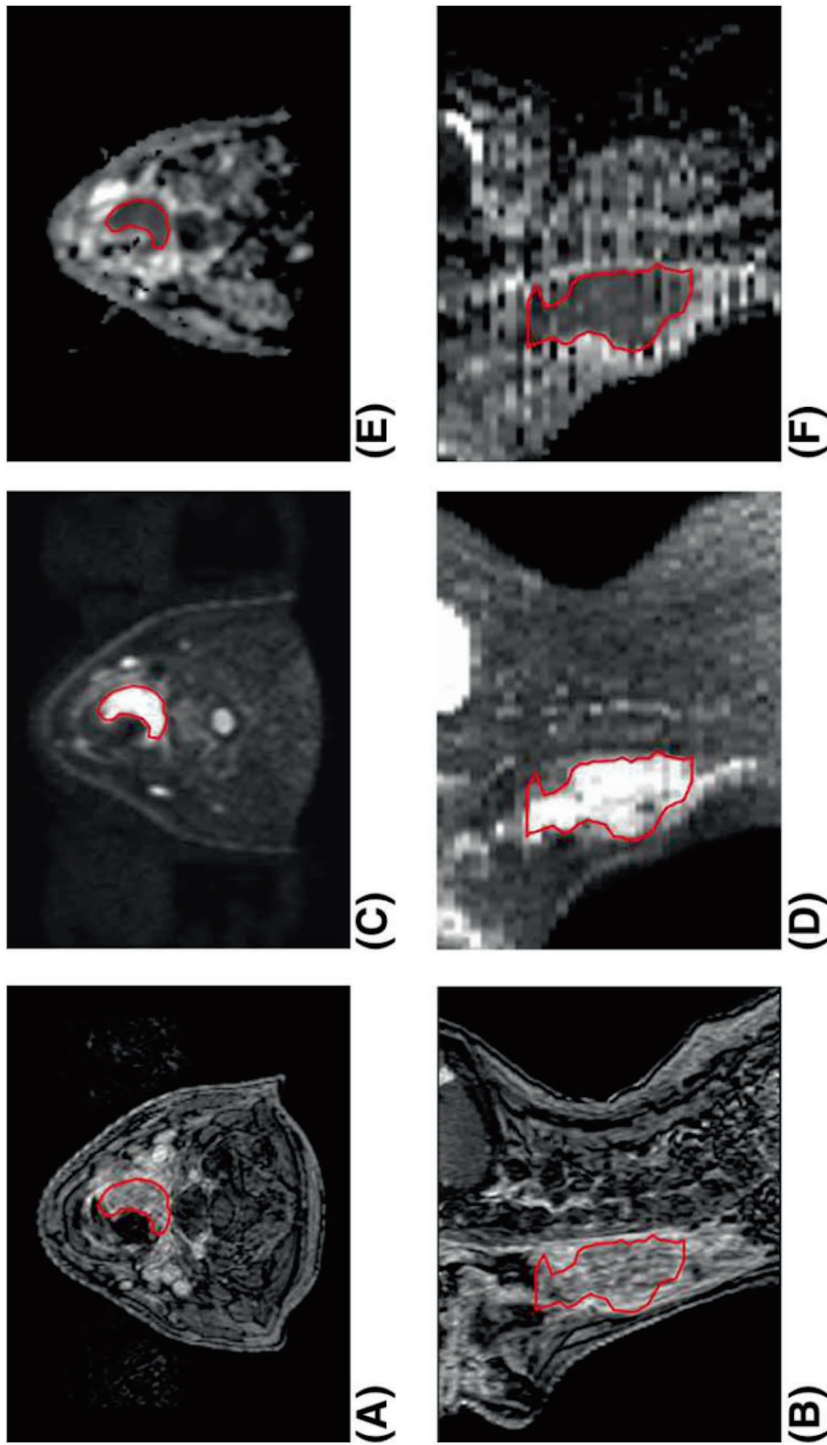


FIGURE 1. (A-F) Images in a 68-year-old man with a human papillomavirus (HPV)-negative oropharyngeal carcinoma shows tumor delineation on axial and sagittal post contrast T1-weighted MRI with fat suppression (A and B), axial and sagittal diffusion-weighted image (b= 800 s/mm²) (C and D) and corresponding axial and sagittal apparent diffusion coefficient map (E and F).

Results

Seventy-five patients with T2 or larger HNSCC were included. Two patients were excluded because HPV status could not be assessed because of the lack of vital DNA for sampling, leaving 73 patients for further analyses. Sixty patients (82%) scored p16-negative versus 13 (18%) p16-positives. Of the 13 patients who were p16-positive, only 6 (8.2% of total patients analyzed) were confirmed to be HPV-positive. Mean tumor size for HPV-positive HNSCC was 15.9 mL compared to HPV-negative HNSCC, which showed a volume of 17.1 mL. This difference was not statistically significant ($p = .92$). In addition, other baseline characteristics showed no significant differences between patients who were HPV-positive and HPV-negative (table 1).

TABLE 1. Characteristics of 73 patients sorted by human papillomavirus

Patient or tumor Characteristics	HPV positive n=6	%	HPV negative n=67	%	p value
Age (yr)	57 ±10		62 ±9		0.28
Sex					0.18
male	2	33	45	67	
female	4	67	22	33	
Tumor site					0.95
oropharynx	3	50	29	43	
larynx	2	33	29	43	
hypopharynx	1	17	8	12	
oral cavity	0		1	2	
AJCC tumor stage					0.82
T2	4	66	29	43	
T3	1	17	23	34	
T4	1	17	15	33	
Nodal stage					0.09
N0	2	33	31	46	
N1	2	33	7	10	
N2	2	33	29	44	
Tumor volume (ml)	15.9 ±21.9		17.1 ±27.4		0.92
Treatment					0.91
Radiotherapy	4	67	44	66	
Chemoradiotherapy	2	33	23	34	

HPV: human papillomavirus, AJCC: American Joint Committee on Cancer

Mean apparent diffusion coefficient followed normal distribution ($p = .15$). Both p16-positive and HPV-positive tumors showed significant lower mean apparent diffusion coefficient compared to p16-negative and HPV-negative tumors. The mean apparent diffusion coefficient of HPV-positive tumors was $1.327 \pm 0.267 \times 10^{-3} \text{ mm}^2/\text{s}$ compared to $1.740 \pm 0.338 \times 10^{-3} \text{ mm}^2/\text{s}$ in HPV-negative tumors ($p = .005$; table 2; figure 2).

TABLE 2. Mean apparent diffusion coefficient according to human papillomavirus status

HPV status	N	Mean ADC ($\times 10^{-3} \text{ mm}^2/\text{s}$)	p value
P16 positive	13	1.476 ± 0.309	0.008
P16 negative	60	1.756 ± 0.341	
HPV positive	6	1.327 ± 0.267	0.005
HPV negative	67	1.740 ± 0.338	

HPV: human papillomavirus, ADC: apparent diffusion coefficient

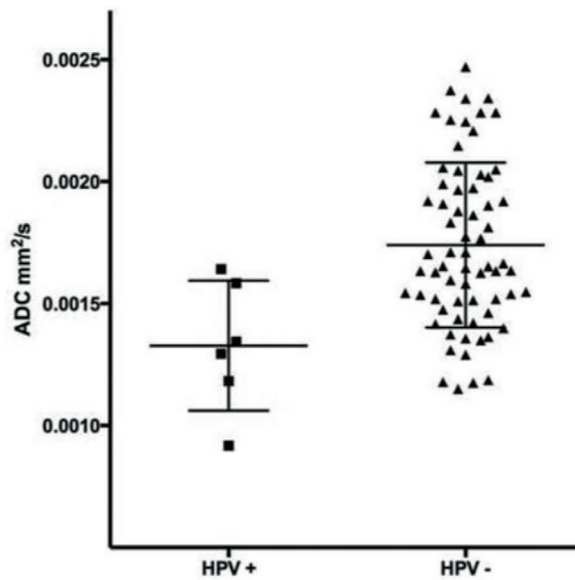


FIGURE 2. Scatterplot showing mean apparent diffusion coefficient by human papillomavirus (HPV) status.

Correlation between apparent diffusion coefficient and HPV status had a Spearman’s rho of 0.31 ($p = .008$). Multivariate logistic regression showed this correlation to be independent of age, tumor site, T classification, N classification, and volume (table 3).

TABLE 3. Correlation human papillomavirus status with prognostic factors

Patient or tumor characteristics	p value	OR	95% CI
Sex	0.58	5.03	0.79 – 31.71
Age (yr)	0.63	1.01	0.91 – 1.12
Tumor site	0.17	3.15	0.62 – 15.98
T classification	0.09	5.03	0.79 – 31.77
N classification	0.89	1.06	0.48 – 2.32
Volume (ml)	0.29	0.98	0.94 – 1.02
ADC mean	0.03	6.9	1.12 – 41.76

OR: odds ratio, CI: confidence interval, ADC: apparent diffusion coefficient

In HPV-positive tumors, diffusion-weighted images showed high signal intensity and the corresponding apparent diffusion coefficient maps showed low apparent diffusion coefficient values (figure 3A–3C). In comparison, HPV-negative tumors showed more signal loss in diffusion-weighted images and thus higher apparent diffusion coefficient values (figure 4A–4C).

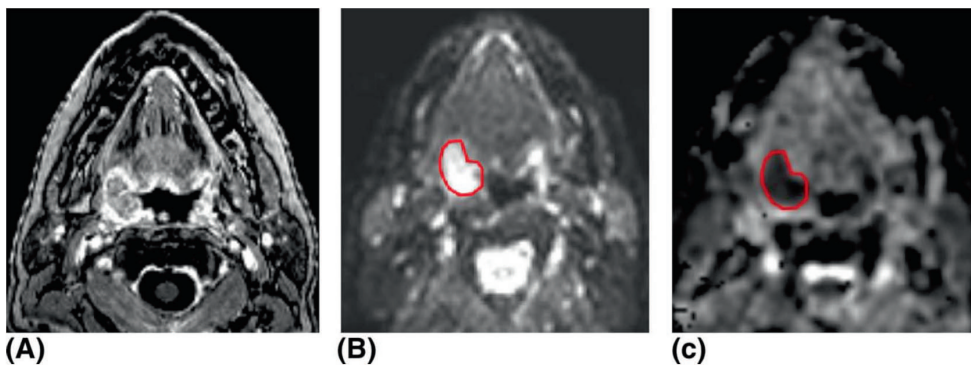


FIGURE 3. (A–C) Images in a 65-year-old man with a human papillomavirus (HPV)-positive oropharyngeal carcinoma. **(A)** Axial post contrast T1-weighted MRI with fat suppression shows a right tonsillar mass with limited extension in the glossotonsillar sulcus. **(B)** Axial diffusion-weighted image ($b = 800 \text{ s/mm}^2$) showing increased signal intensity in the tumor and **(C)** corresponding axial apparent diffusion coefficient map showing marked signal loss corresponding with a low apparent diffusion coefficient value.

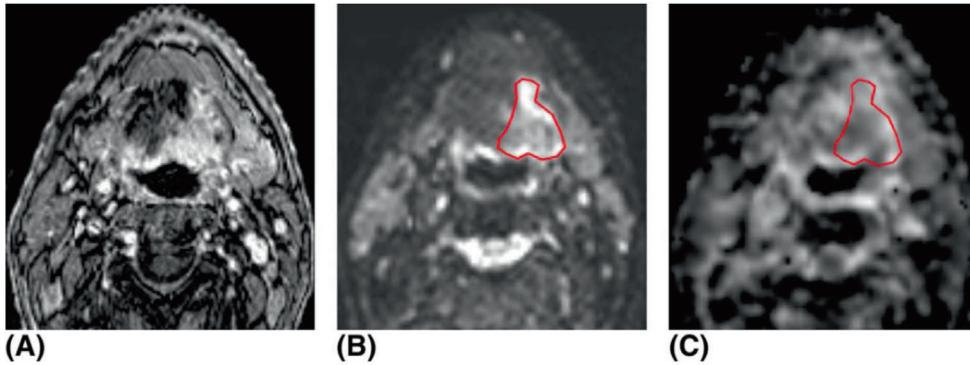


FIGURE 4. (A-C) Images in a 68-year-old man with a human papillomavirus (HPV)-negative oropharyngeal carcinoma. **(A)** Axial post contrast T1-weighted MRI with fat suppression shows an infiltrative lesion centered in the left tongue base with anterior extension in the floor of the mouth. **(B)** Axial diffusion-weighted image ($b=800$ s/mm²) showing somewhat increased signal intensity in the tumor. This signal intensity is far less than in HPV-positive carcinoma shown in Figure 3. **(C)** Corresponding axial apparent diffusion coefficient map showing less signal loss in comparison to HPV-positive carcinoma, indicative of a higher apparent diffusion coefficient value.

Discussion

The results of this study showed a correlation between HPV status and apparent diffusion coefficient derived from diffusion-weighted imaging. HPV-positive HNSCC showed a significantly lower mean pretreatment apparent diffusion coefficient in comparison to the HPV-negative HNSCC. This difference was independent of other patient characteristics, such as tumor volume, subsite, age, T classification, and N classification.

Although the exact reason for the correlation found remains partly unknown, a hypothesis can be proposed. Apparent diffusion coefficient is described as being an imaging biomarker reflecting tumor microanatomy. A positive correlation between apparent diffusion coefficient and total percentage area of stroma was reported, and an inverse correlation between apparent diffusion coefficient and cell density in tumors. (5) HPV-associated tumors are described to have multiple morphologic features distinct from their HPV-negative equivalents. HPV-negative HNSCCs show a keratinizing morphology with large central necrosis. In contrast, HPV-positive HNSCCs often show a partially or nonkeratinizing morphology. They also demonstrate only small central necrosis with cystic changes as well as the presence of large amounts of tumor infiltrating lymphocytes. Notably absent are surface dysplasia and large stromal volume. (18) The low stromal volume seen in HPV-positive HNSCC might be an explanation for their low apparent diffusion coefficient on diffusion-weighted MRI, as this is known to cause low apparent diffusion coefficient. (5) In addition, it can be hypothesized that the association between a low apparent diffusion coefficient and a positive HPV status might explain the favorable local response to radiotherapy of a low apparent diffusion coefficient. (19,20)

Despite the statistically significant difference found in apparent diffusion coefficient between HPV-positive and HPV-negative HNSCC, the correlation coefficient was only 0.31. Reflecting the fact that HPV status is not the only factor influencing apparent diffusion coefficient. It is more likely that apparent diffusion coefficient is a complex sum of multiple variables all of which influence the microanatomy and perfusion of tissues, of which HPV is one.

The correlation between apparent diffusion coefficient and HPV has been earlier described by Nakahira et al. (21) However our study and theirs have some methodological differences.

The study of Nakahira et al (21) was based on a correlation between p16 expression and apparent diffusion coefficient. However, p16 immunohistochemistry alone is generally not considered suitable to detect HPV status, as sensitivity and specificity of this test is limited. Smeets et al (17) showed that p16 overexpression does not accurately predict HPV-positivity because p16 overexpression can also occur through other mechanisms. Therefore, p16-positive HNSCC may still test HPV-negative in the GP51/61 PCR analysis. Additionally, p16-positive and HPV-negative do not show a significantly better survival. (12) In our study, both p16 and HPV linear array were used to ensure that positive HPV status was reflected by active HPV virus. This validated method ensured that the correlation seen in this study is not corrupted by p16-positive HPV-negative carcinomas. This was illustrated by the fact that of the 13 p16-positive samples in our data, only 6 (46%) tested HPV-positive in linear array analysis. The second difference in the study of Nakahira et al (21) is that they have taken a single axial slice in which the region of interest was drawn. However, we believe that 3D total tumor volume reduces selection bias. Especially in HNSCC, which are known for their heterogeneity, this seems of uttermost importance.

The last point of interest is the diffusion-weighted MRI used to delineate the region of interest. We performed manual delineation on b0, whereas Nakahira et al (21) performed delineation on the apparent diffusion coefficient map. We believe that by delineation on the apparent diffusion coefficient map, a bias is introduced by the fact that only areas with restricted water diffusion are delineated, causing the risk of a bias for low apparent diffusion coefficient. On b0, however, delineation is not directly influenced by apparent diffusion coefficient but based on high signal intensity on this T2-weighted image. The disadvantage of this method is the possibility of inclusion of peritumoral edema and healthy tissue around the tumor.

Despite the interesting correlation found between apparent diffusion coefficient and HPV status, the following limitations of our study should be noted. Of the total of 73 patients assessed, only 6 (8%) tested HPV-positive. Several reasons have contributed to this low incidence. The incidence of HPV-positive tumors is said to be 80% in the oropharynx and 28% in the larynx in the United States. (22) In the Netherlands, however, this number ranges between 20% and 29% in oropharyngeal cancer. (23,24) Furthermore, we chose to include

R1 multiple subsites besides the oropharynx, leading to a lower total incidence as HPV-positive
R2 HNSCCs are predominantly found in the oropharynx. However, we assume that HPV-induced
R3 changes will have similar effects on the microanatomy of HNSCC in all subsites. Moreover,
R4 the small number might be due to patient selection; because it was a retrospective study
R5 with inclusion of patients who already had a preexistent diffusion-weighted MRI available.
R6 Although our number of HPV-positive HNSCC only was 8.2%, we found a significant correlation
R7 with pretreatment apparent diffusion coefficient. Moreover, our study did include a large
R8 negative control group diminishing the chance of a coincidental finding.
R9

R10 **Conclusion**

R11 The results of this study show that HPV-positive HNSCC has a significantly lower pretreatment
R12 apparent diffusion coefficient in comparison to the HPV-negative HNSCCs. Diffusion-weighted
R13 MRI is an upcoming MRI method that reflects tumor microanatomy; where a low pretreatment
R14 apparent diffusion coefficient has shown to be a positive predictor for locoregional control
R15 after (chemo)radiotherapy. The favorable prognostic value of low pretreatment apparent
R16 diffusion coefficient might be partially attributed to patients with a positive HPV status. Better
R17 understanding of the histological reflection of modern imaging modalities might contribute
R18 to patient selection for personalized cancer care in the future.
R19
R20
R21
R22
R23
R24
R25
R26
R27
R28
R29
R30
R31
R32
R33
R34
R35
R36
R37
R38
R39

1. Parkin DM, Bray F, Ferlay J, Pisani P. Estimating the world cancer burden: Globocan 2000. *Int J Cancer* 2001;94(2):153-6.
2. Argiris A. Update on chemoradiotherapy for head and neck cancer. *Curr Opin Oncol* 2002;14(3):323-9.
3. Kamangar F, Dores GM, Anderson WF. Patterns of cancer incidence, mortality, and prevalence across five continents: defining priorities to reduce cancer disparities in different geographic regions of the world. *J Clin Oncol* 2006;24(14):2137-50.
4. Kasperts N, Slotman B, Leemans CR, Langendijk JA. A review on re-irradiation for recurrent and second primary head and neck cancer. *Oral Oncol* 2005;41(3):225-43.
5. Driessen JP, Caldas-Magalhaes J, Janssen LM, et al. Diffusion-weighted MR Imaging in Laryngeal and Hypopharyngeal Carcinoma: Association between Apparent Diffusion Coefficient and Histologic Findings. *Radiology* 2014;272(2):456-63.
6. Wang J, Takashima S, Takayama F, et al. Head and neck lesions: characterization with diffusion-weighted echo-planar MR imaging. *Radiology* 2001;220(3):621-30.
7. Koh DM, Padhani AR. Diffusion-weighted MRI: a new functional clinical technique for tumour imaging. *Br J Radiol* 2006;79(944):633-5.
8. Kim S, Loevner L, Quon H, et al. Diffusion-weighted magnetic resonance imaging for predicting and detecting early response to chemoradiation therapy of squamous cell carcinomas of the head and neck. *Clin Cancer Res* 2009;15(3):986-94.
9. Hatakenaka M, Shioyama Y, Nakamura K, et al. Apparent diffusion coefficient calculated with relatively high b-values correlates with local failure of head and neck squamous cell carcinoma treated with radiotherapy. *AJNR Am J Neuroradiol* 2011;32(10):1904-10.
10. Ang KK, Harris J, Wheeler R, et al. Human papillomavirus and survival of patients with oropharyngeal cancer. *N Engl J Med* 2010;363(1):24-35.
11. O'Rourke MA, Ellison MV, Murray LJ, Moran M, James J, Anderson LA. Human papillomavirus related head and neck cancer survival: a systematic review and meta-analysis. *Oral Oncol* 2012;48(12):1191-201.
12. Dayyani F, Etzel CJ, Liu M, Ho CH, Lippman SM, Tsao AS. Meta-analysis of the impact of human papillomavirus (HPV) on cancer risk and overall survival in head and neck squamous cell carcinomas (HNSCC). *Head Neck Oncol* 2010;2:15.
13. Isayeva T, Li Y, Maswahu D, Brandwein-Gensler M. Human papillomavirus in non-oropharyngeal head and neck cancers: a systematic literature review. *Head Neck Pathol* 2012;6 Suppl 1:S104-20.
14. Leemans CR, Braakhuis BJ, Brakenhoff RH. The molecular biology of head and neck cancer. *Nat Rev Cancer* 2011;11(1):9-22.
15. Kimple RJ, Smith MA, Blitzer GC, et al. Enhanced radiation sensitivity in HPV-positive head and neck cancer. *Cancer Res* 2013;73(15):4791-800.
16. van Diest PJ. No consent should be needed for using leftover body material for scientific purposes. *For. BMJ* 2002;325(7365):648-51.
17. Smeets SJ, Hesselink AT, Speel EJ, et al. A novel algorithm for reliable detection of human papillomavirus in paraffin embedded head and neck cancer specimen. *Int J Cancer* 2007;121(11):2465-72.
18. Westra WH. The morphologic profile of HPV-related head and neck squamous carcinoma: implications for diagnosis, prognosis, and clinical management. *Head Neck Pathol* 2012;6 Suppl 1:S48-54.
19. de Kruijf EM, van Nes JG, van de Velde CJ, et al. Tumor-stroma ratio in the primary tumor is a prognostic factor in early breast cancer patients, especially in triple-negative carcinoma patients. *Breast Cancer Res Treat* 2011;125(3):687-96.
20. Huijbers A, Tollenaar RA, v Pelt GW, et al. The proportion of tumor-stroma as a strong prognosticator for stage II and III colon cancer patients: validation in the VICTOR trial. *Ann Oncol* 2013;24(1):179-85.
21. Nakahira M, Saito N, Yamaguchi H, Kuba K, Sugawara M. Use of quantitative diffusion-weighted magnetic resonance imaging to predict human papilloma virus status in patients with oropharyngeal squamous cell carcinoma. *Eur Arch Otorhinolaryngol* 2014;271(5):1219-25.

- 22. Lewis JS, Jr, Thorstad WL, Chernock RD, et al. p16 positive oropharyngeal squamous cell carcinoma:an entity with a favorable prognosis regardless of tumor HPV status. *Am J Surg Pathol* 2010;34(8):1088-96.
- 23. Sturgis EM, Ang KK. The epidemic of HPV-associated oropharyngeal cancer is here: is it time to change our treatment paradigms? *J Natl Compr Canc Netw* 2011;9(6):665-73.
- 24. Rietbergen MM, Leemans CR, Bloemena E, et al. Increasing prevalence rates of HPV attributable oropharyngeal squamous cell carcinomas in the Netherlands as assessed by a validated test algorithm. *Int J Cancer* 2013;132(7):1565-71.
- 25. Braakhuis BJ, Snijders PJ, Keune WJ, et al. Genetic patterns in head and neck cancers that contain or lack transcriptionally active human papillomavirus. *J Natl Cancer Inst* 2004;96(13):998-1006.

R1
R2
R3
R4
R5
R6
R7
R8
R9
R10
R11
R12
R13
R14
R15
R16
R17
R18
R19
R20
R21
R22
R23
R24
R25
R26
R27
R28
R29
R30
R31
R32
R33
R34
R35
R36
R37
R38
R39

R1
R2
R3
R4
R5
R6
R7
R8
R9
R10
R11
R12
R13
R14
R15
R16
R17
R18
R19
R20
R21
R22
R23
R24
R25
R26
R27
R28
R29
R30
R31
R32
R33
R34
R35
R36
R37
R38
R39

5





6

Is pretreatment apparent diffusion coefficient a predictor of radiosensitivity of head and neck squamous cell carcinomas?

J.P. Driessen
M.E.P. Philippens
I. Stegeman
F.A. Pameijer
L.M. Janssen
W. Grolman
C.H.J. Terhaard

Submitted

Abstract

Background and Purpose: Patients with head and neck cancer are increasingly treated with (chemo)radiotherapy, keeping surgery in reserve for salvage treatment. Reliable identification of nonresponders would enable treatment stratification and might improve survival and reduce treatment induced side effects. We aimed to investigate the apparent diffusion coefficient (ADC) as predictor of outcome of treatment with (chemo)radiation.

Materials and Methods: This prospective cohort study included 75 consecutive patients with oropharynx, hypopharynx, larynx or oral cavity squamous cell carcinomas treated with (chemo)radiotherapy. All patients underwent a pretreatment MRI with diffusion-weighted imaging. The ADC of the primary tumor was determined by 3D-tumor delineation and correlated to local outcome and disease specific survival. Multivariate analysis corrected for the effect of volume.

Results: Median total follow-up was 29 months (range 1 – 48). One-year local recurrence rate was 17%; two-year local recurrence rate was 23%. Univariate analysis showed significant correlation between mean tumor ADC and local control within 1 and 2 years after (chemo)radiotherapy ($p=0.04 - 0.02$), however multivariate logistic regression showed that ADC did not remain its significance when corrected for volume. Kaplan Meier survival analysis shows that the prognosis of local outcome is mainly influenced by volume, and not by ADC. Results for disease specific survival showed comparable results.

Conclusion: In the present study we found primary tumor pretreatment ADC not to be an independent predictor for local response. Therefore, at this time, more research is needed to define the exact role of pretreatment ADC as a predictor of local outcome after (chemo)radiotherapy.

Introduction

Patients with head and neck squamous cell carcinomas (HNSCC) are increasingly treated with organ sparing treatments such as (chemo)radiotherapy, keeping surgery in reserve for salvage treatment. With the introduction of new sparing radiotherapy techniques great progress has been made to diminish the therapeutic side effects, however some tumors are insensitive to radiation therapy and these patients will develop locoregional recurrence. Salvage surgery of these recurrences may be disappointing and previous radiotherapy makes surgery more challenging. Reliable pretreatment identification of tumors insensitive for radiation therapy would enable patient selection for primary surgery, avoiding the surgical challenges induced by previous radiation. This kind of treatment stratification might improve disease free survival and reduce treatment induced side effects. However, pre-therapeutic prediction of radiosensitivity in an individual patient is limited. (1) Recent studies have shown that diffusion-weighted MRI (DW-MRI), appears to be an interesting modality for pretreatment identification of non-responders. (2) DW-MRI is a functional MRI technique that quantifies the restriction of random motion of water molecules in tissues by the apparent diffusion coefficient (ADC). (3-5) This diffusion coefficient reflects the microenvironment of tissues, where higher cell density leads to more diffusion restriction of water molecules. (6) A few studies investigated the correlation of pretreatment ADC in the prediction of radiotherapy response, resulting in contrary results. (7-12) However, most studies have limited number of patients and calculate the pretreatment ADC from cervical lymph nodes (9) or a circular region of interest (ROI) placed in the core in the primary tumor (7,8). However, HNSCC are known for their heterogeneity, which questions the reflection of the true ADC of the primary tumor by a random ROI within the tumor. Also, there is no literature that supports the fact that the primary tumor and its metastatic lymph nodes have similar ADC. Therefore, the ADC calculated from the whole primary tumor is the most appropriate when investigating pretreatment ADC as a predictor of local outcome. Therefore, we aimed to investigate whole-tumor ADC as predictor of local outcome of treatment with (chemo)radiation of patients with HNSCC.

Methods and materials

Patient selection

This prospective cohort study included 75 consecutive patients with primary pathologically proven HNSCC, treated with (chemo)radiotherapy with curative intent from April 2009 to April 2012 at the University Medical Center Utrecht. Inclusion criteria were T2, T3 and T4 cancers located in the oropharynx, hypopharynx, larynx or oral cavity. T1 cancer patients were excluded

R1 because of limited conspicuity of the tumors on DW-MRI with inherent low resolution. Patients
R2 were staged, using the T and N classifications according to the American Joint Committee
R3 on Cancer. Clinical charts were retrospectively reviewed for clinical characteristics. Routine
R4 pretreatment examinations included diagnostic (fiberoptic) endoscopy, contrast-enhanced
R5 computed tomography (CT) and MRI including DW-MRI. All patients were treated up to a
R6 minimal dose of 70 Gy in 5–7 weeks and in case of chemotherapy combined with 100 mg
R7 Cisplatin/m² at day 1, 22 and 43. When there was an indication for chemotherapy in patients
R8 with severe comorbidity, radiotherapy was combined with Cetuximab instead of Cisplatin.
R9 After treatment all patients were followed up at the multidisciplinary outpatient clinic
R10 with intervals according to national guidelines; 2 months the first year and 3 months the
R11 second year after treatment. These consultations consisted of physical examination including
R12 fiberoptic endoscopy. Additional imaging was used on indication, for example when there
R13 were complaints or findings suspected for local or regional recurrence.
R14

R15 ***Diffusion-weighted Magnetic Resonance Imaging***

R16 All patients had undergone pretreatment MRI with diffusion-weighted imaging for target
R17 and organ at risk delineation used for radiotherapy treatment planning. The MRIs were
R18 acquired on a 1.5 T MRI scanner (Intera NT, Philips Medical Systems, Best, the Netherlands).
R19 Two surface coils were used as receivers (Flex-M or Flex-S). DW-MRI was acquired using a
R20 single shot spin echo planar imaging with three b-values (0, 150 en 800 s/mm²) in three
R21 orthogonal directions with a 4-mm slice thickness. The acquisition parameters were: TR/TE
R22 5872/70 ms, flip angle 90, acquisition matrix: 112x101, acceleration factor 2 (SENSE), EPI
R23 factor 51, acquired resolution: 2.1x2.1 mm², reconstructed resolution: 1.7x1.7 mm², number
R24 of averages 4. Fat suppression was applied using short tau inversion recovery (STIR) with
R25 an inversion time of 180 ms. As part of the clinical protocol, gadolinium contrast-enhanced
R26 imaging was performed using 3D T1 spoiled gradient echo after contrast administration.
R27 The acquisition parameters consisted of: TR/TE 25/2.7 ms, flip angle 30, acquisition matrix:
R28 256x256x80, acquired resolution: 1.0x1.0x2.2 mm³, reconstructed resolution: 1.0x1.0x1.1
R29 mm³, number of averages 1.
R30

R31 ***Tumor delineation***

R32 ADC maps were calculated from the DW images using all three b-values and a mono-
R33 exponential model. The tumor was delineated on the axial slides of diffusion-weighted MRI
R34 at the b 0 s/mm² by a radiologist and an ENT resident in consensus both blinded by patient
R35 outcome (J.P.D. and F.A.P.). Delineations were performed on institution developed software
R36 (Volumetool), by making a free-hand multi-slice contour around what was regarded as
R37 the total tumor volume based on the DW images using additional information of all other
R38 (conventional) MR images. Evident cystic regions (regarded as bright on T2-weighted images
R39

and bright on b800 and ADC map) were separately delineated and excluded from total tumor volume. Delineation were automatically copied to the ADC map, on which ADC values within the delineation were calculated automatically by Volumetool.

Statistical analysis

Local recurrence was defined as biopsy proven squamous cell carcinoma of the primary tumor region. Pretreatment mean ADC of patients with local response and local recurrence were compared. Shapiro-Wilk test was used to test normality of ADC distribution. Multivariate logistic regression was performed. For this, ADC was categorized in 4 percentiles. Kaplan Meier survival curves were calculated and compared using the log rank test. Statistical analysis was performed using SPSS (Inc. v20.0, Chicago, IL, USA). P-values smaller than 0.05 were considered statistically significant.

Results

Patients

In all 75 consecutively included patients DW-MRI scans were of sufficient quality to be analyzed and all patients completed treatment. Median total follow-up time after end of treatment was 29 months (range 1 – 48 months). Six patients (8%) were lost to follow-up within 1 year, fifteen patients (20%) were lost to follow-up within 2 years. Twelve patients (17%) developed local recurrence within one year; and fourteen patients (23%) developed local recurrence within two years. See table 1 for baseline characteristics.

Prognostic value of ADC for local control

Mean ADC followed normal distribution (Shapiro-Wilk test; p=0.13). Univariate analysis showed significant correlation between mean tumor ADC and local control within 1 year after (chemo)radiotherapy; mean ADC of $1.74 \pm 0.37 \times 10^{-3} \text{ mm}^2/\text{s}$ for local control versus $1.56 \pm 0.24 \times 10^{-3} \text{ mm}^2/\text{s}$ for local recurrence (p=0.04). Additionally, a significant correlation between local control after 1 year and tumor volume was found with significantly smaller tumors in local controls compared to local recurrences ($12.8 \pm 18.1\text{ml}$ versus $29.0 \pm 23.4\text{ml}$, p=0.01). Univariate analyses for local control after 2 years were comparable, showing significant differences in mean ADC and volume between local responders and local recurrences. See table 2 for the results.

R1
R2
R3
R4
R5
R6
R7
R8
R9
R10
R11
R12
R13
R14
R15
R16
R17
R18
R19
R20
R21
R22
R23
R24
R25
R26
R27
R28
R29
R30
R31
R32
R33
R34
R35
R36
R37
R38
R39

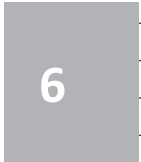


TABLE 1. Patient characteristics

Variable	Included (N=75)	%	1-year FU (N=69)	%	2-year FU (N=60)	%
Lost to follow-up	-		6	8	15	20
Age (y) *	62 (41-81)		62 (41-81)		62 (41-81)	
Sex						
female	26	35	24	35	22	37
male	49	65	45	64	38	63
Tumor site						
oropharynx	34	45	30	43	26	43
larynx	31	41	31	45	28	47
hypopharynx	9	12	8	12	6	10
oral cavity	1	1	-	-	-	-
AJCC tumor stage						
T2	34	45	30	44	25	42
T3	24	32	23	33	21	35
T4a	13	17	12	17	11	18
T4b	4	5	4	6	3	5
Nodal stage						
N0	34	45	32	46	29	48
N1	8	11	8	12	7	12
N2a	1	1	1	1	1	2
N2b	19	25	17	25	15	25
N2c	13	17	11	16	8	13
Tumor volume (ml) *	17.2 (1-175)		15.6 (1-86)		15.9 (1-86)	
Treatment						
Radiotherapy	49	65	45	65	39	65
Chemoradiotherapy	20	27	19	27	17	28
Radiotherapy + Cetuximab	6	8	5	7	4	2

* Median and range

FU: follow-up, AJCC: American Joint Committee on Cancer

TABLE 2. Univariate analysis of local outcome and tumor characteristics

Local tumor status	N	Pretreatment ADC x 10 ⁻³ mm ² /s	P-value	Volume ml	P-value
1 Year after treatment			0.04		0.01
Local control	57	1.74 ±0.37		12.8±18.1	
Local recurrence	12	1.56 ±0.24		29.0±23.4	
2 Years after treatment			0.02		<0.01
Local control	46	1.74 ±0.36		10.6±14.6	
Local recurrence	14	1.54 ±0.22		33.3±26.3	

ADC: apparent diffusion coefficient

Multivariate logistic regression showed that volume was the only significant prognostic factor for local control two years after treatment, and that ADC did not remain its significance when corrected for volume (table 3).

TABLE 3. Multivariate logistic regression of local recurrence and tumor characteristics

Tumor Characteristic	P=value	OR	95% CI
1 Year after treatment (n=69)			
Volume	0.05	1.03	1.01- 1.06
ADC mean	0.52	0.81	0.43- 1.53
2 Years after treatment (n=60)			
Volume	<0.01	1.05	1.02- 1.09
ADC mean	0.34	0.73	0.39- 1.40

OR: odds ratio, CI: confidence interval, ADC: apparent diffusion coefficient

Actuarial analysis by Kaplan Meier showed no significant difference in local outcome between high and low ADC ($p=0.19$). But when divided by volume this was significant ($p<0.01$). Figure 1 shows in Kaplan Meier survival analysis that the prognosis of local outcome is mainly influenced by volume, and not by ADC. There is no significant difference between the high and low ADC when divided by volume. ($p>0.50$) There is a significant difference between high and low volume within tumors with high ADC. ($p<0.01$) This difference is also visible for the tumors with low ADC, but not significant when tested ($p=0.09$)

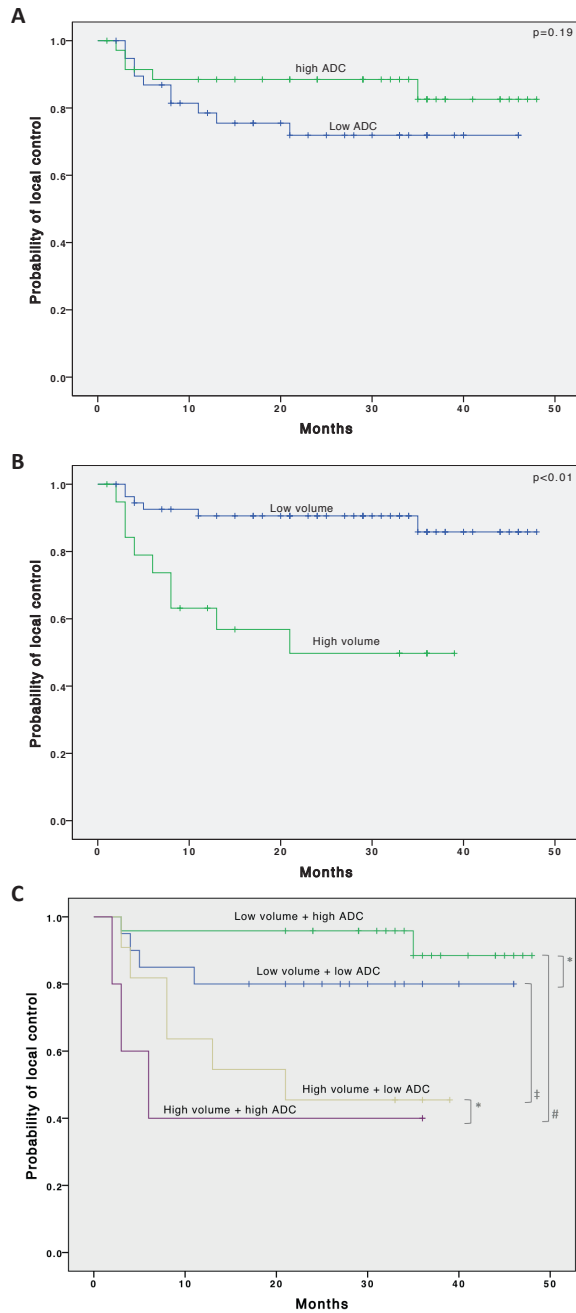


FIGURE 1. Kaplan-Meier survival analysis
(A) Probability of local control divided by apparent diffusion coefficient is not significantly different ($p=0.19$). **(B)** Probability of local control divided by volume is significantly different ($p<0.01$). **(C)** Probability of local control divided by volume and ADC shows that the volume is the main predictor of local outcome. * $P>0.50$, # $P=0.01$, ‡ $P=0.09$.

Discussion

In this prospective cohort study we studied the prognostic value of pretreatment ADC for local control after (chemo)radiotherapy. Our results show that volume and ADC both are correlated to local outcome one and 2 years after treatment. However, when combined in a multivariate model, only volume shows independent prognostic value two years after treatment. Larger tumors show significant worse probability of local control in time, where ADC does not show this. In literature, conflicting results are reported on ADC and its predictive value and ability of ADC-based prediction of tumor (chemo)radiosensitivity varies from one institution to another. Therefore, more research is needed to define the exact value of pretreatment ADC as a predictor of local outcome.

Diffusion-weighted MRI

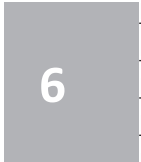
Although the biological origin of ADC remains partly unknown, it is correlated to cell density, stromal components of the tumor, infiltration of inflammatory cells and also correlates to HPV status. (6, 13-15) High stromal proliferation is associated with poor outcome, and also with high ADC. (16, 17) HPV positive tumors, which are known for their prognostic favorable outcome compared to their HPV negative counterparts, have significantly lower ADC compared to HPV negative tumors. (13, 18, 19) This supports the idea that ADC could be able to serve as a predictor of outcome.

Current literature

In our results, pretreatment ADC shows a significant correlation to local control in univariate analysis, however in multivariate analysis only volume remained.

Previous studies concerning the use of pretreatment ADC in the prediction of radiotherapy response reported conflicting results. A few of these studies showed, in contrast to our study, a significant correlation between pretreatment ADC and local outcome. (7-9, 12) A methodology difference between the present study and these studies is the technique of the tumor delineation; Most studies calculated ADC on only one axial slice of the MRI. (7,8) Due to the fact that HNSCC are known for their heterogeneity this might introduce a bias as it can be questioned if that represents the true ADC of the primary tumor. (7, 8) In the study of Kim et al. ADC of the metastatic nodes were used instead of the ADC of the primary lesion, which implies a selection bias as it excludes patients with a NO neck. Also, they determined local control immediately at the end of radiotherapy without follow-up afterwards. (9) For this study we used hand-free multi-slice delineation of the whole primary tumor. This represented the total 3D volume of what was regarded as the primary tumor. This does not have the bias of only having the core, and often most compact part of the tumor, but it does come with the risk of partial volume effects. When using total tumor delineation, you introduce partial

R1
R2
R3
R4
R5
R6
R7
R8
R9
R10
R11
R12
R13
R14
R15
R16
R17
R18
R19
R20
R21
R22
R23
R24
R25
R26
R27
R28
R29
R30
R31
R32
R33
R34
R35
R36
R37
R38
R39



R1 volume effects in the periphery of the lesion. This might cause the inclusion of healthy tissue
R2 surrounding the tumor and will increase the mean ADC of the lesion. Srinivasan et al. used
R3 comparable tumor delineation to ours (e.g. total 3D volume of primary tumor), however they
R4 correlated ADC with overall survival instead of local control or disease specific survival. (12)
R5 Preferably, when discussing tumor radiosensitivity disease specific survival or local control is
R6 more appropriate. In addition, these studies used only univariate analysis and did not correct
R7 for volume. (7-9)

R8 One study that also found pretreatment ADC to be predictive of local outcome is the
R9 study of Lambrecht et al. (11) This study included 161 patients, calculated total tumor ADC
R10 and performed multivariate analysis. Although their methodology is similar to ours, they did
R11 find pretreatment ADC to be predictive independent of tumor volume, in contrary to our
R12 results. However, this effect was only visible when using high b-values (500, 750 and 1000)
R13 and was not the case then using average (0, 50, 100, 500, 750 and 1000) and low b-values
R14 (0, 50 and 100). Our study used b-values of 0, 150 and 800, so would be most comparable to
R15 their average b-value results, which both showed no significant correlation to local outcome.
R16 However, even in the high b-value, although significant the hazard ratio was quite low,
R17 especially when compared to to the hazard ratio of volume (Hazard ratio 1.14 versus 5.38).

R18 In correspondence to our study, King et al. found no significant predictive value of
R19 pretreatment ADC. (10) Their methodology was similar to ours, including the delineation
R20 of whole tumor volume to determine ADC and correlate ADC to local status at 2 years after
R21 radiotherapy in 37 patients.

R22 In addition, all of these studies, except the one of Lambrecht et al (11), suffered from
R23 small sample sizes and are from a sparse number of institutions which enlarges the risk of a
R24 positive publication bias.

R26 **Methodology and acquisition of DW-MRII**

R27 The above mentioned differences in results in current literature, might be due to differences
R28 in methodology. As mentioned, the results are greatly influenced by the method of tumor
R29 delineation. The heterogeneity of HNSCC makes the delineation of only one axial slide of
R30 the total tumor questionable to resemble the true ADC. Also the choice of b-values can be
R31 of influence. The choice of b-values influences the sensitivity for slow or fast diffusion water
R32 molecules. Low b-values are known to be influenced also by perfusion rather than solely
R33 diffusion. In accordance, Lambrecht et al. reported ADC calculated with high b-values to have
R34 a stronger correlation to outcome compared to ADC calculated with lower b-values. (11)
R35 This might explain the differences in results across studies, as for example King et al. who
R36 found no correlation, only included low b-values up to 500. (10) The fact that the choice of
R37 b-values influences the result of the ADC and is of influence on the strength of correlation
R38 with outcome is an important fact to realize when using the results in clinical setting.
R39

Early assessment

As this study focused on pretreatment prediction of radiosensitivity in HNSCC, there are studies reporting on early prediction of treatment response. Vandecaveye et al. found the increase of pretreatment ADC of the primary tumor and ADC 3 weeks after start of (chemo) radiotherapy to correspond with the outcome 2 years after treatment. (20) Also other studies showed the capacity of ADC to predict response during and early after (chemo)radiotherapy of HNSCC. (9, 21, 22)

Limitations

Our study did suffer from limitations. We have 20% of the patients lost to follow-up at two years. This is based on the study population which as known has high co-morbidity and risk of secondary cancers. Also, our events were low, only 14 patients suffered from local recurrence. This limits the possibility of multivariate analysis. Generally, it is accepted to include an extra variable for each 10 events. Therefore, we could only include volume as a predictor and not other known prognostic patient characteristics. (23) Primary tumor volume is a known predictor of local control. (24).

Conclusion

In the future, personalized cancer treatment requires therapy stratification before onset of therapy. Therefore, we need prognostic features for therapy response prediction. ADC is described to be one of them. However, these studies are sparse, differ in methodology and outcome measures, and reported contradicting results. In the present relatively large study we found pretreatment ADC not to be an independent predictor for local response. The ability of ADC-based prediction of tumor (chemo)radiosensitivity varies from one institution to another. Therefore, at this time, more studies should explore the role of pretreatment ADC in treatment stratification. For future studies we recommend delineation of the total primary tumor for ADC calculation, as a random ROI might introduce bias and not reflect the true ADC of the primary lesion. Further, we recommend the use of high b-values, as they trend to have a stronger correlation to outcome compared to lower b-values. Studies should always perform multivariate analysis and correct for as many confounding factors as possible based on the number of events. To enable this, we need large datasets, but the applicability of a multicenter trial remains questionable due to interscanner reproducibility.

R1
R2
R3
R4
R5
R6
R7
R8
R9
R10
R11
R12
R13
R14
R15
R16
R17
R18
R19
R20
R21
R22
R23
R24
R25
R26
R27
R28
R29
R30
R31
R32
R33
R34
R35
R36
R37
R38
R39

- R1
R2
R3
R4
R5
R6
R7
R8
R9
R10
R11
R12
R13
R14
R15
R16
R17
R18
R19
R20
R21
R22
R23
R24
R25
R26
R27
R28
R29
R30
R31
R32
R33
R34
R35
R36
R37
R38
R39
1. Bourhis J, Overgaard J, Audry H, Ang KK, Saunders M, Bernier J, et al. Hyperfractionated or accelerated radiotherapy in head and neck cancer: a meta-analysis. *Lancet*. 2006;368(9538):843-54. Epub 2006/09/05.
 2. Driessen JP, van Kempen PM, van der Heijden GJ, Philippens ME, Pameijer FA, Stegeman I, et al. Diffusion-weighted imaging in head and neck squamous cell carcinomas: a systematic review. *Head Neck*. 2015;37(3):440-8. Epub 2013/12/19.
 3. Koh DM, Padhani AR. Diffusion-weighted MRI: a new functional clinical technique for tumour imaging. *Br J Radiol*. 2006;79(944):633-5. Epub 2006/06/24.
 4. Wang J, Takashima S, Takayama F, Kawakami S, Saito A, Matsushita T, et al. Head and neck lesions: characterization with diffusion-weighted echo-planar MR imaging. *Radiology*. 2001;220(3):621-30. Epub 2001/08/30.
 5. Padhani AR. Diffusion magnetic resonance imaging in cancer patient management. *Semin Radiat Oncol*. 2011;21(2):119-40. Epub 2011/03/02.
 6. Driessen JP, Caldas-Magalhaes J, Janssen LM, Pameijer FA, Kooij N, Terhaard CH, et al. Diffusion-weighted MR imaging in laryngeal and hypopharyngeal carcinoma: association between apparent diffusion coefficient and histologic findings. *Radiology*. 2014;272(2):456-63. Epub 2014/04/23.
 7. Hatakenaka M, Nakamura K, Yabuuchi H, Shioyama Y, Matsuo Y, Ohnishi K, et al. Pretreatment apparent diffusion coefficient of the primary lesion correlates with local failure in head-and-neck cancer treated with chemoradiotherapy or radiotherapy. *Int J Radiat Oncol Biol Phys*. 2011;81(2):339-45. Epub 2010/09/14.
 8. Hatakenaka M, Shioyama Y, Nakamura K, Yabuuchi H, Matsuo Y, Sunami S, et al. Apparent diffusion coefficient calculated with relatively high b-values correlates with local failure of head and neck squamous cell carcinoma treated with radiotherapy. *AJNR Am J Neuroradiol*. 2011;32(10):1904-10. Epub 2011/07/23.
 9. Kim S, Loevner L, Quon H, Sherman E, Weinstein G, Kilger A, et al. Diffusion-weighted magnetic resonance imaging for predicting and detecting early response to chemoradiation therapy of squamous cell carcinomas of the head and neck. *Clin Cancer Res*. 2009;15(3):986-94. Epub 2009/02/04.
 10. King AD, Chow KK, Yu KH, Mo FK, Yeung DK, Yuan J, et al. Head and neck squamous cell carcinoma: diagnostic performance of diffusion-weighted MR imaging for the prediction of treatment response. *Radiology*. 2013;266(2):531-8. Epub 2012/11/16.
 11. Lambrecht M, Van Calster B, Vandecaveye V, De Keyzer F, Roebben I, Hermans R, et al. Integrating pretreatment diffusion weighted MRI into a multivariable prognostic model for head and neck squamous cell carcinoma. *Radiother Oncol*. 2014;110(3):429-34. Epub 2014/03/19.
 12. Srinivasan A, Chenevert TL, Dwamena BA, Eisbruch A, Watcharotone K, Myles JD, et al. Utility of pretreatment mean apparent diffusion coefficient and apparent diffusion coefficient histograms in prediction of outcome to chemoradiation in head and neck squamous cell carcinoma. *J Comput Assist Tomogr*. 2012;36(1):131-7. Epub 2012/01/21.
 13. Driessen JP, van Bommel AJ, van Kempen PM, Janssen LM, Terhaard CH, Pameijer FA, et al. Correlation of HPV status with apparent diffusion coefficient of diffusion weighted MRI in head and neck squamous cell carcinomas. *Head Neck*. 2015. Epub 2015/03/19.
 14. Sun Y, Tong T, Cai S, Bi R, Xin C, Gu Y. Apparent Diffusion Coefficient (ADC) value: a potential imaging biomarker that reflects the biological features of rectal cancer. *PLoS One*. 2014;9(10):e109371. Epub 2014/10/11.
 15. Choi SY, Chang YW, Park HJ, Kim HJ, Hong SS, Seo DY. Correlation of the apparent diffusion coefficient values on diffusion-weighted imaging with prognostic factors for breast cancer. *Br J Radiol*. 2012;85(1016):e474-9. Epub 2011/12/01.
 16. de Kruijf EM, van Nes JG, van de Velde CJ, Putter H, Smit VT, Liefers GJ, et al. Tumor-stroma ratio in the primary tumor is a prognostic factor in early breast cancer patients, especially in triple-negative carcinoma patients. *Breast Cancer Res Treat*. 2011;125(3):687-96. Epub 2010/04/03.

17. Wang K, Ma W, Wang J, Yu L, Zhang X, Wang Z, et al. Tumor-stroma ratio is an independent predictor for survival in esophageal squamous cell carcinoma. *J Thorac Oncol.* 2012;7(9):1457-61. Epub 2012/07/31.
18. Isayeva T, Li Y, Maswahu D, Brandwein-Gensler M. Human papillomavirus in non-oro-pharyngeal head and neck cancers: a systematic literature review. *Head and neck pathology.* 2012;6 Suppl 1:S104-20. Epub 2012/07/13.
19. Kimple RJ, Smith MA, Blitzer GC, Torres AD, Martin JA, Yang RZ, et al. Enhanced radiation sensitivity in HPV-positive head and neck cancer. *Cancer Res.* 2013;73(15):4791-800. Epub 2013/06/12.
20. Vandecaveye V, Dirix P, De Keyzer F, Op de Beeck K, Vander Poorten V, Hauben E, et al. Diffusion-weighted magnetic resonance imaging early after chemoradiotherapy to monitor treatment response in head-and-neck squamous cell carcinoma. *Int J Radiat Oncol Biol Phys.* 2012;82(3):1098-107. Epub 2011/04/26.
21. King AD, Mo FK, Yu KH, Yeung DK, Zhou H, Bhatia KS, et al. Squamous cell carcinoma of the head and neck: diffusion-weighted MR imaging for prediction and monitoring of treatment response. *Eur Radiol.* 2010;20(9):2213-20. Epub 2010/03/24.
22. Vandecaveye V, Dirix P, De Keyzer F, de Beeck KO, Vander Poorten V, Roebben I, et al. Predictive value of diffusion-weighted magnetic resonance imaging during chemoradiotherapy for head and neck squamous cell carcinoma. *Eur Radiol.* 2010;20(7):1703-14. Epub 2010/02/25.
23. Peduzzi P, Concato J, Feinstein AR, et al. Importance of events per independent variable in proportional hazards regression analysis. II. Accuracy and precision of regression estimates. *J Clin Epidemiol* 1995;48:1503–10.
24. Mancuso A, Mukherji S, Schmalfluss I, et al. Preradiotherapy computed tomography as a predictor of local control in supraglottic carcinoma. *J Clin Oncol*, 17 (1999), pp. 631–637

R1
R2
R3
R4
R5
R6
R7
R8
R9
R10
R11
R12
R13
R14
R15
R16
R17
R18
R19
R20
R21
R22
R23
R24
R25
R26
R27
R28
R29
R30
R31
R32
R33
R34
R35
R36
R37
R38
R39





7

**Prospective comparative study of diffusion-weighted MRI
versus FDG PET-CT for the detection of recurrent head and neck
squamous cell carcinomas after (chemo)radiotherapy**

J.P. Driessen
M.E.P. Philippens
J.E. Huijbregts
F.A. Pameijer
L.M. Janssen
W. Grolman
C.H.J. Terhaard

Submitted

Abstract

Purpose: This prospective study aimed to compare the diagnostic accuracy of diffusion-weighted MRI (DW-MRI) to FDG PET-CT in the detection of local recurrent head and neck squamous cell carcinomas after (chemo)radiation ((C)RT).

Materials and Methods: The institutional ethical committee approved this study and all patients signed written informed consent. Seventy-five patients clinically suspected of local recurrence after (C)RT for laryngeal, hypopharyngeal or oropharyngeal cancer underwent a DW-MRI and an FDG PET-CT. Qualitative assessment of DW-MRI and FDG PET-CT was performed independently by a blinded experienced radiologist and a nuclear medicine physician respectively. Reference standard was the absence of biopsy proven local recurrence within 6 months following imaging.

Results: Seventy patients were suitable for analysis. Fifty percent (35/70) had local recurrence. Seventy-three percent (51/70) of the FDG PET-CTs were positive compared to 46% (32/70) of the DW-MRI. FDG PET-CT had an area under the curve 0.71 compared to 0.73 for MR-DWI ($p=0.85$). The sensitivity of FDG PET-CT was 97% compared to 69% for DW-MRI ($p<0.01$). The specificity of FDG PET-CT was 46% compared to 77% for DW-MRI ($p<0.01$).

Conclusions: DW-MRI showed similar diagnostic accuracy, superior specificity but inferior sensitivity compared to FDG PET-CT. False negative results will cause delay in the detection of a recurrence and this will potentially influence the chance of successful salvage surgery. Therefore, based on these results, we consider FDG PET-CT to be superior to MR-DWI for the detection of early recurrent oropharyngeal, hypopharyngeal or laryngeal cancer after (chemo)radiation.

Advances in knowledge:

- Diffusion-weighted MRI and FDG PET-CT have similar diagnostic accuracy for the detection of local recurrence in oropharyngeal, hypopharyngeal or laryngeal cancer after (chemo)radiation (area under the curve 0.73 resp. 0.71; $p=0.85$)
- The sensitivity of FDG PET-CT was 97% compared to 69% for diffusion-weighted MRI ($p<0.01$).
- The specificity of FDG PET-CT was 46% compared to 77% for diffusion-weighted MRI (<0.01).
- FDG PET-CT has a false positive rate of 54% compared to 23% of diffusion-weighted imaging.
- Diffusion-weighted MRI has a false negative rate of 31% compared to 3% for FDG PET-CT.

Implications for patient care:

- FDG PET-CT is superior to DW-MRI in the early detection of local recurrence of head and neck cancer after (chemo)radiation due to the superior sensitivity of FDG PET-CT.

Introduction

Patients with head and neck squamous cell carcinomas (HNSCC) are increasingly treated with (chemo)radiotherapy ((C)RT) due to improved radiotherapy techniques and its advantage of organ preservation. Depending on subsite and tumor stage, loco-regional recurrence rates vary from less than 5% up to 55% after (C)RT. (1, 2) Early detection of local recurrences is one of the main objectives during follow-up as delayed detection reduces the chance of successful salvage surgery and may decrease survival rates. However, discrimination between local recurrence and post-radiation effects is known to be a difficult clinical problem. (3) Post-radiation effects such as fibrosis, edema and inflammation may mimic tumor recurrence. Approximately 50% of patients who present with these symptoms will have local recurrence. (4)

Gold standard for the existence of a local recurrence is biopsy-proven squamous cell carcinomas. However, a negative biopsy does not exclude a local recurrence due to sampling error. Unnecessary biopsies in previously radiated areas are undesirable as they can lead to wound healing problems. (5) An accurate selection strategy that reduces the number of patients requiring a biopsy without compromising early detection of residual disease is therefore of great interest. Several studies have shown the value of fluorine 18 (¹⁸F) fluorodeoxyglucose (FDG) PET-CT in the detection of local recurrence after (C)RT. (6, 7) This technique is described to have high negative predictive value, but is limited by false positive results due to FDG avidity in inflammation. (8)

A relative new imaging technique in head and neck cancer is diffusion-weighted magnetic resonance imaging (DW-MRI). DW-MRI is a functional MRI technique that quantifies the restriction of random motion of water molecules in tissues by the apparent diffusion coefficient (ADC). This diffusion coefficient reflects the microenvironment of tissues, where higher cell density leads to more diffusion restriction of water molecules. DW-MRI is described to accurately discriminate malignant lesions from benign and is increasing subject of research in several oncologic imaging applications. (9, 10) Recent results suggest that DW-MRI might be superior to PET-CT in the detection of local recurrences. (11-13) The present prospective study aimed to compare the diagnostic accuracy of DW-MRI to PET-CT in the detection of local recurrent HNSCC after (C)RT in patients with clinical suspicion of local residual or recurrence disease.

Methods

The institutional ethical committee approved this study and written informed consent was obtained from all participants.

Patients

Seventy-five patients were consecutively and prospectively included in this study between April 2011 and November 2014. Patients clinically suspected of local recurrence after (C)RT for HNSCC underwent as standard procedure an FDG PET-CT and an additional investigational MRI with diffusion-weighted MRI. Inclusion criteria were patients with laryngeal, hypopharyngeal or oropharyngeal cancer with clinical suspicion of local recurrence between 3 months and 3 years after the end of primary (chemo)radiation with curative intent. Oropharyngeal tumors received 69 Gy in 33 fractions in 6 weeks. Small glottic tumors received 60 Gy in 25 fractions in 5 weeks. In all other cases a total dose of 70 Gy in 35 fractions in 7 weeks was given. In case of concurrent chemotherapy 100 mg/m² intravenous Cisplatin was added at day 1, 22 en 43. In case of contraindication for chemotherapy the radiation was combined with Cetuximab. Clinical suspicion of local recurrence was defined by presentation with new, persistent or progressive symptoms, or suspicious findings during physical examination. Patients in whom, based on physical examination, local recurrence was so obvious that there was no reasonable doubt were not included in this study. Qualitative assessment of DW-MRI and FDG PET-CT was performed by an experienced radiologist resp. nuclear medicine physician blinded for the other modality. Reference standard was the absence of a biopsy proven local recurrence within 6 months following imaging. See figure 1 for study flow-chart.

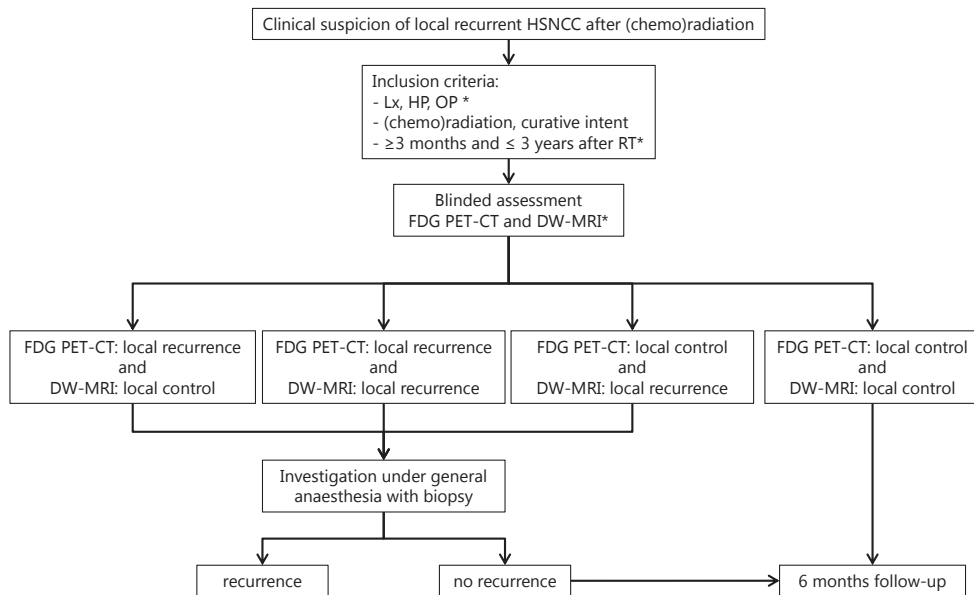


FIGURE 1. Flow-chart of study design

Lx: laryngeal cancer, HP: hypopharyngeal cancer, OP: oropharyngeal cancer, RT: radiotherapy, DW-MRI: diffusion-weighted MRI.

Imaging

MRI was performed on a 3 Tesla unit (Intera NT, Philips Medical Systems, Best, the Netherlands) using a dedicated head and neck coil. The conventional MRI included a transverse T1-weighted turbospin-echo (TSE) before and after gadolinium, a transverse and coronal T1-weighted spectral presaturation with inversion recovery (SPIR) after admission of gadolinium and a transverse and coronal proton density SPIR. Echo-planar DWI was performed in the transverse plane. Four diffusion gradient b values (0, 100, 500 and 1,000 s/mm²) were applied in three orthogonal directions, minimizing the effects of diffusion anisotropy. For the latest 20 patients an extra diffusion sequence with split acquisition of fast spin-echo (SPLICE) technique was added due to progress in the development of protocols without the characteristic geometric distortions in conventional DW-MRI. ADC maps were calculated from the DW images using all three b values and a mono-exponential model. See table 1 for the imaging parameters.

TABLE 1. Imaging parameters

	ST (mm)	S	IG (mm)	RT (ms)	ET (ms)	FS	M	FOV (mm ²)
Transverse T1w TSE	4	33	0	653	16	-	268x211	240x218
Transverse PD TSE SPIR	4	33	0	2818	25	SPIR	240x183	240x200
Coronal PD TSE SPIR	3	30	0.3	2486	25	SPIR	220x171	220x196
Transverse T1w TSE Gd	5	43	0.8	653	16	-	240x209	240x220
Transverse T1w TSE SPIR Gd	4	33	0	703	16	SPIR	240x192	240x222
Coronal T1w TSE SPIR Gd	3	30	0.3	703	16	SPIR	220x175	220x196
Transverse DWI EPI SPIR	4	27	1	2588	68	SPIR	116x116	230x266
Transverse DWI SPLICE	4	30	0	17305	165	SPIR	124x124	250x250

ST: slice thickness, S: number of slices, IG: intersection gap, RT: repetition time, ET; echo time, FS: fat suppression, M: matrix, FOV: field of view, T1w: T1-weighted, TSE: turbospin-echo, PD: proton density, SPIR: spectral presaturation with inversion recovery, Gd: gadolinium, DWI: diffusion-weighted imaging, EPI: echo-planar imaging, SPLICE: split acquisition of fast spin-echo

The FDG PET-CTs were performed on a whole body PET-CT scanner (Biograph mCT, Siemens Medical Systems, Erlangen, Germany) approximately one hour after injection of 2,0 MBq/

R1 kg of ^{18}F -FDG after a 6-hour fasting period. To increase the detection sensitivity, both a
R2 dedicated head and neck scan and a whole body scan were performed. First, dedicated
R3 head and neck imaging was performed with the arms placed beside the body to minimize
R4 artifacts in the head and neck area. Subsequently, a whole body scan was performed ranging
R5 from the shoulders to the upper thigh with the patient's arms placed above the head. PET
R6 acquisition was preceded by a low dose CT scan (40mAs, slice thickness 3mm). PET images
R7 were acquired in 3D mode with Time of Flight for 4 minutes per bed position for the head
R8 and neck scan and 3 minutes per bed position for the whole body scan. High resolution PET
R9 reconstructions were made with FWHM of 5mm (whole body scan) or FWHM 4mm (head/
R10 neck scan), 4 iterations and 21 subsets.
R11

R12 ***Image assessment***

R13 The MRI including DWI and the FDG PET-CT scan were independently reviewed, blinded
R14 for the other imaging modality and report. The FDG PET-CT scan was assessed by a nuclear
R15 medicine physician with 5 years of experience in head and neck PET-CT scanning (J.H.). The
R16 DW-MRI was assessed in consensus by a radiologist, with more than 15 years of experience
R17 in head and neck imaging, and an ENT resident, with 4 years of experience in head and neck
R18 DWI (F.A.P. and J.P.D.). DWI analysis was performed in conjunction with the conventional
R19 images due to the fact that poor spatial resolution of DWI prevents interpretation on its
R20 own. Both DWI and FDG PET-CT were assessed based on qualitative/visual analysis, e.g.
R21 no apparent diffusion coefficient (ADC) or standard uptake value (SUV) were calculated of
R22 the region of interest. For the DWI hyper-intense signal on the heavily diffusion-weighted
R23 image with a b-value of 1000 s/mm² with corresponding low diffusion coefficients in the
R24 corresponding ADC map was considered positive for local recurrence. Absence of low signal
R25 on the ADC map was considered negative for local recurrence. Only the primary tumor site
R26 was evaluated, lymph nodes were not a subject of this study. Cases could be scored as local
R27 recurrence, local control or inconclusive. All clinical information and all previous imaging,
R28 including pre-treatment imaging were available of all patients.
R29

R30 ***Reference standard***

R31 The local outcome of the patients was determined as follows; If at least one of the imaging
R32 modalities was suspicious for a local recurrence, investigation under general anesthesia was
R33 performed with biopsy of the primary tumor region. If this was negative, or if both imaging
R34 modalities were suggestive of local control, disease free follow-up of 6 months was considered
R35 reference standard for local control.
R36
R37
R38
R39

Sample size and statistical analysis

For the use of DW-MRI to be clinically relevant, the positive and negative predictive value of the DW-MRI should be comparable to the current results of FDG PET-CT. We expect 70% of the DW-MRI to be positive for local recurrence. To prove a positive predictive value of $\geq 70\%$, comparable to the current results of FDG PET-CT, with a precision of $\sim 10\%$ we need to include 75 patients. (7, 14) Diagnostic accuracy, sensitivity, specificity, negative predictive value (NPV), positive predictive value (PPV) and area under the curve (AUC) were calculated for MRI with diffusion-weighted imaging and FDG PET-CT. Sensitivity and specificity were compared with the McNemar test, and the AUC were compared according to the method of Hanley & McNeil (paired data). To explore learning curve we divided our dataset in 3 subsequent time frames; the first 23 DW-MRIs, the subsequent 24 DW-MRIs and the last 23 DW-MRIs and compared sensitivity and specificity using Pearson Chi-square (unpaired data). Data was processed using SPSS (SPSS Inc. v20.0, Chicago, IL, USA) and MedCalc (MedCalc Software v 12.5, Ostend, Belgium)

Results**Patients**

Seventy-five patients were included in this study. Five patients were excluded after inclusion. Four patients due to contraindications or disruption of the MRI (e.g. claustrophobia or patients' stature). One patient was excluded due to the lack of histopathology or follow-up; this patient had a positive DW-MRI and a positive FDG PET-CT, however died of a pneumosepsis 24 hours after the last imaging without biopsy or autopsy. The seventy remaining patients were included due to clinical suspicion of local recurrence, due to new or persistent symptoms including pain, stridor, dysphonia, dysphagia, edema, irregular mucosal surface or vocal cord impairment. Fifty-one patients were male (73%), the median age was 61 years (range 42-81). Thirty-four patients (49%) had laryngeal, 12 (17%) hypopharyngeal and 24 (34%) oropharyngeal cancer. Primary T stage ranged from 1 to 4b, N stage 0 to N2c. All patients were treated with primary fractionated radiotherapy: radiotherapy alone (n=50, 71%), combined with cisplatin (n=11, 16%) or combined with Cetuximab (n=9, 13%). All patients and tumor characteristics are presented in table 2.

TABLE 2. Baseline patient characteristics

Variable	N	%
Age (y) *	61 (42-81)	
Sex		
female	19	27
male	51	73
Tumor site		
larynx	34	49
supraglottic	17	50 †
glottic	16	47 †
subglottic	1	3 †
hypopharynx	12	17
oropharynx	24	34
AJCC tumor stage		
T1	12	17
T2	20	29
T3	23	33
T4a	14	20
T4b	1	1
Nodal stage		
N0	39	56
N1	7	10
N2a	2	3
N2b	12	17
N2c	10	14
Treatment		
Radiotherapy	50	71
Chemoradiotherapy	11	16
Radiotherapy + Cetuximab	9	13

* Median (range), † Percentage within subsite, AJCC: American Joint Committee on Cancer

Histopathology

Thirty-five patients (50%) had local recurrence, of which 33 were histologically proven by the first biopsy after imaging. One patient had initially negative biopsy, but due to persistent clinical suspicion for recurrence a second endoscopy with biopsy was performed after 4 weeks which confirmed recurrent disease. Finally, one patient with a positive DW-MRI and a positive FDG PET-CT refrained from biopsy. This patient had clinical progressive local disease combined with progressive alterations seen on repeated imaging (CT and conventional MRI). Therefore, this patient was considered as having recurrent disease. The remaining thirty-five patients had no biopsy proven recurrence within 6 months after inclusion for this study. Twenty-one had negative biopsy, and fourteen of these patients had no biopsy but at least 6 months' disease free follow-up.

Imaging

Median time between DW-MRI and FDG PET-CT was one day (0-31 days). All images were of sufficient quality to be evaluated. For the FDG PET-CT the plasma glucose of each patient was <10 mmol/l, except for one who had a plasma glucose of 12.5 mmol/l. Seventy-three percent (51/70) of the FDG PET-CTs were positive for local recurrence compared to only 46% (32/70) of the DW-MRI. Two FDG PET-CTs were inconclusive. For the calculation of the diagnostic accuracy, inconclusive imaging results were regarded as positive, because in clinical practice, these patients you would not refrain from endoscopy with biopsy. FDG PET-CT had a similar diagnostic accuracy compared to DW-MRI (area under the curve of 0.71 versus 0.73 for DW-MRI ($p=0.85$)). The sensitivity of FDG PET-CT was significantly superior compared to MR-DWI (97% versus 69%; $p<0.01$). The specificity of FDG PET-CT was significantly inferior compared to DW-MRI (46% versus 77%; $p<0.01$). DW-MRI had a false negative rate of 31% (11/35) compared to 3% for FDG PET-CT (1/35). See table 3 and 4 for the complete results. See figure 2 and 3 for an example of the images obtained from an included patient.

TABLE 3. Results of DW-MRI and FDG PET-CT

Imaging	Local recurrence	Local control	total
DW-MRI positive	24	8	32
DW-MRI negative	11	27	38
FDG PET-CT positive	33	18	51
FDG PET-CT negative	1	16	17
FDG PET-CT inconclusive	1	1	2

DW-MRI: diffusion-weighted MRI, FDG PET-CT: 18F-fluorodeoxyglucose positron emission tomography-computed tomography

TABLE 4. Diagnostic accuracy of DW-MRI and FDG PET-CT

	FDG PET-CT	(95% CI)	DW-MRI	(95% CI)	p-value
Sensitivity	97	(85-100)	69	(51-83)	<0.01 *
Specificity	46	(29-63)	77	(60-90)	<0.01 *
Area under the curve	0.71	(0.59-0.82)	0.73	(0.61-0.83)	0.85 †
Accuracy	72		73		
Positive predictive value	64	(50-77)	75	(57-89)	
Negative predictive value	94	(71-100)	71	(54-85)	
False positive rate	54		23		
False negative rate	3		31		

DW-MRI: diffusion-weighted MRI, FDG PET-CT: 18F-fluorodeoxyglucose positron emission tomography-computed tomography, * McNemar test, † Hanley & McNeil

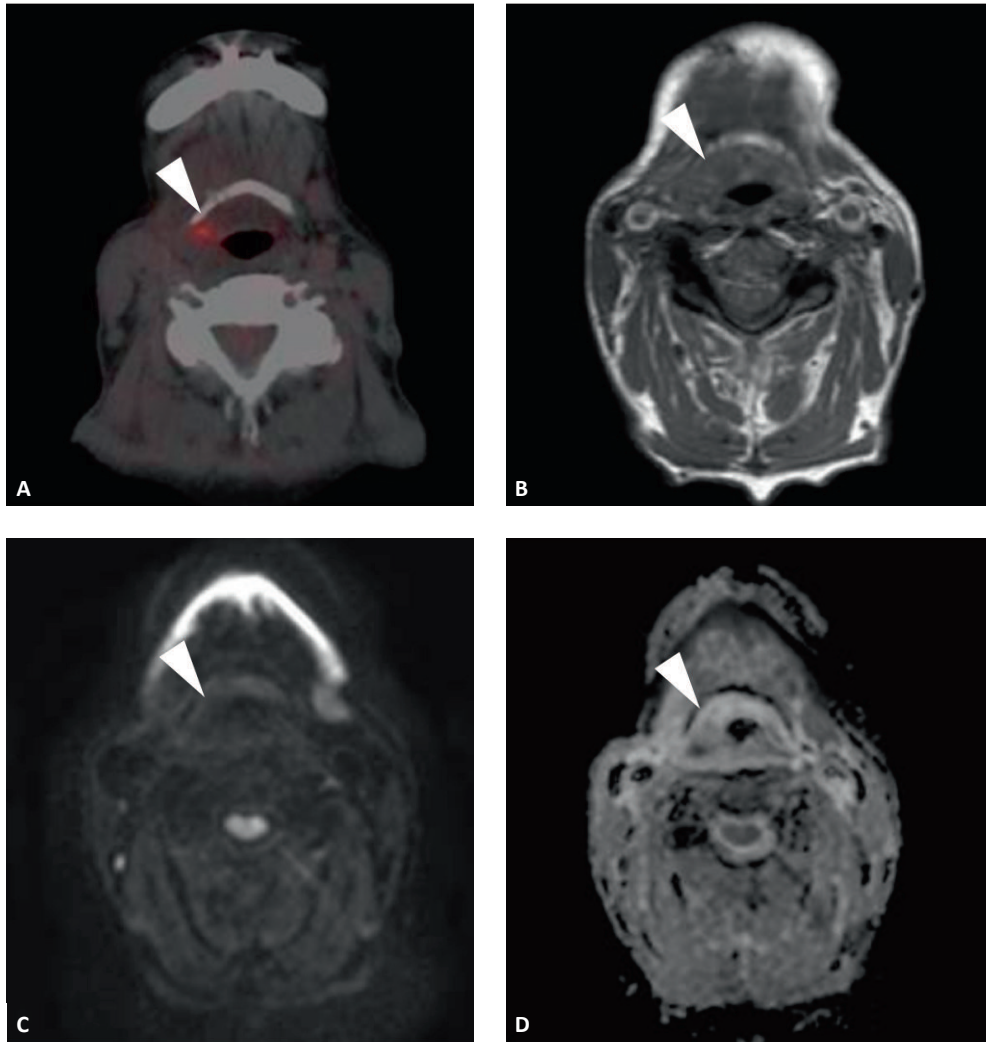


FIGURE 2. (A-D) Example of an included patient. 42-year-old-man with T2N1M0 oropharyngeal carcinoma in the right vallecula. Seven months after radiotherapy he presented with asymmetry in the vallecula and an ulcer in the right vallecula. **(A)** FDG PET-CT shows metabolic activity at the primary site suspicious of a recurrent carcinoma (arrow). **(B)** T1w MRI shows swelling of the vallecula at the primary tumor site (arrow). **(C)** DWI B1000 shows no increased signal intensity and no diffusion restriction on ADC therefore there was no suspicion of recurrence based on the DW-MRI **(D, arrow)**. Histology confirmed recurrence of a squamous cell carcinoma.

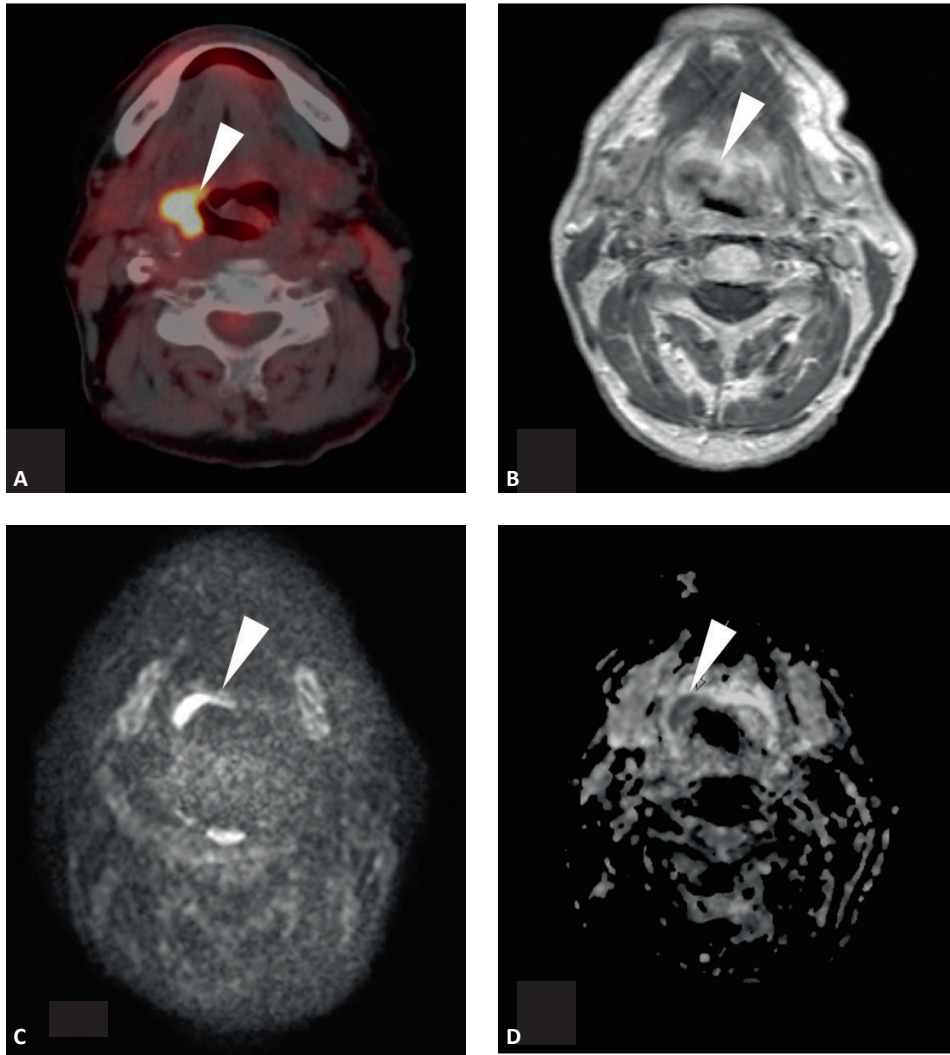


FIGURE 3. (A-D) Example of an included patient. 81-year-old-man with T4aN2cM0 oropharyngeal carcinoma in the right base of tongue. Thirteen months after chemoradiotherapy with Cetuximab he presented with progressive otalgia. **(A)** FDG PET-CT shows metabolic activity at the primary site suspicious of a recurrent carcinoma (arrow). **(B)** T1w contrast-enhanced MRI shows a hypodense region at the primary tumor site (arrow). **(C)** DWI B1000 shows increased signal intensity with corresponding diffusion restriction on ADC **(D, arrow)**. Histology confirmed recurrence of a squamous cell carcinoma.

R1
R2
R3
R4
R5
R6
R7
R8
R9
R10
R11
R12
R13
R14
R15
R16
R17
R18
R19
R20
R21
R22
R23
R24
R25
R26
R27
R28
R29
R30
R31
R32
R33
R34
R35
R36
R37
R38
R39

Diagnostic accuracy in time and according to imaging-protocol

For our institution diffusion-weighted imaging was a relative new sequence added to the regular protocol when this study started. Our head and neck radiologist had approximately one-year experience with DWI in head and neck, but mostly in imaging of primary tumors. Therefore, our results might reflect a learning curve for DW-MRI. When analyzed divided by time frame (first 23, subsequent 24 and the last 23 DW-MRIs) sensitivity ranged from 62% for the first timeframe, 58% for the second and 80% for the last timeframe ($p=0.44$). Specificity ranged from 93% to 58% to 75% ($p=0.10$). When dividing the dataset to the patients scanned with the DWI-EPI protocol and with both the DWI-EPI and the SPLICE protocol, no substantial differences were found; sensitivity was 64% versus 78% ($p=0.41$) and specificity 75% versus 86% ($p=0.55$).

Discussion

The present prospective study is the first study comparing FDG PET-CT and DW-MRI regarding the detection of recurrence of oropharyngeal, hypopharyngeal or laryngeal cancer. It shows that DW-MRI has a similar diagnostic accuracy as FDG PET-CT (AUC 0.73 compared to 0.71; $p=0.85$). DW-MRI has superior specificity but inferior sensitivity compared to FDG PET-CT (specificity 77% versus 46%, sensitivity 69% versus 97%; $p<0.01$). During follow-up after (chemo)radiation, early detection of residual or recurrent disease is one of the main objectives as salvage surgery might still be a curative option for a local recurrence. Delayed recognition of recurrent disease might lead to irresectability, regional or distant metastasis and therefore decreased survival rates. (15-17) When imaging is used as a selection strategy to prevent unnecessary endoscopy with biopsy under general anesthesia, the most important aim is to reliably rule out the existence of a recurrence and hereby safely refraining from endoscopy. Therefore, in this scenario, a high sensitivity is the most important feature of an imaging modality. False negative results of a selection strategy can have tremendous effects; they will cause delay in detection of recurrences and therefore will potentially influence the chance of successful salvage surgery. Therefore, based on these results, we consider FDG PET-CT to be superior to MR-DWI in the early diagnosis of recurrence of HNSCC after (C)RT.

Few studies have shown the diagnostic accuracy of DW-MRI in head and neck cancer after (C)RT, most of them showing excellent results with accuracies up to 98%. (12, 13) Compared to literature our results concerning DW-MRI are somewhat disappointing. This might be because we included patients based on 'clinical suspicion of local recurrence'. This is prone to subjectivity, which might be physician, institution and study dependent. Also the design of this study facilitates the inclusion of very early recurrences and therefore very small lesions which may be under or at the border of the detection limit. Diffusion-weighted imaging

suffers from relative low spatial resolution, making it less suitable for detection of very small tumor residues. Partial volume effects will prevent diffusion restriction to stand out at the ADC map. However, the results of FDG PET-CT are comparable to literature, so that disputes the fact that our study design does not resembles clinical practice.

Forty-nine percent of the patients had laryngeal tumors. The larynx, compared to other regions of the head and neck is especially known for movement and susceptibility artefacts. FDG PET-CT will be more forgivable for movement artefacts such as swallowing and breathing cause of the faster acquisition. In addition, previous studies on DW-MRI, reported on small number of patients and used repeated imaging to detect the recurrent or residual tumors. (12) Repeated imaging will always lead to better results, because findings on imaging can be related to previous imaging and progression of suspicious findings makes a recurrence more likely.

There are no studies available comparing the diagnostic accuracy of DW-MRI with other imaging modalities in the same set of patients. In our study, we chose visual e.g. qualitative assessment of DW-MRI instead of quantitative ADC measurements because it closely resembles clinical practice. Radiologists usually visually judge MRIs and base their final decision on the existence of recurrence on a combination of information given by all sequences, rather than based on one solitary measure of for example ADC. Also, quantitative ADC measurements is dependent on the placement of a region of interest within an ADC map, and therefore highly variable with low repeatability. Furthermore, using ADC as a discriminating tool for recurrence or benign lesions also comes with challenges and questions such as which ADC threshold to use and its reproducibility on other type of scanners and protocols. Even though quantitative ADC measures are described to have significantly different mean values in benign compared to malignant lesions, there is extensive overlap between ADC values of malignant and benign lesions. (11, 18) This limits its use on individual patients. Qualitative e.g. visual assessment has limitations as well; as it is subjective and might have a learning curve; however, our data of the diagnostic accuracy divided in three time-frames showed no time trends.

One strength of this study is the design, in which biopsy served as the reference standard or disease free follow-up of six months. The extra time frame of six months' disease free follow-up was incorporated to prevent sampling errors of negative biopsies. Indeed, there was one subject in which biopsy was negative at first but turned out positive after 4 weeks during a second endoscopy because of persistent clinical suspicion of local disease. One could argue that 6 months might be too short, however a longer interval might introduce a scenario where a recurrent disease developed after the imaging.

Our study has limitations. First, the diffusion-weighted MRI was evaluated in combination with the anatomical images of the conventional MRI. This resembles clinical practice, as the diffusion-weighted images suffer from low resolution and lack anatomical landmarks these images should always be viewed in context of other MRI sequences. Therefore, our results

R1
R2
R3
R4
R5
R6
R7
R8
R9
R10
R11
R12
R13
R14
R15
R16
R17
R18
R19
R20
R21
R22
R23
R24
R25
R26
R27
R28
R29
R30
R31
R32
R33
R34
R35
R36
R37
R38
R39

R1 reflect MRI including DWI, and does not study the addition of DWI to conventional MRI
R2 sequences. Secondly, the images could be compared to pre-therapeutic imaging available.
R3 However, both the radiologist, reviewing the DW-MRI, and the nuclear medicine physician,
R4 examining the FDG PET-CT had access to the same pre-therapeutic scans and patient
R5 information. Pre treatment imaging consisted of conventional CT, MRI and sometimes FDG
R6 PET-CT. None of the patients had diffusion-weighted MRI as pre-therapeutic imaging, neither
R7 there was any post therapeutic baseline imaging available. Finally, not all patients had biopsy
R8 as a reference standard, since 14 patients were considered as local control based on negative
R9 DW-MRI and negative FDG PET-CT combined with 6 months' disease free follow-up. Because
R10 of the high negative predictive value of FDG PET-CT we felt that it was ethically incorrect to
R11 expose these patients to unnecessary general anesthesia with biopsy.

R12 In conclusion, FDG PET-CT is superior to DW-MRI in the early detection of recurrent
R13 oropharyngeal, hypopharyngeal or laryngeal cancer after (chemo)radiation. Though having
R14 similar accuracies, DW-MRI suffers from false negative results. When early detection of
R15 recurrences is the main goal, false negatives lead to delayed detection and might lead to
R16 irresectability and decreased survival rates. FDG PET-CT has significantly inferior specificity
R17 compared to DW-MRI due to its relatively high false positive rate of 54%. However, this is
R18 less fateful in a post-therapeutic setting where early detection of residual disease is the main
R19 objective. Based on current results, we consider FDG PET-CT to be superior to MR-DWI as the
R20 choice of imaging when local recurrent disease of HNSCC after (C)R is suspected.
R21
R22
R23
R24
R25
R26
R27
R28
R29
R30
R31
R32
R33
R34
R35
R36
R37
R38
R39

1. Forastiere AA, Goepfert H, Maor M, Pajak TF, Weber R, Morrison W, et al. Concurrent chemotherapy and radiotherapy for organ preservation in advanced laryngeal cancer. *N Engl J Med*. 2003;349(22):2091-8. Epub 2003/12/03.
2. Spector GJ, Sessions DG, Lenox J, Newland D, Simpson J, Haughey BH. Management of stage IV glottic carcinoma: therapeutic outcomes. *Laryngoscope*. 2004;114(8):1438-46. Epub 2004/07/29.
3. Zbaren P, Weidner S, Thoeny HC. Laryngeal and hypopharyngeal carcinomas after (chemo)radiotherapy: a diagnostic dilemma. *Curr Opin Otolaryngol Head Neck Surg*. 2008;16(2):147-53. Epub 2008/03/11.
4. O'Brien PC. Tumour recurrence or treatment sequelae following radiotherapy for larynx cancer. *J Surg Oncol*. 1996;63(2):130-5. Epub 1996/10/01.
5. Valentino J, Spring PM, Shane M, Arnold SM, Regine WF. Interval pathologic assessments in patients treated with concurrent hyperfractionated radiation and intraarterial cisplatin (HYPERRADPLAT). *Head Neck*. 2002;24(6):539-44. Epub 2002/07/12.
6. Krabbe CA, Pruim J, Dijkstra PU, Balink H, van der Laan BF, de Visscher JG, et al. 18F-FDG PET as a routine posttreatment surveillance tool in oral and oropharyngeal squamous cell carcinoma: a prospective study. *J Nucl Med*. 2009;50(12):1940-7. Epub 2009/11/17.
7. Terhaard CH, Bongers V, van Rijk PP, Hordijk GJ. F-18-fluoro-deoxy-glucose positron-emission tomography scanning in detection of local recurrence after radiotherapy for laryngeal/ pharyngeal cancer. *Head Neck*. 2001;23(11):933-41. Epub 2002/01/05.
8. de Bree R, van der Putten L, Brouwer J, Castelijns JA, Hoekstra OS, Leemans CR. Detection of locoregional recurrent head and neck cancer after (chemo)radiotherapy using modern imaging. *Oral Oncol*. 2009;45(4-5):386-93. Epub 2008/12/20.
9. Koh DM, Padhani AR. Diffusion-weighted MRI: a new functional clinical technique for tumour imaging. *Br J Radiol*. 2006;79(944):633-5. Epub 2006/06/24.
10. Padhani AR. Diffusion magnetic resonance imaging in cancer patient management. *Semin Radiat Oncol*. 2011;21(2):119-40. Epub 2011/03/02.
11. Abdel Razek AA, Kandeel AY, Soliman N, El-shenshawy HM, Kamel Y, Nada N, et al. Role of diffusion-weighted echo-planar MR imaging in differentiation of residual or recurrent head and neck tumors and posttreatment changes. *AJNR Am J Neuroradiol*. 2007;28(6):1146-52. Epub 2007/06/16.
12. Tshering Vogel DW, Zbaeren P, Geretschlaeger A, Vermathen P, De Keyzer F, Thoeny HC. Diffusion-weighted MR imaging including bi-exponential fitting for the detection of recurrent or residual tumour after (chemo)radiotherapy for laryngeal and hypopharyngeal cancers. *Eur Radiol*. 2013;23(2):562-9. Epub 2012/08/07.
13. Vandecaveye V, De Keyzer F, Nuyts S, Deraedt K, Dirix P, Hamaekers P, et al. Detection of head and neck squamous cell carcinoma with diffusion weighted MRI after (chemo)radiotherapy: correlation between radiologic and histopathologic findings. *Int J Radiat Oncol Biol Phys*. 2007;67(4):960-71. Epub 2006/12/05.
14. Brouwer J, de Bree R, Comans EF, Akarriou M, Langendijk JA, Castelijns JA, et al. Improved detection of recurrent laryngeal tumor after radiotherapy using (18)FDG-PET as initial method. *Radiother Oncol*. 2008;87(2):217-20. Epub 2008/03/11.
15. Davidson J, Keane T, Brown D, Freeman J, Gullane P, Irish J, et al. Surgical salvage after radiotherapy for advanced laryngopharyngeal carcinoma. *Arch Otolaryngol Head Neck Surg*. 1997;123(4):420-4. Epub 1997/04/01.
16. Goodwin WJ, Jr. Salvage surgery for patients with recurrent squamous cell carcinoma of the upper aerodigestive tract: when do the ends justify the means? *Laryngoscope*. 2000;110(3 Pt 2 Suppl 93):1-18. Epub 2000/03/14.
17. Ho AS, Kraus DH, Ganly I, Lee NY, Shah JP, Morris LG. Decision making in the management of recurrent head and neck cancer. *Head Neck*. 2014;36(1):144-51. Epub 2013/03/09.
18. Gouhar G, El-Hariri M. Feasibility of diffusion weighted MR imaging in differentiating recurrent laryngeal carcinoma from radionecrosis. *The Egyptian Journal of Radiology and Nuclear Medicine*. 2011(42):169-75.





8

Summary and general discussion

Chapter 8

R1
R2
R3
R4
R5
R6
R7
R8
R9
R10
R11
R12
R13
R14
R15
R16
R17
R18
R19
R20
R21
R22
R23
R24
R25
R26
R27
R28
R29
R30
R31
R32
R33
R34
R35
R36
R37
R38
R39

In this thesis we study the use of diffusion weighted MRI (DW-MRI) in head and neck squamous cell carcinomas (HNSCC). DW-MRI is an established technique in the early detection of acute stroke, and is increasingly subject of research in several oncologic imaging applications. (1-3) DW-MRI can be performed with most standard MR systems, takes only a few minutes and needs no contrast agent administration. The main goal of this thesis is to evaluate the potential of DW-MRI to add value to the current clinical practice in treatment of HNSCC. From early after diagnosis, in tumor characterization, to later on in the post treatment phase in early detection of recurrent disease.

Challenges in the treatment of HNSCC

With the rise of intensity modulated radiotherapy it became possible to give a high dose of radiation to the tumor with simultaneous preservation of surrounding organs at risk. (4) The development of this technique has led to increased use of primary (chemo)radiotherapy for HNSCC. Unfortunately, depending on primary stage and subsite, up to 50% of the patients will develop recurrence. (5-7) Consequently, salvage surgery has become an important procedure in case of recurrence. The success of secondary salvage surgery depends on the extent of the tumor. The tumor must be operated with radical margins because no additional radiotherapy can be given. Therefore, early detection of recurrent or residual disease after (chemo)radiation ((C)RT) is of uttermost importance. (8, 9) In the follow-up of HNSCC after (C)RT it is one of the main objectives. (10, 11) Local recurrence often presents with symptoms or clinical findings at physical examination. These symptoms or findings include dysphonia, dysphagia, otalgia or suspect mucosal lesions. However, post radiation effects may present with similar complaints. (12) Local recurrence is proven by biopsy of the site of the index tumor. For HNSCC this often needs general anesthesia. In addition, biopsies in previous radiated tissue can cause pain and wound healing problems. Ideally, an accurate selection strategy would reduce the number of patients requiring a biopsy without compromising early detection of residual disease. Using computed tomography (CT), magnetic resonance imaging (MRI) and nuclear imaging such as fluorodeoxyglucose positron emission tomography combined with CT (FDG PET-CT) the differentiation of recurrence and post therapeutic alterations remains a challenge. (13) A second challenge in the treatment of HNSCC is the pretreatment stratification of patients for the optimal treatment, considering quality of life and cure. Some tumors are less sensitive to radiation than expected. Accurate and reliable identification of these radiotherapy non-responders would be a step towards personalized cancer care for patients suffering from HNSCC. (14) These patients could then be selected for primary surgical intervention.

Current practice in the Netherlands

As mentioned, after primary (C)RT for HNSCC, early detection of residual or recurrent disease is crucial for successful salvage surgery. However, national and international guidelines have no consensus concerning the content of the follow-up of HNSCC after (C)RT. International guidelines widely differ in the recommendation on the frequency of consultation, duration of follow-up and use of imaging modalities in the follow-up after (C)RT for HNSCC. In **chapter 2** we have performed an online survey among clinical physicians treating HNSCC in the Netherlands which are connected to the Dutch Head and Neck Society. With detection of recurrences being one of the main objectives, it is important to have knowledge of the most effective strategy. Regrettably, international guidelines have well defined pretreatment and therapy recommendations, but their suggestions concerning follow-up is limited. This nation-wide survey revealed that most institutions have a follow-up of 5 years after (C)RT. Follow-up is intensive in the first 3 years after (C)RT, when risk of loco-regional recurrence is known to be high. Consultation once every 2-3 months within the first year, and every 6 months for the subsequent 2 years. However, the survey revealed that especially the use and timing of imaging during follow-up of HNSCC varied widely. About half of the respondents systematically performed baseline post-treatment imaging, while others only used it when local recurrence was suspected. They responded that a high positive predictive value (PPV) was the most important feature of an imaging modality. It should be noticed that, if early detection of recurrence is the main objective, a high negative predictive value (NPV) might be more relevant than a high PPV. In that situation, the main objective is to accurately rule out recurrence; and that is mostly reflected by a high NPV or high sensitivity. The use of DW-MRI during follow-up of HNSCC was only mentioned by only a few respondents. The substantial variation of answers illustrates the need for international guidelines. These guidelines should not only focus on the duration and interval of consultations, but also include recommendations concerning the indication and use of additional imaging modalities as well as the imaging modality of preference. DW-MRI could be one of the imaging modalities with great potential.

The potential of DW-MRI

Chapter 3 describes a systematic review of the current literature on the use of DW-MRI in HNSCC. (15) We divided this review into three review questions; the diagnostic accuracy of DW-MRI in detection of primary tumors, nodal staging and detection of local recurrences. We selected studies according to the recommendations of the QUADAS (Quality Assessment of Diagnostic Accuracy Studies). (16) The first striking point of our search was the sparseness of literature with a suitable methodology to address our research question. In the end, we could

only include 10 studies. Most studies were excluded because of a case-control design. To study diagnostic accuracy an appropriate design is to include patients suspected or at risk of a specific diagnosis, as case-control studies risk the chance of overestimation of the diagnostic accuracy. (16) Our review revealed that DW-MRI shows no added value in detection of primary HNSCC, since the reported NPV was not superior to conventional MRI, CT and FDG PET-CT. It also revealed that DW-MRI might have potential in nodal staging, and discrimination of recurrence from post treatment changes. For nodal staging, the three included studies showed a sensitivity of 84-92% and a NPV of 91-99%. These results are superior to those reported of FDG PET, where a recent meta-analysis of Kyzas et al. found a pooled sensitivity of 79%, and other studies reported NPV from 71-93%. For the detection of recurrent HNSCC after (C)RT, the reported NPV of DW-MRI ranged from 77-100%, comparable to the results of FDG PET-CT. However, the PPV of DW-MRI was 91-100%, much higher than the 64-77% PPV of FDG PET-CT. In conclusion, DW-MRI might be promising in the use of nodal staging and detection of recurrence of HNSCC after (C)RT.

The reflection of tumor characteristics by DW-MRI

In HNSCC, current therapy stratification is mainly based on the TNM-classification and not on tumor-specific characteristics. Ideally, treatment could be tailored on individual characteristics of patient and tumor specific features. It has been reported that pre-treatment apparent diffusion coefficient (ADC) derived from DW-MRI is able to predict local outcome. (17-19) This might become an important application for treatment personalization and pave the road for more personalized cancer treatment. Several studies report a correlation between high pretreatment ADC and local failure of (C)RT. (20, 21) However, the microanatomical background of this correlation has not been fully understood; it is often hypothesized that this correlation is explained by necrotic parts of the tumor. Necrotic parts within the tumor will cause a higher ADC. Tumors with high percentage of necrosis due to hypoxia are known to be less sensitive for radiotherapy treatment, so it is often hypothesized that a pretreatment high ADC is prognostic less favorable. (22) To explore this hypothesis, we studied the microanatomical background of DW-MRI in **chapter 4 and 5**. These two chapters aim to give us insight and understanding of the reflection of ADC on microscopic level. In **chapter 4** we correlated histopathological findings on whole mount laryngectomy specimens with the presurgical ADC derived from DW-MRI. (23) We investigated the correlation between cellular density, amount of nuclear, cytoplasmic and stromal area to ADC. We showed that high ADC reflects low cell density and a large stromal area. The inverse correlation between ADC and cell density reinforces the hypothesis that higher cellularity, with more densely packed cells, causes restriction of water diffusion and as a results a low ADC. Stroma plays

R1
R2
R3
R4
R5
R6
R7
R8
R9
R10
R11
R12
R13
R14
R15
R16
R17
R18
R19
R20
R21
R22
R23
R24
R25
R26
R27
R28
R29
R30
R31
R32
R33
R34
R35
R36
R37
R38
R39

R1 an important role in the support of tumor growth, and has shown to be an independent
R2 prognostic factor for relapse-free period in breast, colon and esophageal carcinomas. (24-
R3 26) This might suggest that the poor prognostic value of a high pre-treatment ADC might be
R4 partly attributed to the tumor-stromal component. In addition, all tumors showed less than
R5 5% necrosis, which enervates the hypothesis that the poor prognosis of a low ADC can be
R6 attributed to necrotic areas.

R7 In **chapter 5** we investigated the correlation between human papillomavirus (HPV) status
R8 and ADC. (27) In the last decade, an increase of the incidence of HNSCC has been observed,
R9 especially in oropharyngeal cancer. (28-30) In contrary to traditional HNSCC patients, these
R10 patients are younger and do not have a typical history of excessive tobacco and alcohol
R11 consumption. Instead, these tumors have been found to contain a high proportion of high
R12 risk HPV. (31, 32) This makes HPV status, besides tobacco and alcohol consumption, an
R13 important risk factor in the development of HNSCC especially in the oropharynx. Just like
R14 HNSCC with low pretreatment ADC, also HPV positive HNSCC have favorable response to (C)
R15 RT. (19, 20, 33, 34) A reason for this favorable response is not exactly known. Therefore, we
R16 investigated the correlation between HPV status and ADC. In **chapter 5** we correlated HPV
R17 status and ADC of 73 oropharyngeal and laryngeal carcinomas. Although we only had 8% HPV
R18 positive tumors, we did find a significant lower ADC in HPV positive tumors compared to
R19 HPV negative tumors. This difference was independent of other patient characteristics such
R20 as tumor volume, subsite, age, T-stage and N-stage. Taken into account that we found low
R21 ADC to correlate with high cell density and low stromal area, it might be that HPV positive
R22 tumors reflect tumors with high cell density and low stromal area. This is supported by the
R23 fact that indeed HPV positive HNSCC often histologically present with small stromal volume.
R24 (35) In addition, it can be hypothesized that the association between a low ADC and a positive
R25 HPV status might explain the favorable local response to radiotherapy of a low ADC.
R26
R27

R28 **Treatment stratification using DW-MRI**

R29
R30 As mentioned before, one of the major challenges in the management of HNSCC is selecting
R31 the right treatment for the individual patient. Identification of nonresponders to radiotherapy
R32 would enable surgery to be given earlier in the treatment process and avoid treatment
R33 induced side effects of failed radiotherapy. Some studies have described DW-MRI to have
R34 potential in prediction of radiosensitivity. (18, 19, 21, 36) However, these studies are sparse,
R35 differ in methodology and outcome measures, and reported contradicting results. The results
R36 of **chapter 4 and 5** in which ADC correlates to stromal area and HPV status supports the
R37 idea that ADC could be able to serve as a predictor of outcome. In **chapter 6** we aimed to
R38 investigate ADC as predictor of local outcome after (C)RT. We studied pretreatment ADC of 75
R39

patients and correlated pretreatment ADC to local outcome and disease specific survival. Our results showed that tumor volume and ADC both were correlated to local outcome. However, when combined in a multivariate model, only volume remained an independent predictor for local response. Few other studies showed, in contrast to our study, a significant correlation between pretreatment ADC and local outcome. These studies differed in methodology, especially in delineation method of the tumor and in the outcome parameter (local, regional, disease specific or overall survival). When discussing tumor radiosensitivity local response or disease specific survival would be the most appropriate outcomes.

Post treatment surveillance using DW-MRI

Another challenge in the management of HNSCC is detection of residual or recurrent disease after (C)RT. As described, an accurate imaging based selection strategy would reduce the number of unnecessary biopsies in radiated areas. Post therapeutic effect mimic tumor recurrence both in symptoms and in findings on imaging. FDG PET-CT is often used after (C)RT, due to its high negative predictive value, but it is limited in its predictive value. (37, 38) Some studies have investigated the diagnostic accuracy of DW-MRI for the detection of local recurrences and showed impressive results with accuracies up to 98%. (39, 40) Therefore, we performed a prospective comparative study of diffusion weighted MRI versus FDG PET-CT for the detection of recurrent HNSCC after (C)RT, described in **chapter 7**. It is the first study comparing FDG PET-CT and DW-MRI regarding the detection of recurrence of oropharyngeal, hypopharyngeal or laryngeal cancer. Our results show that DW-MRI has a similar diagnostic accuracy as FDG PET-CT. However, DW-MRI has inferior sensitivity compared to FDG PET-CT (69% versus 97%). During follow-up after (C)RT, most important is to reliably rule out the existence of a recurrence and hereby safely refraining from biopsy. Therefore, a high sensitivity is the most important as false negative results cause delay in detection of recurrences, which will potentially influence the chance of successful salvage surgery. Based on these results, we consider FDG PET-CT to be superior to MR-DWI in the early diagnosis of recurrence of HNSCC after (C)RT. Compared to literature our results concerning DW-MRI are somewhat disappointing, which might be explained by the inclusion criteria. Inclusion based on 'clinical suspicion of local recurrence' is prone to subjectivity and might cause inclusion even when suspicion is low. The prevalence of recurrence within the study population will influence the diagnostic accuracy. Lower prevalence will make it more likely to find a high negative predictive value. This might partly explain the difference across studies, as other studies had lower prevalence of recurrence compared to our study. (40) Also, other studies had different methodology, included repeated imaging which is inappropriate when testing diagnostic accuracy and will lead to artificial favorable results.

Limitations of extrapolation of DW-MRI results

Current literature, including the content of this thesis on DW-MRI has some limitations. ADC derived from DW-MRI is reported to differ among MRI systems, centers and imaging protocols. Therefore, ADC thresholds used to discriminate malignant versus benign lesions, but also to define low or high pretreatment ADC are not always interchangeable. They are dependent on the variety of b-values, pulse sequences, field strength and anatomic subsite. The choice of b-values influences the sensitivity for slow or fast diffusion water molecules. Low b values are known to reflect perfusion in addition to diffusion. Therefore, when studying diffusion one might be better of choosing higher b-values. (20) When using pretreatment ADC, it is not only highly dependent on the acquisition of the ADC, but also on the technique of tumor delineation. Delineation of tumors might prove difficult on DW-MRI as these images suffer from geometrical distortions compared to native MR images. Furthermore, they are susceptible to artifacts, especially in the inhomogeneous head and neck region. Some authors delineate one axial slide of the tumor to resemble the true ADC of the total tumor. This method remains questionable due to the heterogeneity of HNSCC. (23) This might explain the differences in results across studies, and is an important fact to realize when using the results of studies in clinical setting.

Conclusion and future perspectives

This thesis describes the use of DW-MRI for HNSCC in a broad scope. DW-MRI has not often been used in the management of HNSCC in the Netherlands (**chapter 2**). Recent literature describes DW-MRI to be promising especially in nodal staging and detection of recurrences (**chapter 3**). It is a valuable technique which reflects microanatomy in HNSCC and therefore suitable to characterize HNSCC (**chapter 4 and 5**). Although reported in literature, we found pretreatment ADC not to be an independent predictor for local response (**chapter 6**). With a prospective comparative study, we found DW-MRI to have similar diagnostic accuracy as FDG PET-CT. But due to the superior sensitivity of FDG PET-CT it is superior to DW-MRI when used for early detection of recurrence of HNSCC after (C)RT (**chapter 7**).

Future studies should focus on monitoring of treatment response. Recent studies have reported promising results; strong increase in ADC value early in radiotherapy corresponds to significant better local tumor control. (41-43) If long-term response can be predicted early after the start of therapy it still enables therapy alterations with dose escalation, the addition of chemotherapy or even switching towards surgery. In addition, uniform DW-MRI protocols with identical b-values across studies will enable comparison of study results and meta-analysis. Preferably high b-values are incorporated to reflect diffusion instead of perfusion. In

addition, research should focus on the development of new sequences and reduce artifacts and geometrical distortions.

This thesis shows that DW-MRI is a promising technique in the management of HNSCC, however the exact clinical applications of this technique needs to be established. The results of this thesis will be helpful for future studies investigating the clinical use of DW-MRI in HNSCC.

R1
R2
R3
R4
R5
R6
R7
R8
R9
R10
R11
R12
R13
R14
R15
R16
R17
R18
R19
R20
R21
R22
R23
R24
R25
R26
R27
R28
R29
R30
R31
R32
R33
R34
R35
R36
R37
R38
R39

1. Dunitan, A.J., L.A. Cox, and B.W. Long, Detection of acute stroke with diffusion-weighted MRI. *Radiol Technol*, 1998. 69(6): p. 559-65.
2. Koh, D.M. and A.R. Padhani, Diffusion-weighted MRI: a new functional clinical technique for tumour imaging. *Br J Radiol*, 2006. 79(944): p. 633-5.
3. Padhani, A.R., Diffusion magnetic resonance imaging in cancer patient management. *Semin Radiat Oncol*, 2011. 21(2): p. 119-40.
4. Gregoire, V., et al., Intensity-modulated radiation therapy for head and neck carcinoma. *Oncologist*, 2007. 12(5): p. 555-64.
5. Ritoe, S.C., et al., Screening for local and regional cancer recurrence in patients curatively treated for laryngeal cancer: definition of a high-risk group and estimation of the lead time. *Head Neck*, 2007. 29(5): p. 431-8.
6. Spector, G.J., Distant metastases from laryngeal and hypopharyngeal cancer. *ORL J Otorhinolaryngol Relat Spec*, 2001. 63(4): p. 224-8.
7. Terhaard, C.H., et al., F-18-fluoro-deoxy-glucose positron-emission tomography scanning in detection of local recurrence after radiotherapy for laryngeal/ pharyngeal cancer. *Head Neck*, 2001. 23(11): p. 933-41.
8. Ho, A.S., et al., Decision making in the management of recurrent head and neck cancer. *Head Neck*, 2014. 36(1): p. 144-51.
9. Goodwin, W.J., Jr., Salvage surgery for patients with recurrent squamous cell carcinoma of the upper aerodigestive tract: when do the ends justify the means? *Laryngoscope*, 2000. 110(3 Pt 2 Suppl 93): p. 1-18.
10. Cooney, T.R. and M.G. Poulsen, Is routine follow-up useful after combined-modality therapy for advanced head and neck cancer? *Arch Otolaryngol Head Neck Surg*, 1999. 125(4): p. 379-82.
11. Merckx, M.A., et al., Effectiveness of routine follow-up of patients treated for T1-2N0 oral squamous cell carcinomas of the floor of mouth and tongue. *Head Neck*, 2006. 28(1): p. 1-7.
12. Brouwer, J., et al., Detecting recurrent laryngeal carcinoma after radiotherapy: room for improvement. *Eur Arch Otorhinolaryngol*, 2004. 261(8): p. 417-22.
13. de Bree, R., et al., Advances in imaging in the work-up of head and neck cancer patients. *Oral Oncol*, 2009. 45(11): p. 930-5.
14. Bourhis, J., Hypoxia response pathways and radiotherapy for head and neck cancer. *J Clin Oncol*, 2006. 24(5): p. 725-6.
15. Driessen, J.P., et al., Diffusion-weighted imaging in head and neck squamous cell carcinomas: a systematic review. *Head Neck*, 2015. 37(3): p. 440-8.
16. Whiting, P.F., et al., QUADAS-2: a revised tool for the quality assessment of diagnostic accuracy studies. *Ann Intern Med*, 2011. 155(8): p. 529-36.
17. Srinivasan, A., et al., Utility of pretreatment mean apparent diffusion coefficient and apparent diffusion coefficient histograms in prediction of outcome to chemoradiation in head and neck squamous cell carcinoma. *J Comput Assist Tomogr*, 2012. 36(1): p. 131-7.
18. Lambrecht, M., et al., Integrating pretreatment diffusion weighted MRI into a multivariable prognostic model for head and neck squamous cell carcinoma. *Radiother Oncol*, 2014. 110(3): p. 429-34.
19. Kim, S., et al., Diffusion-weighted magnetic resonance imaging for predicting and detecting early response to chemoradiation therapy of squamous cell carcinomas of the head and neck. *Clin Cancer Res*, 2009. 15(3): p. 986-94.
20. Hatakenaka, M., et al., Apparent diffusion coefficient calculated with relatively high b-values correlates with local failure of head and neck squamous cell carcinoma treated with radiotherapy. *AJNR Am J Neuroradiol*, 2011. 32(10): p. 1904-10.
21. Hatakenaka, M., et al., Pretreatment apparent diffusion coefficient of the primary lesion correlates with local failure in head-and-neck cancer treated with chemoradiotherapy or radiotherapy. *Int J Radiat Oncol Biol Phys*, 2011. 81(2): p. 339-45.

22. Stadler, P., et al., Influence of the hypoxic subvolume on the survival of patients with head and neck cancer. *Int J Radiat Oncol Biol Phys*, 1999. 44(4): p. 749-54.
23. Driessen, J.P., et al., Diffusion-weighted MR imaging in laryngeal and hypopharyngeal carcinoma: association between apparent diffusion coefficient and histologic findings. *Radiology*, 2014. 272(2): p. 456-63.
24. Wang, K., et al., Tumor-stroma ratio is an independent predictor for survival in esophageal squamous cell carcinoma. *J Thorac Oncol*, 2012. 7(9): p. 1457-61.
25. de Kruijf, E.M., et al., Tumor-stroma ratio in the primary tumor is a prognostic factor in early breast cancer patients, especially in triple-negative carcinoma patients. *Breast Cancer Res Treat*, 2011. 125(3): p. 687-96.
26. Huijbers, A., et al., The proportion of tumor-stroma as a strong prognosticator for stage II and III colon cancer patients: validation in the VICTOR trial. *Ann Oncol*, 2012.
27. Driessen, J.P., et al., Correlation of human papillomavirus status with apparent diffusion coefficient of diffusion-weighted MRI in head and neck squamous cell carcinomas. *Head Neck*, 2015.
28. Chaturvedi, A.K., et al., Human papillomavirus and rising oropharyngeal cancer incidence in the United States. *J Clin Oncol*, 2011. 29(32): p. 4294-301.
29. Chaturvedi, A.K., et al., Incidence trends for human papillomavirus-related and -unrelated oral squamous cell carcinomas in the United States. *J Clin Oncol*, 2008. 26(4): p. 612-9.
30. Marur, S., et al., HPV-associated head and neck cancer: a virus-related cancer epidemic. *Lancet Oncol*, 2010. 11(8): p. 781-9.
31. Hafkamp, H.C., et al., Marked differences in survival rate between smokers and nonsmokers with HPV 16-associated tonsillar carcinomas. *Int J Cancer*, 2008. 122(12): p. 2656-64.
32. Syrjanen, K.J., et al., Immunohistochemical demonstration of human papilloma virus (HPV) antigens in oral squamous cell lesions. *Br J Oral Surg*, 1983. 21(2): p. 147-53.
33. Ang, K.K., et al., Human papillomavirus and survival of patients with oropharyngeal cancer. *N Engl J Med*, 2010. 363(1): p. 24-35.
34. O'Rourke, M.A., et al., Human papillomavirus related head and neck cancer survival: a systematic review and meta-analysis. *Oral Oncol*, 2012. 48(12): p. 1191-201.
35. Westra, W.H., The morphologic profile of HPV-related head and neck squamous carcinoma: implications for diagnosis, prognosis, and clinical management. *Head Neck Pathol*, 2012. 6 Suppl 1: p. S48-54.
36. King, A.D., et al., Head and neck squamous cell carcinoma: diagnostic performance of diffusion-weighted MR imaging for the prediction of treatment response. *Radiology*, 2013. 266(2): p. 531-8.
37. de Bree, R., et al., Detection of locoregional recurrent head and neck cancer after (chemo)radiotherapy using modern imaging. *Oral Oncol*, 2009. 45(4-5): p. 386-93.
38. Kyzas, P.A., et al., 18F-fluorodeoxyglucose positron emission tomography to evaluate cervical node metastases in patients with head and neck squamous cell carcinoma: a meta-analysis. *J Natl Cancer Inst*, 2008. 100(10): p. 712-20.
39. Vandecaveye, V., et al., Detection of head and neck squamous cell carcinoma with diffusion weighted MRI after (chemo)radiotherapy: correlation between radiologic and histopathologic findings. *Int J Radiat Oncol Biol Phys*, 2007. 67(4): p. 960-71.
40. Tshering Vogel, D.W., et al., Diffusion-weighted MR imaging including bi-exponential fitting for the detection of recurrent or residual tumour after (chemo)radiotherapy for laryngeal and hypopharyngeal cancers. *Eur Radiol*, 2013. 23(2): p. 562-9.
41. Vandecaveye, V., et al., Predictive value of diffusion-weighted magnetic resonance imaging during chemoradiotherapy for head and neck squamous cell carcinoma. *Eur Radiol*, 2010. 20(7): p. 1703-14.
42. Vandecaveye, V., et al., Diffusion-weighted magnetic resonance imaging early after chemoradiotherapy to monitor treatment response in head-and-neck squamous cell carcinoma. *Int J Radiat Oncol Biol Phys*, 2012. 82(3): p. 1098-107.

43. King, A.D., et al., Squamous cell carcinoma of the head and neck: diffusion-weighted MR imaging for prediction and monitoring of treatment response. *Eur Radiol*, 2010. 20(9): p. 2213-20.

R1
R2
R3
R4
R5
R6
R7
R8
R9
R10
R11
R12
R13
R14
R15
R16
R17
R18
R19
R20
R21
R22
R23
R24
R25
R26
R27
R28
R29
R30
R31
R32
R33
R34
R35
R36
R37
R38
R39

- [R1](#)
- [R2](#)
- [R3](#)
- [R4](#)
- [R5](#)
- [R6](#)
- [R7](#)
- [R8](#)
- [R9](#)
- [R10](#)
- [R11](#)
- [R12](#)
- [R13](#)
- [R14](#)
- [R15](#)
- [R16](#)
- [R17](#)
- [R18](#)
- [R19](#)
- [R20](#)
- [R21](#)
- [R22](#)
- [R23](#)
- [R24](#)
- [R25](#)
- [R26](#)
- [R27](#)
- [R28](#)
- [R29](#)
- [R30](#)
- [R31](#)
- [R32](#)
- [R33](#)
- [R34](#)
- [R35](#)
- [R36](#)
- [R37](#)
- [R38](#)
- [R39](#)





9

Summary in Dutch - Nederlandse samenvatting

Acknowledgments - Dankwoord

Curriculum Vitae

R1
R2
R3
R4
R5
R6
R7
R8
R9
R10
R11
R12
R13
R14
R15
R16
R17
R18
R19
R20
R21
R22
R23
R24
R25
R26
R27
R28
R29
R30
R31
R32
R33
R34
R35
R36
R37
R38
R39

In dit proefschrift staat het gebruik van diffusie gewogen MRI (DW-MRI) bij hoofd-hals tumoren centraal. DW-MRI is een moderne MRI-techniek, reeds veel gebruikt in de vroege detectie van herseninfarcten, en is de laatste jaren toenemend het onderwerp van onderzoek in diverse oncologische toepassingen. DW-MRI meet de microscopische mobiliteit van watermoleculen. Watermoleculen zullen zich in een vrije omgeving verplaatsen gedreven door thermische energie. Deze verplaatsing wordt diffusie genoemd en wordt beïnvloed door de eigenschappen van de microscopische omgeving. De afstand die de moleculen afleggen wordt gekwantificeerd als de schijnbare diffusie coëfficiënt, waarvoor meestal de Engelse term ‘apparent diffusion coefficient’ (ADC) gebruikt wordt. Water op lichaamstemperatuur (37°C) heeft een diffusie coëfficiënt van $3 \times 10^{-3} \text{ mm}^2/\text{sec}$. Echter, in het menselijk lichaam worden de watermoleculen gehinderd door bijvoorbeeld celmembranen, andere moleculen en cel compartimenten. Hierdoor zijn watermoleculen niet volledig vrij in hun diffusie, maar zijn beperkt afhankelijk van de samenstelling van de omgeving waarin ze zich bevinden. DW-MRI geeft door middel van de ADC een kwantitatieve meting van de diffusie van watermoleculen. Omdat diffusie-restrictie wordt veroorzaakt door onderdelen die zich bevinden in de microanatomie, correspondeert de diffusie coëfficiënt met cel dichtheid. Weefsels met hogere cel dichtheid, zoals de meeste tumoren, zullen zich presenteren met een lagere ADC. De correlatie tussen de microanatomie en ADC maakt dat DW-MRI een interessante beeldvormende techniek is in de vaak uitdagende radiodiagnostiek van hoofd-hals kanker.

De drie pijlers in de behandeling van hoofd-hals kanker zijn chirurgie, radiotherapie en systemische therapie. Met de opkomst van intensiteit gemoduleerde radiotherapie (IMRT) is radiotherapie een steeds aantrekkelijker alternatief ten opzichte van chirurgische behandeling. Bij IMRT wordt gebruik gemaakt van meerdere stralenbundels. Tijdens de bestraling wordt het veld van iedere bundel meerdere malen aangepast. Op deze wijze komt men tot een dosisverdeling die de tumor contour volgt en het gezonde weefsel zo veel mogelijk spaart. Dit heeft geleid tot afname van straling geïnduceerde bijwerkingen en maakt daarmee chirurgische interventie toenemend van belang in het geval van een residu of recidief na (chemo)radiatie ((C)RT).

Het toenemend gebruik van radiotherapie als primaire behandeling en chirurgie als therapie bij recidief, maakt ook de uitdaging van post-therapie controle groter. Vroege detectie van recidieven na (C)RT is van uitermate groot belang, omdat daarmee de kans op een succesvolle chirurgische excisie toeneemt. Met conventionele beeldvormende technieken zoals CT en MRI en nucleaire beeldvorming zoals FDG PET-CT blijft de discriminatie tussen recidief en radiotherapie effecten een uitdaging. Een tweede uitdaging bij de behandeling van hoofd-hals kanker is de pretherapeutische stratificatie van patiënten voor de juiste therapie. Er zijn tumoren die minder goed reageren op radiotherapie dan verwacht. Nauwkeurige en betrouwbare identificatie van deze niet-stralingsgevoelige tumoren zou een

R1
R2
R3
R4
R5
R6
R7
R8
R9
R10
R11
R12
R13
R14
R15
R16
R17
R18
R19
R20
R21
R22
R23
R24
R25
R26
R27
R28
R29
R30
R31
R32
R33
R34
R35
R36
R37
R38
R39

R1 waardevolle toevoeging zijn voor de behandeling van deze patiënten. Deze patiënten zouden
R2 dan niet onnodig bestraald worden, maar direct geselecteerd kunnen worden voor primaire
R3 chirurgische interventie.

R4 Dit proefschrift richt zich op bovenstaande uitdagingen en onderzoekt of DW-MRI bij kan
R5 dragen de hedendaagse knelpunten in de behandeling van hoofdhal kanker. Dit proefschrift
R6 bestrijkt het gebied van fundamentele correlatie van DW-MRI met histologische kenmerken
R7 tot aan diagnostische studies bij patiënten met een recidiverende tumor.

R9 In de eerste twee hoofdstukken ligt de focus op de huidige praktijk en bewijslast ten
R10 gunste van DW-MRI bij hoofdhal kanker. In **hoofdstuk 2** hebben we door middel van een
R11 vragenlijst onder alle leden van de Nederlands Werkgroep HoofdHals-Tumoren de huidige
R12 gebruikte beeldvormende technieken tijdens de follow-up van oropharynx-, larynx- en
R13 hypopharynx tumoren geïnventariseerd en de rol van DW- MRI daarin. Hieruit blijkt dat er
R14 een grote variatie is aan gebruikte protocollen wanneer een patiënt verdacht wordt van een
R15 lokaal recidief na (C)RT. DW-MRI wordt slechts spaarzaam gebruikt en over het algemeen is
R16 men ontevreden over de huidige richtlijnen ten aanzien van follow-up na (C)RT. Daarnaast
R17 geven wij in **hoofdstuk 3** een overzicht van de huidige bewijslast ten aanzien van DW-MRI in
R18 het gebruik van primaire locoregionale stadiëring en opsporen van recidieven.

R20 De twee daaropvolgende hoofdstukken richten zich op de microanatomische achtergrond
R21 van DW-MRI. In **hoofdstuk 4** bestudeerden we de histopathologische bevindingen van
R22 laryngectomie preparaten met de pre-chirurgische DW-MRI beelden. Daarbij vonden we
R23 een positieve correlatie tussen een diffusie coëfficiënt en het percentage stroma, en een
R24 negatieve correlatie met de cel dichtheid, percentage kernoppervlak en de kern-cytoplasma
R25 ratio. Daarnaast vonden we in **hoofdstuk 5** dat humaan papilloma virus (HPV) positieve
R26 tumoren een lagere ADC hebben dan HPV negatieve tumoren. Deze bevindingen kunnen
R27 mogelijk een verklaring vormen voor de prognostisch gunstige waarde van tumoren met een
R28 lage diffusie coëfficiënt (ADC).

R30 **Hoofdstuk 6** richt zich op de predictie van radiosensitiviteit door middel van de ADC. Hierbij
R31 bleek de ADC geen onafhankelijk factor in de predictie van lokale controle na (C)RT. Tenslotte
R32 gaan we in **hoofdstuk 7** in op het gebruik van DW-MRI voor de detectie van lokale recidieven
R33 na (C)RT. Daarbij blijkt DW-MRI vergelijkbare diagnostische accuratesse te hebben als FDG
R34 PET-CT. Echter, de sensitiviteit en negatief voorspellende waarde van FDG PET-CT is superieur
R35 ten opzichte van DW-MRI.

Hoofdstuk 8 is een samenvattende discussie van de voorgaande hoofdstukken van dit proefschrift. Zoals we eerder beschreven, wordt DW-MRI in Nederland slechts zelden gebruikt tijdens de behandeling van hoofdhal kanker. Daarnaast zijn kwalitatief goede studies betreffende DW-MRI bij hoofdhal kanker schaars. Dit vormde de basis van dit proefschrift. Samenvattend toont dit proefschrift nieuwe inzichten ten aanzien van het gebruik van DW-MRI bij hoofdhal tumoren, in het bijzonder bij orofarynx-, larynx- en hypofarynxcarcinomen.

[R1](#)
[R2](#)
[R3](#)
[R4](#)
[R5](#)
[R6](#)
[R7](#)
[R8](#)
[R9](#)
[R10](#)
[R11](#)
[R12](#)
[R13](#)
[R14](#)
[R15](#)
[R16](#)
[R17](#)
[R18](#)
[R19](#)
[R20](#)
[R21](#)
[R22](#)
[R23](#)
[R24](#)
[R25](#)
[R26](#)
[R27](#)
[R28](#)
[R29](#)
[R30](#)
[R31](#)
[R32](#)
[R33](#)
[R34](#)
[R35](#)
[R36](#)
[R37](#)
[R38](#)
[R39](#)

R1
R2
R3
R4
R5
R6
R7
R8
R9
R10
R11
R12
R13
R14
R15
R16
R17
R18
R19
R20
R21
R22
R23
R24
R25
R26
R27
R28
R29
R30
R31
R32
R33
R34
R35
R36
R37
R38
R39



9

Summary in Dutch - Nederlandse samenvatting

Acknowledgments - Dankwoord

Curriculum Vitae

R1
R2
R3
R4
R5
R6
R7
R8
R9
R10
R11
R12
R13
R14
R15
R16
R17
R18
R19
R20
R21
R22
R23
R24
R25
R26
R27
R28
R29
R30
R31
R32
R33
R34
R35
R36
R37
R38
R39

Promotie-onderzoek combineren met de opleiding tot medisch specialist is een enorme uitdaging. Het was niet mogelijk geweest zonder de hulp van velen.

Allereest wil ik mijn bijzondere dank uitspreken aan de patiënten die deel hebben genomen aan mijn onderzoek. Zij hebben zich belangeloos ingezet om in de toekomst de behandeling van hun lotgenoten te optimaliseren. Dank voor de bereidwilligheid bij te dragen aan de wetenschap en in het bijzonder mijn proefschrift.

Professor Grolman, beste Wilko, ik wil u bedanken voor de mogelijkheid om naast mijn opleiding tot KNO-arts dit promotietraject te voltooien. U had het vertrouwen dat ik onder de vleugels van een andere afdeling een gezamenlijk project op kon zetten. Ik denk dat het tot een vruchtbare samenwerking heeft geleid!

Professor Terhaard, beste Chris, bij jou mocht ik, vanuit de afdeling KNO, onder de vleugels van de radiotherapie mijn promotietraject opstarten. Toen ik de eerste dag bij je binnen stapte was ik je halverwege je verhaal kwijt. *‘Waar gaat dat promotietraject nou over?!’* Later heb ik geleerd dat dit enthousiasme en je eindeloze ideeën juist jouw kracht zijn. Wetenschap is allesbehalve puur theoretisch; de beste wetenschap wordt gevoed door nieuwsgierigheid, creativiteit en fantasie. Ik ben je dankbaar voor je persoonlijke betrokkenheid bij dit project en dat je mij de mogelijkheid hebt gegeven het laatste jaar één dag in de week te besteden aan alleen dit boekje; ik weet zeker dat het er beter door is geworden.

Dr. Janssen, beste Luuk. Mijn dank naar jou is groot. In de afwezigheid van professor Grolman het eerste half jaar van mijn aanstelling heb jij je geprofileerd als mijn ankerpunt op de afdeling KNO. Mede door jouw enthousiasme en jouw vermogen je collegae hoofd-hals chirurgen te overtuigen van het belang van de RETURNED-studie, is onze inclusie zo voorspoedig gegaan. Tijdens mijn oncologie stage heb ik van jou ongelooflijk veel geleerd in de operatie- en spreekkamer.

Dr. Philippens, beste Mariëlle. Als iemand bedankt moet worden voor de inhoud van dit proefschrift dan ben jij het. Jij introduceerde me op het gebied van diffusie gewogen MRI. Ik heb me pas veel later beseft hoe lastig dat geweest moet zijn; een KNO-georiënteerde, praktisch ingestelde, technisch ongeschoolde, klinische, jonge dokter die onder jouw vleugels een promotie traject startte. Jouw brede en inhoudelijke kennis is het fundament van dit proefschrift. Dit proefschrift was er niet geweest als jij niet de schakel was geweest tussen Chris z’n eindeloze ideeën en de dagelijkse wetenschapspraktijk. Je bent een begeleider in alle opzichten; inhoudelijk, methodologisch maar ook persoonlijk. Dank daarvoor.

R1
R2
R3
R4
R5
R6
R7
R8
R9
R10
R11
R12
R13
R14
R15
R16
R17
R18
R19
R20
R21
R22
R23
R24
R25
R26
R27
R28
R29
R30
R31
R32
R33
R34
R35
R36
R37
R38
R39

R1 Dr. Pameijer, beste Frank. Dat iemand mij zo enthousiast heeft kunnen maken over de
R2 radiologie is een wonder. Je oefent met zoveel passie je vak uit; dat werkt aanstekelijk. Ik
R3 weet dat je die rommelige, lelijke diffusie gewogen plaatjes niet altijd kon waarderen, en
R4 dat je weleens met tegenzin een oordeel 'recidief' of 'respons' hebt moeten geven over een
R5 DW-MRI. Desalniettemin hoefde ik nooit achter een uitslag aan te bellen; je was altijd eerder
R6 dan ikzelf. Inhoudelijk heb ik zoveel van je geleerd. Het is een groot genoegen geweest om zo
R7 nauw met je samen te hebben mogen werken.
R8

R9 Dr. Huijbregts, beste Julia. Voor de RETURNED-studie beoordeelde jij de FDG PET scans. Ik kan
R10 me de herhaaldelijke mailtjes nog goed herinneren waarin je vroeg om de mogelijkheid van
R11 een 'inconclusief' als oordeel omdat je je niet kon vinden in een positieve of negatieve uitslag.
R12 De uitkomsten van de RETURNED zijn een bevestiging van jouw kunde in de beoordeling van
R13 PET scans. Dank voor je inzet voor dit project.
R14

R15 Geachte leden van de promotiecommissie. Ik wil u allen danken voor uw tijd en inzet om dit
R16 proefschrift te beoordelen.
R17

R18 Lieve (oud) collega's van de research-gang in het Q-gebouw en later op H.02; Tim D., Martijn,
R19 Maarten, Stephanie, Marlien, Sarah, Marc, Joost, Yvette, Huib en Inge. Het is jullie aanwezigheid
R20 die fulltime research voor mij een stuk leuker maakte. Ondanks de stoffige materie viel er
R21 altijd wat te lachen! Collega's uit de hoofd-hals research groep, in het bijzonder Nicolien,
R22 Homan, Niels, Tim S., Joana, Lisanne, Hanneke en Stefan, dank voor de fijne interdisciplinaire
R23 samenwerking. Ook dank aan de wetenschaps-studenten, in het bijzonder Robbert Puijk, die
R24 een speciale bijdrage hebben gedaan aan een hoofdstuk uit dit boekje.
R25

R26 Lieve (oud) arts-assistenten en arts-onderzoekers van de afdeling KNO UMC Utrecht. Wat
R27 een ontzettend leuke collega's heb ik! Elke dag merk ik hoe fijn het is om te werken met
R28 mensen die niet alleen de collega's zijn maar ook je maatjes. In het bijzonder wil ik Pauline,
R29 Xander en Boris bedanken, omdat zij direct bij dit proefschrift en mijn onderzoek betrokken
R30 zijn geweest. Pauline en Xander, wat een leuke tijd hebben we gehad in Poznań!
R31

R32 Stafleden van de afdeling KNO van het UMC Utrecht, St. Antonius ziekenhuis Nieuwegein en
R33 Gelre ziekenhuis Apeldoorn, hartelijk dank voor de passie waarmee jullie mij opleiden. Ivonne,
R34 hartelijk dank voor jouw aandeel hierin en je persoonlijk benadering van de combinatie van
R35 mijn opleiding en promotietraject.
R36

R37 Beste Hanneke, Daphne en Therèse. Dank voor jullie administratieve ondersteuning en
R38 gezelligheid in de afgelopen tijd.
R39

Lieve Annemijn, Elisa, Ingrid en Marlies; wat een groepje zijn we toch. Water en vuur en tegelijk met niemand zo eensgezind. Wat hebben we een hoop meegemaakt met z'n vijf. Het is zo fijn om zo'n onvoorwaardelijk vangnet te hebben. Tussen de opleiding, diensten, onderzoek en verplichtingen door weten we elkaar altijd te vinden en kan ik bij niemand m'n hart luchten zoals bij jullie. Dank dat jullie bereid waren naar mijn oersaaie onderzoeksverhalen te luisteren en begrip te hebben voor het tijdgebrek wat ik de afgelopen jaren heb gehad.

Lieve Emma, Kirstin en Liora; vriendinnetjes vanuit het eerste studiegroepje! Wat kunnen we heerlijk kletsen en wat vind ik het fijn dat jullie mijn vriendinnetjes zijn.

Lieve Anke, Carin, Carien, Evelyne en Stefanie. Wat zijn we allemaal verschillend! En wat leer ik daar veel van. Wat is het mooi om een vriendschap te hebben die zo veel ruimte laat voor ieders eigen 'ik'. Ik vind het zo leuk om jullie (andere) visie op de wereld te horen.

Lieve Ingrid, naast vriendinnetje ook mijn paranimf. Wie anders dan degene die ook een promotietraject heeft lopen kan zich voorstellen hoe het voelt om dit boekje af te hebben. Het is fijn om iemand te hebben die de frustraties van een METC-aanvraag snapt. Ik hoop dat jij ook snel mag beginnen aan je dankwoord.

Lieve Elisa. Het was voor mij direct vanzelfsprekend om jou als paranimf achter me te hebben staan. Ik heb zoveel respect voor hoe jij de afgelopen jaren alle ballen hoog hebt gehouden. Ik vind het heerlijk om jouw kritisch noot, maar verpakt in gouden papier, toegespeeld te krijgen. Nooit heb ik me beseft dat psychiater je op zo erg het lijf geschreven is, tot nu.

Lieve familie Booms, Theo, Marjo, Theo jr, Janneke, Vera, Jos, Paul en Angelique. Wat een voorrecht om onderdeel te mogen zijn van zo'n warme familie. Theo en Marjo, als pubermeisje kwam ik bij jullie binnen en jullie hebben mij als jullie eigen dochter ontvangen. Dank voor jullie interesse in mijn promotie en opleiding.

Lieve zus, lieve Eef. Ik geniet van die eindeloze telefoontjes van ons in de auto. Jij hebt het altijd feilloos door als er iets is, en ik eigenlijk even mijn hart moet luchten. Ik geniet van jou, Robin en de kinderen en bewonder je als moeder. Robin, bedankt dat jij mijn zus zo gelukkig maakt.

Lieve papa en mama. In de voetsporen van... Dank voor alle steun en eindeloze mogelijkheden die jullie mij geboden hebben. Van jullie heb ik geleerd wat ambitie en drive is. Het is fijn om ruggespraak te kunnen houden over de belangrijke beslissingen in het leven. Jullie

R1
R2
R3
R4
R5
R6
R7
R8
R9
R10
R11
R12
R13
R14
R15
R16
R17
R18
R19
R20
R21
R22
R23
R24
R25
R26
R27
R28
R29
R30
R31
R32
R33
R34
R35
R36
R37
R38
R39

R1 onvoorwaardelijk steun heeft ervoor gezorgd dat ik mijn kansen durfde te nemen op de
R2 afdeling KNO. Ik ben ontzettend blij dat wij dit bijzondere moment als familie kunnen vieren.

R3
R4 Lieve Mark. Waar moet ik beginnen? In alle aspecten van mijn leven geef jij me de helpende
R5 hand die ik nodig heb. Je ondersteunt mijn beslissingen en voert mijn enthousiasme. Hobbels
R6 die ik in de weg zie, weet jij weg te nemen of samen te trotseren. Nu we samen in het oosten
R7 van het land zitten bewijst zich eens te meer: mijn thuis is alleen maar daar waar jij je bevindt.
R8 Dank voor je geduld, humor en eindeloze interesse rondom de afronding van deze promotie.
R9 Bedankt dat je me af en toe laat winnen op de golfbaan. Ik hou van jou en koester ons.
R10 Bedankt dat jij jij bent, mijn lief.

R11

R12

R13

R14

R15

R16

R17

R18

R19

R20

R21

R22

R23

R24

R25

R26

R27

R28

R29

R30

R31

R32

R33

R34

R35

R36

R37

R38

R39

R1
R2
R3
R4
R5
R6
R7
R8
R9
R10
R11
R12
R13
R14
R15
R16
R17
R18
R19
R20
R21
R22
R23
R24
R25
R26
R27
R28
R29
R30
R31
R32
R33
R34
R35
R36
R37
R38
R39





9

Summary in Dutch - Nederlandse samenvatting

Acknowledgments - Dankwoord

Curriculum Vitae

R1
R2
R3
R4
R5
R6
R7
R8
R9
R10
R11
R12
R13
R14
R15
R16
R17
R18
R19
R20
R21
R22
R23
R24
R25
R26
R27
R28
R29
R30
R31
R32
R33
R34
R35
R36
R37
R38
R39

Juliette Pauline Driessen was born on October 9th in 's-Gravenhage, the Netherlands. After graduating from secondary school (gymnasium) at the Vrijzinnig Christelijk Lyceum, she started to study Medicine at the Erasmus University in Rotterdam. She obtained her medical degree, cum laude, in March 2011. During her final year, she participated in a research project on facial anthropometry at the Sophia Children's Hospital, where she studied protruding ears. Afterwards, she followed an internship at the department of Otorhinolaryngology at the Erasmus MC. During this year her interest in otorhinolaryngology was sparked, and in April 2011 she started her PhD project at the University Medical Center Utrecht. This PhD project was a collaboration between the department of Otorhinolaryngology- Head & Neck surgery and the department of Radiation Oncology and supervised by Prof. dr. Grolman and Prof. dr. Terhaard. Her daily supervisors were dr. Janssen and dr. Philippens.



The result of her PhD project is described in this thesis and has been presented at national and international conferences. In January 2013, she became a resident Otorhinolaryngology at the University Medical Center Utrecht under the supervision of Prof. dr. Grolman. During her residency, she also worked at the St. Antonius Hospital in Nieuwegein (supervised by Dr. Copper) and at the Gelre Hospital in Apeldoorn (supervised by Dr. Bruintjes).

R1
R2
R3
R4
R5
R6
R7
R8
R9
R10
R11
R12
R13
R14
R15
R16
R17
R18
R19
R20
R21
R22
R23
R24
R25
R26
R27
R28
R29
R30
R31
R32
R33
R34
R35
R36
R37
R38
R39

